JOURNAL OF APPLIED PHYSICS

JOURNAL OF APPLIED

PHYSICS

DECEMBER, 1940 Vol. 11, No. 12

In This Issue

		Page
"A Way of Total Peace"		**749**
Qualitative Spectrochemical Analysis in Agriculture and Geochemistry	STANLEY S. BALLARD	**750**
Contributed Original Research		
Flow of Air Through Porous Media	R. R. SULLIVAN AND K. L. HERTEL	**761**
Spark Gaps with Short Time Lag	JOSEPH SLEPIAN AND W. E. BERKEY	**765**
Thermoplastic Behavior of Linear and Three-Dimensional Polymers	S. S. KISTLER	**769**
Changes in the Absorption Spectrum of Pb and Ni Films at Low Temperatures	CHARLES F. SQUIRE	**779**
Theory of the Cyclotron	ROBERT R. WILSON	**781**
Electrolytic Polishing. II	W. C. ELMORE	**797**
Graphical Method for Selecting Suitable Radiations for the Precision Determination of Noncubic Lattice Constants and for Indexing Back-Reflection Lines in Powder X-Ray Photograms	LOUIS A. CARAPELLA	**800**
Introduction to the Problem of the Isochronous Hairspring	S. GOUDSMIT AND MING-CHEN WANG	**806**
Concentrator of Eddy Currents for Zonal Heating of Steel Parts	G. BABAT AND M. LOSINSKY	**816**
Annual Indexes		
Author Index to Volume 11		**824**
Subject Index to Volume 11		**827**
Volume Table of Contents		**III**
In Every Issue		
Here and There		**759**
Contributors to This Issue		**760**
Index to Advertisers		**viii**

BOARD OF EDITORS

ELMER HUTCHISSON, *Editor*

Associate Editors

F. BITTER
W. E. FORSYTHE
L. A. JONES
B. E. WARREN
J. B. WHITEHEAD

Publication of the American Institute of Physics

ADMINISTRATIVE STAFF

HENRY A. BARTON, *Director*

MADELINE M. MITCHELL, *Publications Manager*

JOHN T. TATE, *Adviser on Publications*

GOVERNING BOARD

PAUL E. KLOPSTEG, *Chairman*
GEORGE B. PEGRAM, *Secretary*
KARL T. COMPTON
WHEELER P. DAVEY
FLOYD A. FIRESTONE
HARVEY FLETCHER
R. C. GIBBS
ARTHUR C. HARDY
GEORGE R. HARRISON
A. STUART HUNTER
H. R. LILLIE
FREDERIC PALMER, JR.
GEORGE B. PEGRAM
W. B. RAYTON
JOHN T. TATE
WALLACE WATERFALL

THE JOURNAL OF APPLIED PHYSICS, published monthly at Prince and Lemon Sts., Lancaster, Pa., is devoted to physics in its role as the science basic to other natural sciences and to the arts and industries. Previous to 1937 this publication was known as PHYSICS. It aims to be of service not only in physical laboratories, but also in the laboratories of industrial, chemical, geological, geophysical, meteorological, radio, and similar concerns. THE JOURNAL OF APPLIED PHYSICS publishes editorials, news of physicists and reviews, as well as technical papers of applied physics.

Manuscripts should be submitted to Elmer Hutchisson, Editor, University of Pittsburgh, Pittsburgh, Pennsylvania.

SUBSCRIPTION PRICE

	U. S., POSS. AND CANADA	FOREIGN
To members of scientific societies	$5.00	$5.70
To all others	7.00	7.70

Single copies are $.70 each.

Changes of address and proofs should be addressed to the Publications Manager.

Subscriptions and orders for back numbers should be addressed to Prince and Lemon Streets, Lancaster, Pa. or to the American Institute of Physics, 175 Fifth Avenue, New York, N. Y.

Advertising rates supplied on request. Orders, advertising copy and cuts should be sent to the American Institute of Physics.

Entered as second class matter at the Post Office at Lancaster, Pennsylvania, under the Act of March 3, 1897. Accepted for mailing at the special rate of postage provided for in the Act of February 28, 1925, authorized May 2, 1932.

Copyright 1940, by the American Institute of Physics.

Journal of Applied Physics

Volume 11 December, 1940 Number 12

"A Way of Total Peace"

IN an interesting and thought provoking lecture* at the Bicentennial Celebration of the University of Pennsylvania, Dr. Frank B. Jewett, Chairman of the Board of Directors of the Bell Telephone Laboratories and President of the National Academy of Sciences, and Dr. Robert W. King, also of the Bell Telephone Laboratories, formulated a plan for a more efficient and vigorous operation of our government in peace times as well as war times. They pointed out that the governments of the totalitarian states have directed every ounce of intellectual and physical man power toward a single purpose —that of total war against the democracies. Such tremendous effort in which everyone was forced to cooperate naturally led to a powerful machine of war. Is it not possible, Drs. Jewett and King ask, after this conflict is settled, to put as much thought and physical effort into a "way of total peace" as has gone into this preparation for a total war?

A government aimed at total peace must take into account the fact that technological advances have not only been a great boon to civilization, but also have provided tools very useful to a single man or to a small minority who happens temporarily to be in power and who wishes to perpetuate that power. In a primitive society a man who could overpower two or three others was chosen leader. In a group of any appreciable size he was unable to oppose the will of the majority. Under such circumstances democracy was a natural and easy form of government. In our modern society the situation is quite different; with machine guns, radio propaganda and dive bombers a small minority can force its will, not only on people of its own nationality, but also on those of other nations. In view of the great advantages which an ambitious minority now has, constraints must be devised so that society can protect itself and a way of total peace be achieved.

Drs. Jewett and King are convinced that the primary need of society is a "mass intellectual attack on social and political problems" similar to the mass intellectual attacks of large research laboratories upon technological problems. They believe that governments should set up organizations of technical experts whose existence is permanent and whose function is advisory to the elected representatives of the people. They point out that many of our important political, economic and social problems are settled by a "hunch" or whim. Millions of dollars are spent by the government with much less investigation of possible results than that which goes into an expenditure of a few thousand dollars by a well-organized research laboratory. During times of emergency advisory boards such as the National Defense Research Committee have been created. It seems reasonable that if such advisory boards are essential when the direction in which a government is moving is self-evident, they become all the more essential in peace times when the goal is evident but all of the intelligence that can be brought to bear upon the problem is none too much to find the shortest and surest path to permanent peace and good will among men.

* "Engineering Progress and the Social Order," Science 92, 365 (1940).

Qualitative Spectrochemical Analysis in Agriculture and Geochemistry

BY STANLEY S. BALLARD*
University of Hawaii, Honolulu, Hawaii

OF the several physical instruments that are employed in the chemical analysis of materials, the spectrograph is perhaps the most firmly intrenched and the most widely used. The current literature of analytical chemistry contains an increasing number of references to what is known as spectrochemical analysis. *Quantitative* methods are now being emphasized particularly, but this should not cause one to overlook the value of a good *qualitative* technique. It is the purpose of this article to outline qualitative analytical methods applicable to the fields of agriculture and geochemistry and to give illustrations of their use.

The general advantages of spectrochemical analysis are well known—the speed, the adequacy of very small samples, and the high sensitivity for many elements. Marked advantages of a spectrochemical technique for qualitative analysis are the following: first, a single analysis serves to determine many elements, including all the metals, and the nonmetals silicon, phosphorus, boron, arsenic, and fluorine (in the presence of calcium); second, the technique is adaptable to any type of sample, be it liquid or solid, metallic or nonmetallic; third, permanent records in the form of the original spectrograms are obtained, which can be consulted later for additional information not desired at the time of making the original analysis. An example of this occurred recently, regarding the presence of lead in Hawaiian soils; all spectrograms of soils taken since the establishment of the laboratory in 1931 could be consulted readily, and lead was found to be a rarely occurring trace soil constituent. The fourth, and final advantage is that semi-quantitative estimates can be made with little added work, giving results that are much more valuable than those of the "present or not present" type of qualitative analysis. The estimates are made on a logarithmic scale and should be accurate to the nearest factor of 10.

The fact that only small samples are used in spectrographic analysis is a great advantage when working with samples difficult to obtain. But, curiously enough, the smallness of the portion needed for testing may be a disadvantage if a large amount of material is at hand, when a difficult problem of sampling results. Since the maximum amount of material that can be used in an analysis is about 50 milligrams, considerable difficulty is encountered in obtaining a representative sample of this size from a ten-acre soil plot or a lava flow that may cover a fraction of a mountain side!

The analytical methods about to be described have been found most useful in two types of investigations. The first is the determination of the approximate composition of a totally unknown sample. In the course of one hour to one working day, depending on the complexity of the sample, the spectroscopist can determine the identity of the major, minor, and trace arc-sensitive elements present. This information should be of considerable value to the chemist who may wish to obtain quantitative data on certain constituents. An example which can be quoted here concerns a white, crystalline incrustation deposited in areas of solfataric activity on the crater floor of Kilauea volcano. This incrustation had been designated as "gypsum" to the writer by geologists. The spectroscope immediately revealed, however, that there was entirely too much silicon present for this to be a pure gypsum. In Table I is given the composition estimated spectrographically, and the accurate quantitative elemental composition recomputed by K. T. Mau from the subsequent gravimetric

* Assistant Professor of Physics. The present paper is an outgrowth of the activities of the writer as Consultant in Spectroscopy in the Experiment Station of the Hawaiian Sugar Planters' Association, 1937–40.

chemical analysis. The spectrographic estimation was too low for calcium, and included traces of magnesium, manganese and sodium that were not detected chemically. Chemical analysis revealed the presence of a small amount of phosphorus, an amount below the spectrographic threshold (for the technique employed). The chemical results also revealed 36.52 percent SO_3, and 13.60 percent H_2O. These data, combined with the results of a mineralogical examination, indicated that the substance was a gypsum ($CaSO_4 \cdot 2H_2O$) – opal ($SiO_2 \cdot nH_2O$) combination along with some other silicate mineral containing the excess of SO_3. These results are discussed elsewhere by Mau and Payne.[1]

The second field of especial usefulness of the spectrographic technique is the determination of the identities and estimation of the amounts of minor and trace elements in samples whose major constituents are known. Indeed, a comparison among the amounts of trace elements in substances of similar major composition can readily be made. Good examples of this can be drawn from geochemistry, since 99 percent of the earth's crust is made up of only ten elements.[2] The spectrograph appears to be an ideal instrument for learning the composition of the remaining one percent.

Experimental Technique

The experimental work described in the present paper was carried on in the spectroscopic laboratory of the Chemistry Department of the Experiment Station of the Hawaiian Sugar Planters' Association, in Honolulu. In this laboratory, spectra are excited by the direct-current arc and are produced and photographed by a large quartz Littrow spectrograph (Bausch and Lomb). This technique is perhaps the best for most agricultural analyses, since the direct-current arc method is particularly applicable to the nonconducting powders so often encountered, and an instrument of high resolving power is necessary due to the abundant iron in Hawaiian soils.

Direct current is supplied by a 3-kva motor-generator. The striking potential for the arc is 250 volts. Sufficient resistance is put in series to hold the arc current at a desired value within the range 4 to 10 amperes, whereupon the voltage drop across the arc is of the order of 30 to 50 volts. The arc current selected depends upon the volatility of the sample and the exposure time desired. In work of this sort, electrodes of the highest obtainable purity should be used. It is now possible to obtain graphite electrodes that contain only occasional impurities —copper, boron and silicon. Copper electrodes free of boron and silicon, but with traces of lead, tin, iron, nickel and silver can be obtained. Therefore, only copper remains as a possible contaminant, and is of importance only when it is present in the sample in concentrations of less than one part per million. Electrodes must be prepared with extreme care to avoid inadvertent contamination. The steps employed in this laboratory are described elsewhere.[3] A bare electrode strip is photographed on the plate for each pair of electrodes used, in order to be sure that no accidental impurity is present. Lower electrodes are now prepared with a conical cavity, the ratio of the diameter to the depth of the cone being 2 to 1, 1 to 1, or 1 to 2 for small, medium, or large samples, respectively.

TABLE I. *Elementary metallic composition of a white incrustation, as estimated spectrographically and as determined chemically.*

ELEMENT	SPECTROGRAPHIC ESTIMATION, PERCENT	CHEMICAL DETERMINATION, PERCENT
Silicon	more than 10	15.31
Calcium	more than 1	12.2
Iron	approximately 0.1	0.14
Magnesium	approximately 0.01	not found
Manganese	approximately 0.01	not found
Sodium	approximately 0.01	not found
Phosphorus	less than 0.1	0.07

Experiments showed that the arc ran more steadily when the lower electrode was of positive polarity. This arrangement has the added advantage (at least when refractory samples are being arced) that the positive electrode gets much hotter than the negative. For these two reasons the lower electrode is always made the positive. Figure 1 shows the plateholder end of the spectrograph, and various accessories.

Two different techniques are available, and the one chosen depends upon the sensitivity and reproducibility desired. For the highest sensitivity a short arc of 2-mm length is used, and

the arc is focused on the spectrograph slit by a spherical quartz condensing lens. The effective instrumental speed is regulated by the use of rectangular apertures over the condensing lens. As described elsewhere,[3] this allows the speed to be changed during the course of the exposure, as is important in the detection of traces of the volatile elements, whose sensitive lines may be lost unless the photographic speed is high during the first few seconds of exposure. When comparing samples of similar general constitution in order to note minor differences of composition, a technique of lower sensitivity but better reproducibility is employed. A longer arc, 4–5 mm, is focused on the collimator lens of the spectrograph by the condensing lens. Speed regulation is effected by the use of rectangular apertures placed over the collimating lens. These apertures cannot be changed during the course of the exposure. When high reproducibility is desired, it is important that each sample shall be entirely volatilized, as emphasized by Slavin[4] and others.

In order to photograph sensitive lines of all arc-sensitive elements with the large Littrow instrument, it is necessary to take two spectrograms, one in the wave-length range 5900 to 3100A and the other in the range 3100 to 2360A. In the former range, Eastman spectroscopic plates type I–D are used, and in the latter, type I–O. Plates are developed in Eastman high contrast developer D–19 and are fixed, washed and dried in the conventional manner.

Analysis of Spectrograms

Plates are analyzed by comparing the unknown spectrograms in a Judd Lewis comparator (Adam Hilger, Ltd.) with standard plates upon which are marked the ultimate and other sensitive lines of the various elements. We have a file of some 60 of these plates, each of which, of course, was taken with one or the other of the two regular instrumental settings. The use of comparison spectrograms of Hilger's "R. U. Powder" that show the "*raies ultimes*," or ultimate lines, of three or four dozen of the common arc-sensitive elements has not been found practical in this laboratory, since sensitive lines of trace elements may so easily be confused with weaker lines of the more abundant elements. Much time is saved by using a pair of "elimination plates," on which are photographed and identified all the stronger lines of the elements common in agricultural materials, namely, calcium, magnesium, sodium, potassium, aluminum, manganese, copper, boron, silicon, phosphorus, and iron. To this list might well be added strontium and barium, in trace quantities. Lines are dotted with colored ink as they are identified, and the symbols of the appropriate elements are written in the margin. Of course, for provisional analysis the plates can be inspected while still washing, and the presence or absence of the sensitive lines of a dozen or more elements can often be noted without delay.

Because of the occurrence of seeming coincidences of spectrum lines, to the non-uniform wave-length sensitivity of photographic plates, to the wave-length range available, and to the virtual obliteration of certain regions by cyanogen bands, the "*raies ultimes*" are not always the most sensitive lines, from the point of view of practical spectrochemical analysis. We have found that in general the "best lines for trace analysis" are those listed by Milbourn.[5]

Semiquantitative estimates may sometimes be made by comparing the unknown spectrum with that of some substance of analyzed compo-

TABLE II. *Estimated composition of a meteorite-like metallic specimen, and the average composition of iron meteorites, as given by Watson.*[13]

ELEMENT	SPECTROSCOPIC ESTIMATION	CHEMICAL AVERAGE, IRON METEORITES, PERCENT*
Iron	approx. 90%	88.3
Nickel	approx. 1%	8.15
Silicon	approx. 5%	0.76
Cobalt	strong trace	.53
Phosphorus	weak trace	.15
Calcium	trace	.05
Copper	strong trace	.05
Magnesium	trace	.03
Manganese	strong trace	.03
Chromium	not found	.03
Zinc	weak trace	—
Molybdenum	trace	—
Sodium	trace	—
Tin	trace	—
Aluminum	trace	—
Sulphur	not detectable	1.70
Carbon	not detectable	0.04

* Watson (reference 13, p. 430) states: "Many elements present only as traces in meteorites have been omitted as being relatively unimportant."

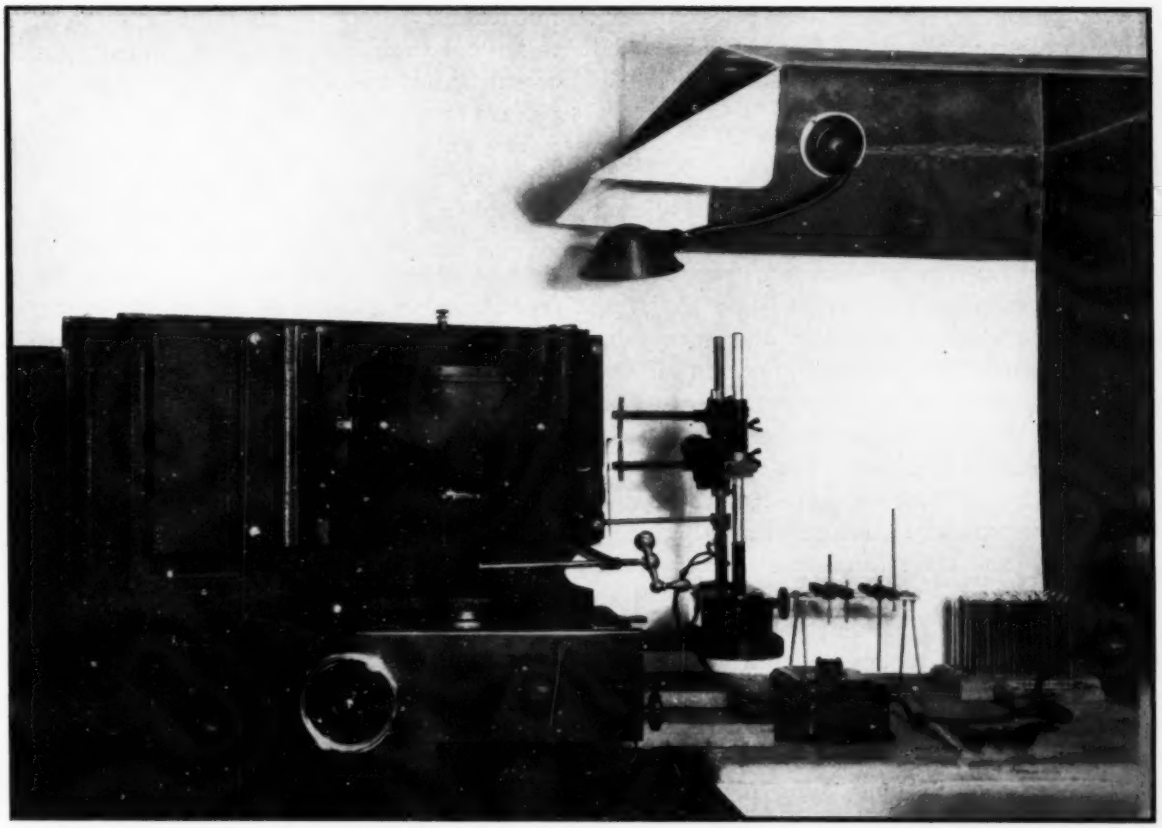

FIG. 1. Plateholder end of spectrograph. The hood draws off fumes from the arc. Note the arc stand (with short graphite electrodes in place), the arc height indicator, the rack with copper and iron electrodes, the prepared graphite electrodes (protected by inverted test tubes), and the reversing switch in the arc electrical supply line.

sition. For example, it was desired to analyze a piece of iron pipe for copper and molybdenum. The spectrum of this sample was compared with that of Hilger's "H.S." brand analyzed iron electrodes, and it was reported that copper was present in the sample in amount exceeding 0.1 percent, while molybdenum was present in amount exceeding 0.01 percent. Subsequent chemical analysis showed 0.2 percent copper and less than 0.05 percent molybdenum.

If no analyzed substance of appropriate composition is available it is still possible to make semiquantitative estimations, on a somewhat *a priori* basis. The two steps are: first, to estimate the relative amount of the element present, in terms of the strength of its sensitive lines and the degree of development of its spectrum; and second, to weight this information in view of the known spectroscopic sensitivity of the various elements. In arriving at a judgment of the first point, one must have a knowledge of the behavior of the spectrum of each element as increasing amounts of the element are present. This, therefore, requires considerable practical experience founded on a knowledge of the fundamental theory of spectrum analysis. Thus equipped, the experienced spectroscopist will have no difficulty in making these judgments, reporting them on a fivefold scale such as "high, medium, low, trace, not detected." The writer has found that he can reproduce such judgments with only minor changes after months or years have elapsed. The relative arc-sensitivity of the various elements has been given by Ryde and Jenkins.[6] It has been found that each step in sensitivity of a factor of 10 corresponds approximately to one of the steps in the scale-of-five given for the development of the spectrum. Combining the original estimate and the weighting in terms of spectral sensitivity, the final

percentage of the element can be estimated. Table I gives an example of the results obtained by the application of this method, as do Tables II and III.

Applications to Agriculture

Chemical methods are used regularly and successfully in agriculture to determine the major plant nutrients: nitrogen, phosphorus, potassium, calcium, magnesium, and so forth. The use of the spectrograph is, therefore, relegated ordinarily to the determination of the so-called minor elements: those that are essential to normal plant growth but are needed in only minute amounts. Hoagland[7] has recently given a good review of this subject. He favors the term "micronutrient elements." Boron, copper, manganese, and zinc are now accepted as "minor" essential elements, and others such as molybdenum have been suggested. Traces of cobalt are essential for animal nutrition, so its presence in plant material is of interest. It should be noted that the beneficial effect of certain of the minor elements changes to a toxicity when they are present in only 5 or 10 times the concentration necessary for normal plant growth. Therefore, not only the lower but also the upper limit of concentration should be determinable.

In an article entitled "The role of the spectrograph in the analysis of agricultural materials"[8] the writer has set forth the principal advantages of the spectrograph in this field, and has given a number of examples of its use. An all-important point, when analyzing such materials for trace elements, is to reduce the chance of accidental contamination by giving the sample the minimum amount of treatment. The methods of preparation of various types of materials for spectrographic analysis will hence be outlined:

(1) Soils

Fusion analysis of soils to determine the total amounts of the various nutrients present is almost a thing of the past, since it is now known that the *availability* of the element is far more important. However, an exception to this general rule is found in the case of the minor elements, where total amounts are still determined. In addition to determining these "micronutrient elements," the agriculturist often wishes to have data on certain other elements, such as arsenic, lead, and fluorine, that may be toxic if present in too large amounts.

The soil sample is first air-dried, then broken up with a wooden mallet until it will pass through a 2-mm screen. It is then spread out on a large piece of wrapping paper, is mixed thoroughly, and is quartered repeatedly, until a representative sample of about 10 grams has been withdrawn. The 10-gram sample is ground in an agate mortar until it will pass through a 100-mesh screen. A representative sample of a few milligrams can then be taken from this finely ground material.

(2) Fertilizers

The spectrochemical analysis of fertilizers is useful in detecting the presence of minor and of toxic elements, and traces of major nutrient elements. In many cases the soil may receive certain minor elements only from fertilizer applications, and, therefore, it is a matter of some importance to know their trace composition. This situation has been of greater importance in recent years, since synthetic fertilizers of rather high chemical purity are being substituted for the natural products that have a large trace element content. The writer has analyzed a dozen of the common commercial fertilizers used in Hawaii in order to determine the identity

Table III. *Spectroscopic estimations and subsequent chemical determinations for four lava samples. All figures are percent of total.*

	Black		Yellow		Gray		Red	
Element	Spec.	Chem.	Spec.	Chem.	Spec.	Chem.	Spec.	Chem.
Silicon	10	24.21	10	33.52	15	23.73	5	12.06
Aluminum	1	8.12	0.1	0.33	5	7.51	1	13.66
Iron	5	6.79	0.01	0.07	5	8.01	1	14.49
Calcium	10	7.51	0.1	0.074	10	7.59	0.01	0.11
Magnesium	1	3.58	0.01	0.006	1	4.05	0.1	0.048
Sodium*	0.01	1.53	N.F.	0	0.01	1.56	0.001	0.19
Potassium	1	0.32	<0.1	0	<0.1	0.72	<0.1	0.10
Titanium	0.5	1.53	10	6.53	1	1.26	0.5	2.16
Zirconium	N.F.	0	0.1	0.10	0.05	0.04	N.F.	0
Phosphorus	<0.1	0.09	<0.1	0	<0.1	0.10	<0.1	0.12
Chromium	0.1	0.039	0.01	0.025	0.05	0.050	0.05	0.138
Vanadium	0.1	0.037	N.F.	0	0.01	0.040	N.F.	0
Nickel	0.01	0.035	N.F.	0	0.01	0.013	0.01	0.018
Copper	0.1	0.079	0.01	0	0.1	0.053	0.1	0.055
Manganese	0.5	0.112	N.F.	0	0.5	0.255	0.1	0.107
Strontium	0.01	0.017	N.F.	0	0.01	0.025	N.F.	0
Barium	N.F.	0	N.F.	0	0.01	0.009	N.F.	0
Cobalt	0.001	0	N.F.	0	0.005	0	0.005	0

* See discussion in text of low sodium sensitivity.

of their major, minor and trace metallic constituents.[9] Fully twenty-one elements were detected in this investigation, although the spectroscopic methods were not the most searching.

The method of preparing fertilizers for analysis is similar to that for soils, except that the sampling procedure is ordinarily not so laborious.

(3) Plant Materials

In order to concentrate the mineral portion of plant materials, they are ordinarily ashed, thereby destroying the organic matter. This ashing is done in platinum dishes, and at low temperature so that the more volatile elements will not be driven off. Wet ashing may be faster, but it involves the use of reagents, whose trace impurities must be carefully determined, and should be checked from time to time. In qualitative spectroscopic analysis the use of reagents should be kept down to the minimum, since the impurities in the reagents may be the very elements concerning which information is desired.

Examples of the analysis of sugar cane have been given elsewhere[8,11] by the writer. One series attempted to determine the distribution of mineral elements throughout the sugar cane plant by comparing ash samples of leaves and various parts of the stalk. A preliminary survey[10] indicated that the lower part of the stalk contained the highest concentration of minerals. It was then realized that this state of affairs was doubtless more apparent than real, due to the variation in ash content of different parts of the plant. The older stalk material is heavier in sugar and, therefore, gives a much smaller ash than does any other part of the plant. In an effort to overcome this difficulty, the spectra of ash samples of different weights were compared, the weights being those representing equal weights of oven-dry material. Data furnished by A. S. Ayres, Assistant Chemist, Experiment Station H. S. P. A., were used in making these computations, and final analyses were made on samples taken from a single stalk of 16 months old sugar cane. 1.0 mg of dry leaf cane ash (24 hours at 300°C), was compared spectrographically with the following ash weights: 1.6 mg of green leaf cane, 4.4 mg of nonmillable top, and 6.2 mg each of green leaves and dead leaves. Chemical results for the major elements phosphorus, potassium, calcium, magnesium and silicon, and spectrographic results for nine minor and trace elements, are presented and discussed elsewhere.[11] This type of comparison, which involves different weights of the various samples and hence quite different arc-burning conditions, doubtless pushes the present technique to its very limits.

(4) Miscellaneous Agricultural Materials

Analyses of a number of these are given in the article already referred to.[8] Liquids require no preparation for analysis, for they can be tested directly by soaking the ends of the electrodes in the solution, or by transferring a droplet into the lower electrode cavity with a pipette. Aqueous solutions can be concentrated by evaporation in platinum over a hot plate or a water bath. The mineral content of a more viscous liquid, such as a sugar sirup, can often be concentrated by low temperature ashing, perhaps preceded by caramelization over a hot plate.

Applications to Geochemistry

Rock samples are ordinarily analyzed by the chemical methods recommended by Washington, Hillebrand, and others. The ten elements oxygen, silicon, aluminum, iron, calcium, sodium, potassium, magnesium, hydrogen and titanium account for over 99 percent of the earth's crust, according to Clarke and Washington.[2] In order to achieve sufficient accuracy, these elements must be determined chemically, as must phosphorus, which is not sensitive spectroscopically. The less abundant elements chlorine, carbon, sulphur, and perhaps fluorine cannot be determined with the present spectroscopic technique, hence other methods must be used. The chemical method for manganese is straightforward and accurate. However, the minor metallic elements barium, chromium, zirconium, vanadium, strontium, nickel, copper, etc., are present in amounts of less than 0.1 percent in the "average igneous rock," and hence lie within the accurate analytical range of the spectrograph. Chemical determinations for these elements are laborious, and larger samples must be used. It is here

that the spectrograph has a great advantage, since with a single 20-mg sample of finely powdered material the spectroanalyst can establish within a few hours the identity of all of the metallic trace constituents. Entirely unsuspected constituents are as likely to be found as are the well-established ones. The knowledge of what elements are present in trace amounts should certainly shorten the work of the chemist, and he need not run his samples at all for the metals not found by the spectroscopist. Furthermore, the semiquantitative spectrographic information will allow him to adjust his methods in order more accurately and readily to make these sometimes difficult quantitative determinations. Indeed, if the amount estimated spectroscopically is equal to or less than 0.001 percent, the actual amount present will probably not have to be determined at all, since even with an allowable error in estimation of a factor of 10, the amount present would not exceed 0.01 percent, and the element would ordinarily be termed a chemical "trace." It is the writer's considered opinion that one who has performed a number of such spectrochemical analyses on samples that have previously been analyzed chemically for major, minor and trace elements could give for similar samples semiquantitative estimations on trace elements which should not be in error by more than a factor of 5. In fact, rough quantitative spectrographic methods, in which the average error should not exceed 15 to 20 percent, could be introduced with only a small amount of additional work. (Certain major elements already determined chemically could serve as "internal standards.") However, this matter is outside the scope of the present paper, which is concerned only with qualitative and semiquantitative methods.

It should be remembered that "not detected" may have different meanings for different elements, since the "detection threshold quantities" differ considerably. For many elements this threshold is far below the common 0.01 percent "trace" designation. Quoting Hillebrand[12] regarding the advisability of the determination of trace elements: "If present in little more than traces, that knowledge alone may suffice, for it is often more important to know whether or not an element is present than to be able to say that it is there in amount of exactly 0.02 or 0.06 percent."

An added advantage to the analytical chemist of the present rapid spectrographic technique is the possibility of testing precipitates for traces of elements concentrated therein. The chemical tests may have failed to reveal them because such small amounts were present, or because their presence was unsuspected and they were not sought. Or they may have been incompletely removed in previous steps of the chemical procedure.

Of course no geological sample will have exactly the "average composition of the lithosphere"! Nor will it always be true that the identity of all the major constituents will be known. An example of benefits of determining what major elements are present is the case of the "gypsum" mentioned above (Table I). Another example of the identification of the major elements occurred when the writer was asked to analyze a ferrous material which appeared to be a meteorite. The estimated composition of this sample is shown in Table II, along with the average composition of iron meteorites as given by Watson.[13] The analyzing of such a sample, with iron strongly predominant, is quite different from that discussed above for soils and plant materials, where silicon, calcium, aluminum and the like were the dominating elements. In the first place, the iron may have a different effect on the burning of the arc, so that *a priori* estimates of amounts of other elements present in the sample cannot be reported with confidence until experience has been gained through the use of chemically analyzed samples. In the second place, the complexity of the iron spectrum gives the spectrograms a quite different appearance, and many of the familiar lines of other elements are masked by some of the thousands of iron lines. Analyses must be made by using the few lines that are not blends with iron lines, and so judgments of "the degree of development of the spectrum" become very difficult.

Table II shows that the spectroscopic estimation for the sample and the chemical average for iron meteorites agree fairly well, except for silicon and nickel. It might be instructive to determine the specific gravity of the sample, as

a rough check of its silica content. Examination under the metallographic microscope might also give interesting information, but this is outside the writer's field. Estimates of amounts of the various trace elements are not given, due to lack of experience with ferrous samples. The spectrograms indicated that the five elements not reported by Watson were present in amounts ranging from 0.001 to 0.01 percent.

It was noted that when this specimen was cut or ground so as to expose a fresh metallic surface, there appeared slowly on the surface a viscous liquid exudate, which turned into a brownish powder. This powder was spectrographed, and seemed to be of about the same composition as the parent metal, with the exception that the metal was stronger in phosphorus, magnesium, and manganese, while the powder appeared to be much stronger in zinc.

Another example of the value to the chemist of preliminary spectroscopic analysis is the study recently completed by Mau and Payne[1] of the accelerated decomposition of Kilauea lava by solfataric gases. A visual examination of the various specimens, namely the parent rock, the rock that was decomposing in the presence of steam and carbon dioxide, and the rock decomposing in the presence of steam, carbon dioxide and sulphur dioxide, showed clearly that widespread changes were taking place and that the SO_2 gave a different result from the CO_2 and steam alone. Preliminary spectrographic examinations of the various samples were made by the writer, and these showed the process of disintegration to be accompanied by the concentration of certain elements and the depletion of others, many of them behaving in a totally unexpected fashion. The amounts of all constituents present, as shown by the spectrograph, were estimated, and these data were found to be of great use to the chemists in selecting and adjusting the quantitative analytical methods. As an example of the accuracy that can be expected from such estimation, these spectroscopic estimates are given in Table III along with the accurate values (reduced to element percentages) found subsequently by Mau and Payne. The "black" and "gray" samples are the parent, undecomposed material, and are almost identical in composition. The "yellow" is the decomposition product of "black" lava attacked by steam, CO_2 and SO_2, while the "red" resulted from the decomposition of "gray" by steam and CO_2 only.

The "gray and red" samples were spectrographed approximately six months after the "black and yellow" ones, and with a somewhat modified technique. Nevertheless the spectroscopic estimates for the constituents of the similar undecomposed samples agree more closely than by a factor of 10 in practically every case. Only the arc-sensitive elements are listed in Table III, so the various columns will not total 100 percent. The total time consumed in analyzing the pair of spectrograms for the "gray" and "red" samples, and making the estimates given in Table III, was four hours.

Some twenty other minor elements, in addition to those listed in Table III, were specifically sought, but their sensitive spectrum lines were not found. The chemists did not report amounts less than 0.01 percent, but labeled these "0," which gives no indication of the sensitivity of the various chemical methods. In the spectroscopic columns the abbreviation "N.F." signifies "not found." As conservative estimates of the threshold sensitivities for these experimental conditions, "N.F." for sodium, nickel and cobalt means "less than 0.001 percent," while for zirconium, manganese, vanadium, strontium and barium it means "less than 0.01 percent." Judging by the figures for phosphorus, the limiting spectroscopic sensitivity has been set a bit too low. On the other hand, it is probable that the thresholds just stated for cobalt and nickel are conservatively high, since 0.0001 percent, or one part per million, of these elements can ordinarily be detected with certainty spectrographically. However, the technique employed in the present analyses was of low sensitivity, at least for such volatiles as sodium and potassium. The instrumental speed was very low, and therefore such fast burning elements did not register proportionately; it appears that in subsequent low speed analyses of refractory samples the estimated percentage for sodium should be multiplied by 100. The fact that potassium was detected in the "black" but not in the "gray" sample is explained by the heavy background on the "gray and red" plate. A dark background effectively conceals many of the

weaker lines, and in this case invalidated the "gray" analysis for potassium.

Fortunately, a number of elements each have some sensitive lines in one instrumental range and other sensitive lines in the other range. Thus the uneven or incomplete burning of a sample in the exposure in one range is discovered and can be allowed for. If all the lines of the element lie in one range, as do those of potassium, exposure variations will not be detected, and duplicate plates or duplicate exposures with fresh electrodes should be taken. The present analysis was not run in duplicate, and poor burning of the arc in the case of the "red" sample for the visible range plate is suspected, since the spectra of the major (and refractory) elements, silicon, aluminum, iron, titanium, and particularly calcium, were very weak.

In conclusion, attention is drawn to an application of spectroscopy to petrology. Standard chemical methods have proven the presence of various trace elements in lavas but have given no indication whether they are distributed uniformly throughout the rock or are concentrated in certain of its mineral constituents. Information on this distribution is of particular importance to a petrologist who is studying the process of magmatic differentiation. The spectrograph is an ideal analytical instrument for use in this connection, because of its extreme sensitivity for many metals and its ability to handle minute amounts of material, such as fragments of phenocrysts laboriously separated by hand from a crushed rock specimen. An example of the successful use of the spectrograph for this purpose is a series of analyses performed recently on samples of the groundmass and of various phenocrysts of a Haleakala lava. Nickel was shown by semiquantitative spectrographic analysis to be highly concentrated in the olivine phenocrysts. Vanadium is restricted to the pyroxene, but was found in both larger phenocrysts and smaller groundmass crystals.

Acknowledgments

Thanks are due K. T. Mau and Dr. J. H. Payne for permission to use their analytical data in Tables I and III. The writer wishes to acknowledge the aid of P. L. Gow, Assistant Chemist, Experiment Station H. S. P. A., who was in part responsible for the development of many of the features of the analytical technique reported here. The enthusiasm and encouragement of Dr. F. E. Hance, Chemist, Experiment Station H. S. P. A., under whose cognizance the experimental work was carried on, have been greatly appreciated.

Bibliography

1. K. T. Mau and J. H. Payne, article to be submitted to J. Geol.
2. F. W. Clarke and H. S. Washington, Proc. Nat. Acad. Sci. **8**, 108–115 (1922).
3. S. S. Ballard and P. L. Gow, J. App. Phys. **10**, 556–557 (1939).
4. M. Slavin, Ind. Eng. Chem., Anal. Ed. **10**, 407–411 (1938).
5. M. Milbourn, J. Soc. Chem. Ind. **56**, 205T–209T (1937).
6. F. Twyman and D. M. Smith, *Wavelength Tables for Spectrum Analysis* (Adam Hilger, London, 1931), p. 130.
7. D. R. Hoagland, Science **91**, 557–560 (1940).
8. S. S. Ballard, Hawaiian Planters' Record **44**, 35–48 (1940).
9. S. S. Ballard, Hawaiian Planters' Record **42**, 185–195 (1938).
10. S. S. Ballard, Phys. Rev. **53**, 689A (1938).
11. S. S. Ballard, Hawaiian Planters' Record **44**, 183–186 (1940).
12. W. F. Hillebrand, *The Analysis of Silicate and Carbonate Rocks* (Bull. 700, U. S. Geol. Sur., 1919), p. 23.
13. F. G. Watson, Jr., J. Geol. **47**, 426–430 (1939).

Here and There

Cover Photograph

On the cover of this issue is a photograph of the mass spectrograph of the University of Illinois, constructed under the direction of Professor E. B. Jordan. Two and a half years were required for the design and construction of this instrument, which has an extremely high dispersion and resolving power and employs both velocity and direction focusing. The ions pass through a crossed electric and magnetic field analyzer having an effective length of 115 cm. The effect of this arrangement is to produce a velocity spectrum in front of a slit which allows 0.2 percent of this spectrum to pass on and be focused upon a recording plate by means of a magnetic field. The mean angle of deflection of the ions in the magnetic field is $\pi/3$ radians. The mass spectrum thus produced has a mean dispersion of 14.6 mm for one percent mass difference. The performance of the instrument to date indicates that approximately all of the theoretical resolving power of 29,200 is attainable. The mass differences as obtained by taking the mean of the ratios of the doublet separation to the forward and backward dispersion line separations are accurate to 5 parts in 10^7 when expressed in mass spectra units. Satisfactory spectra of the methane series have been obtained with exposure times of one minute.

★

To Direct Production Engineering

E. W. Ritter, former general manager of radio tube manufacturing of the RCA Manufacturing Company, Inc., Camden, New Jersey, has been elected vice president in charge of all the company's manufacturing and production engineering activities, according to a recent announcement by Robert Shannon, executive vice president of the company. The promotion of E. W. Engstrom, former director of general research, to the post of manager of all research activities for the company, was also announced.

★

Develops Induction Accelerator

Dr. D. W. Kerst, who was recently promoted from an instructorship to an assistant professorship in the Department of Physics of the University of Illinois, has been granted leave from the department until September, 1941, for the purpose of developing his induction accelerator in the research laboratory of the General Electric Company.

★

Company Announces Staff Changes

Dr. Frank B. Jewett has resigned as president of the Bell Telephone Laboratories in New York City to become Chairman of the Board of Directors. He will be succeeded as president of the laboratories by Dr. O. E. Buckley, who has been executive vice president.—*Science.*

Industrial Research Institute Meeting

Problems of industrial research management and of the design of research laboratories were discussed by some fifty active executives in this field at the New England meeting of the Industrial Research Institute on September 27 and 28. Meeting headquarters were at the New Ocean House, Swampscott, Massachusetts. Following the meeting it was announced that an inventory would be made by member companies of the special facilities and key personnel of their research organizations in the interests of the national defense program.

The Industrial Research Institute, an affiliate of the National Research Council, was organized several years ago for the purpose of improving efficiency and effectiveness in the management of industrial research, through cooperation of its members. The membership is composed of industrial concerns maintaining research laboratories as a part of their organizations. The top executives in charge of research of the member-companies represent them in the activities of the Institute.

★

Calendar of Meetings

December

2– 4 American Institute of Chemical Engineers, New Orleans, Louisiana
2– 7 Highway Research Board of National Research Council, Washington, D. C.
3– 6 American Society of Mechanical Engineers, New York, New York
20–21 American Physical Society, Pasadena, California
26–28 American Physical Society, Philadelphia, Pennsylvania
26–28 Geological Society of America, Austin, Texas
28–30 American Association of Physics Teachers, Philadelphia, Pennsylvania
30–Jan. 1 American Mathematical Society, Baton Rouge, Louisiana
27–Jan. 2 American Association for the Advancement of Science, Philadelphia, Pennsylvania

February

21–22 American Physical Society, Cambridge, Massachusetts

April

7–11 American Chemical Society, St. Louis, Missouri
16–19 The Electrochemical Society, Inc., Cleveland, Ohio

May

1– 3 American Physical Society, Washington, D. C.

June

20–21 American Physical Society, Providence, Rhode Island
23–27 American Association for the Advancement of Science, Durham, New Hampshire

★

Visiting Professor at Smith College

Dr. Karl K. Darrow, research physicist at the Bell Telephone Laboratories, has been appointed visiting Professor of Physics on the William Allan Neilson Foundation at Smith College for the second semester 1940–41. He will be the fifth scholar to occupy the chair, which was founded in 1927 as a gift to William Allan Neilson in recognition of his completion of ten years' service as third president of Smith College. The foundation was perma-

nently endowed by alumnae, undergraduates and friends of the college in June, 1935. Dr. Darrow will present a series of lectures in the field of atomic physics suitable for members of the department and for advanced students, seniors and graduate students of other departments. He will also contribute to a seminar in nuclear physics.—*Science.*

★

Chemistry Chairman at Cornell

Professor Peter Debye has been appointed Chairman of the Department of Chemistry at Cornell University, and Bruno Rossi, Associate Professor of Physics, a note in *Science* announces.

Scales for Evaluating Magnetic Anomalies

Magnetic anomalies caused by geologic bodies of any size or shape on any known or assumed distribution of magnetization can be evaluated by means of a set of scales recently developed by the Geophysical Section of the Geological Survey, United States Department of the Interior. Although they were originally constructed for evaluating magnetic anomalies, these scales are equally useful for solving problems involving all fields under the inverse square law; e.g., gravitational attraction, electric fields, and intensity of illumination. Photolithographed charts of this set of 39 scales have been prepared and may be purchased for twenty-five cents each from the Director, Geological Survey, Washington, D. C.

Contributors to This Issue

R. R. Wilson

Robert R. Wilson received his A.B. degree in 1936 and his Ph.D. degree in 1940 from the University of California. His post-graduate work was done in the Radiation Laboratory there. Dr. Wilson has been connected with the research department of the Western Precipitation Corporation and is now an Instructor of Physics at Princeton University.

R. R. Sullivan

R. R. Sullivan received his B.S. degree at the University of Arkansas, his M.A. degree at the University of Missouri, and his Ph.D. degree in physics at the University of Minnesota. He is now Associate Physicist at the University of Tennessee Agricultural Experiment Station.

S. S. Kistler, who has been since 1935 Research Engineer with the Norton Company, received his education at Stanford University, the Kaiser Wilhelm Institute for Physical and Electrochemistry, and the University of Goettingen. He has also been connected with the Engineering Department of the Standard Oil Company of California and has taught chemistry and chemical engineering in the College of the Pacific and the University of Illinois, respectively.

M.-c. Wang

Ming-chen Wang is a graduate student, holding a Barbour Scholarship, in the Department of Physics at the University of Michigan. Miss Wang was graduated from Yenching University, China.

S. A. Goudsmit

S. A. Goudsmit is now Professor of Physics at the University of Michigan, whose faculty he joined in 1927. He received his Ph.D. degree at the University of Leiden in the Netherlands.

Charles F. Squire is now Instructor in Physics at the Massachusetts Institute of Technology and has been doing research in low temperature phenomena at the University of Pennsylvania, the University of Paris, and Johns Hopkins. Dr. Squire's picture and an earlier biographical sketch appeared on p. 250, Vol. 11, No. 4, 1940, *Journal of Applied Physics.*

Pictures and biographies of the following contributors appeared in earlier issues of the *Journal of Applied Physics:*

Stanley S. Ballard, p. 342, Vol. 11, No. 5, 1940.
Louis A. Carapella, p. 563, Vol. 11, No. 8, 1940.
W. C. Elmore, p. 699, Vol. 10, No. 10, 1939.
K. L. Hertel, p. 479, Vol. 11, No. 7, 1940.
Joseph Slepian, p. 618, Vol. 8, No. 9, 1937.

Contributed Original Research

The Flow of Air Through Porous Media*

R. R. Sullivan and K. L. Hertel
The University of Tennessee Agricultural Experiment Station, Knoxville, Tennessee
(Received May 6, 1940)

The values of the constant in the equation which relates permeability of a porous medium to the porosity and specific surface of the medium are determined for three cases. These experimental values are found to be consistent with the theoretical indications of Fowler and Hertel.

Introduction

THE flow of fluids through porous media has been investigated by Carman,[1] Wiggins *et al.*,[2] and Fowler and Hertel[3] as a method for the determination of the specific surface of the media. The importance of the particle orientation was suggested by the introduction of the term "average value of $\cos^2\theta$" in the equation used by Fowler and Hertel. It was decided to determine accurately the constant of the fluid flow equation in the case of glass particles which were so nearly spherical that particle orientation would be meaningless, and also to explore the effect of orientation in the case of fibers.

The laminar flow of homogeneous fluids through porous media is known to follow Darcy's Law,[4] which for linear flow has the form

$$Q=\frac{K}{\mu}\frac{\Delta P}{L}, \tag{1}$$

where Q = rate of flow of fluid in cc/sec., μ = viscosity of fluid in poises, ΔP = pressure drop across medium in dyne/cm², L = length of medium in cm, and K = permeability of medium. For the laminar flow of a gas through the medium one would have,[5]

$$Q=\frac{K}{\mu}\frac{\Delta P}{L}\left\{\frac{P_2^{1+m}-P_1^{1+m}}{(1+m)(P_2-P_1)P_1^{m}}\right\}, \tag{2}$$

$$\Delta P=P_2-P_1,$$

where m is determined by the thermodynamical character of the flow. m takes the value unity for isothermal flow and the value

$$\frac{\text{specific heat at constant volume}}{\text{specific heat at constant pressure}}$$

for adiabatic flow. Several workers[6] have attempted to express K in terms of the physical aspects of the medium. The most successful attempts have led to expressions equivalent to the following form:*

$$K=\epsilon^3 A/kS_0^2(1-\epsilon)^2; \tag{3}$$

where ϵ = porosity = free volume in medium/total volume of medium, S_0 = specific surface = cm² for medium/cm³ of solid portion, A = cross-sectional area of medium, and k = proportionality constant.

While theoretical derivations of (3) are not sufficiently rigorous to determine k, it is interesting to consider the one of Fowler and Hertel,[3] which indicates that k should be closely related to the expression

$$\frac{3}{\langle \sin^2\phi\rangle_{Av}}, \tag{4}$$

* This paper was presented on March 23, 1940, at the Charleston, South Carolina, meeting of the Southeastern Section of the American Physical Society.

[1] P. C. Carman, Trans. Inst. Chem. Eng. **15**, 150–166 (1937), **16**, 168–188 (1938); also J. Soc. Chem. Ind. **57**, 225–235 (1938), **58**, 1–7 (1939).

[2] E. J. Wiggins, W. B. Campbell and O. Maass, Can. J. Research **17**, 318 (1939).

[3] Fowler and Hertel, J. App. Phys. **11**, 496 (1940).

[4] See for instance, M. Muskat, *Flow of Homogeneous Fluids* (McGraw-Hill, 1937).

[5] Reference 4, p. 679.

[6] See Carman, reference 1 for review of field.

* Carman's notation is used.

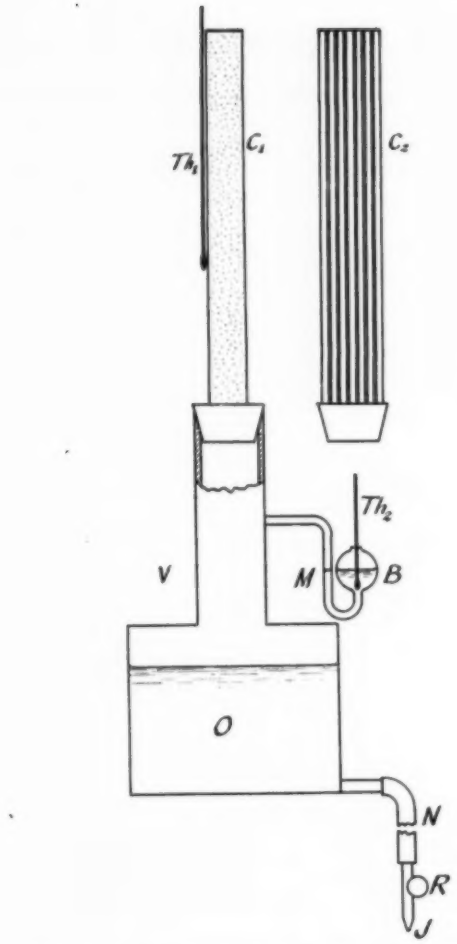

FIG. 1. Diagram of flow apparatus. Th_1, Th_2, thermometers; C_1, single copper tube; C_2, multiple copper tube assembly; V, vessel; O, light mineral oil; M, kerosene manometer; B, bulb; N, Neoprene tubing; J, jet; R, rack and pinion.

where the denominator is the mathematical expectation, or mean value of the square of the sine of the angle ϕ. This angle is taken as that between the direction of macroscopic flow and the normal to an element of surface exposed to the flow. Thus, on the basis of expression (4), k should depend upon the orientation of the particles composing the medium. In fact, if k is equal to expression (4), then for a bed of spheres it should take the value $3/\frac{2}{3}=4.5$, while for a bed of cylinders whose axes are parallel to the direction of flow it should take the value $3/1=3$. Similarly, if circular cylinders were placed perpendicular to the direction of flow, k should be $3/\frac{1}{2}=6.0$. While the theory is not rigorous, yet the experimental data to be presented here agree, within limits of experimental error, with the above predictions.

EXPERIMENTAL

For the major portion of this work the porous medium consisted of a bed of small glass particles the particles being nearly spherical in shape.

Figure 1 is a diagram of the apparatus used in the flow determinations. The glass particles were used to fill the copper tube C_1 or C_2 either of which contained at its lower end a brass screen supported by small brass ribs. The tube was then attached to the top of the vessel V containing air above mineral oil. After preliminary tests with other liquids, the light mineral oil, known as white oil, was chosen because of its relatively low vapor pressure. A jet J, movable vertically by the rack and pinion R, was attached by the Neoprene tubing N to the lower portion of bottle. The rack and pinion allowed sufficient control so that the rate of flow of oil could be kept very constant during a given run. The pressure drop across the tube of particles was then obtained in centimeters of kerosene by reading with a traveling microscope (least count 1/200 mm) the displacement of the kerosene surface in the large bulb B and multiplying by the factor 1.015. This factor was used because the ratio of the areas of the two arms of the manometer M was 0.015. From the known relation between density and temperature for the kerosene, the pressure drop was changed to dynes/cm². A stop watch was used to determine

TABLE I. *Data for tubes.*

	SINGLE TUBE	MULTIPLE TUBE
L	67.21 cm	67.25 cm
A (by water displacement 1)	11.756±.002 cm²	11.662±.006
A (by micrometer)	11.788 cm²	11.657
A (by water displacement 2)	11.786	11.679
A (weighted mean)	11.768±.005	11.664±.004
S	1.0344 cm⁻¹	4.8693 cm⁻¹

TABLE II. *Data for glass particles.*

Density, using pyknometer and water	2.4957 g/cc
Density, using pyknometer and C_6H_6	2.4951 g/cc
From eight groups totaling 13,268 glass particles.	
Mean mass per glass particle	0.00043755±0.00000175 g
Diameter of glass particle of mean mass	0.06945±0.00009 cm
From three groups, totaling 4643 glass particles,	
By projection of images, $\left(\frac{6\Sigma D^2}{\Sigma D^3}\right)\left(\frac{\Sigma D^3}{N}\right)^{\frac{1}{3}}$	5.94177±0.0018
$S_0=5.94177/0.06945=85.555\pm0.171$ cm⁻¹	

TABLE III. *Flow data for air through glass particles.*

Single Tube Mass of particles = 1202.42 g $\epsilon = 0.39077$				Multiple Tube Mass of particles = 1191.82 g $\epsilon = 0.39111$			
μ poises $\times 10^6$	ΔP dynes/cm^2	Q cc/sec.	$\frac{\Delta P}{\mu Q}\frac{\epsilon^3 A}{(1-\epsilon)^2 L}$ $\times 10^{-4}$	μ poises $\times 10^6$	P dynes/cm^2	Q cc/sec.	$\frac{\Delta P}{\mu Q}\frac{\epsilon^3 A}{(1-\epsilon)^2 L}$ $\times 10^{-4}$
185.40	442.869	1.9881	3.38217	185.01	440.622	1.7966	3.71014
185.40	442.731	1.9905	3.37706	185.10	440.278	1.7940	3.71081
185.40	442.501	1.9905	3.37530	185.10	440.605	1.7979	3.70352
185.45	442.448	1.9889	3.37671	185.10	440.924	1.7966	3.70889
185.49	442.299	1.9886	3.37535	185.10	440.498	1.7960	3.70654
185.49	442.506	1.9881	3.37776				
			Mean = 3.37739				Mean = 3.70798
	$k\left(85.555+f\frac{1.0344}{0.60923}\right)^2 = 3.37739\times 10^4$				$k\left(85.555+f\frac{4.8693}{0.60889}\right)^2 = 3.70798\times 10^4$		
	$k = 4.4956$				$f = 0.658$		
Repetition: Mass of particles = 1203.09 g $\epsilon = 0.39043$				Repetition: Mass of particles = 1189.31 g $\epsilon = 0.39240$			
184.76	477.108	2.140	3.38412	184.27	478.657	1.985	3.71461
184.71	467.173	2.100	3.37769	184.31	472.432	1.956	3.71985
184.81	454.341	2.043	3.37472	184.66	511.269	2.099	3.74427
184.86	441.961	1.977	3.39145	184.71	497.670	2.053	3.72532
184.11	458.397	2.055	3.39783	184.76	490.479	2.021	3.72878
184.26	442.294	1.990	3.38280				
184.31	434.941	1.948	3.39737				
			Mean = 3.38657				Mean = 3.72657
	$k\left(85.555+f\frac{1.0344}{0.60957}\right)^2 = 3.38657\times 10^4$				$k\left(85.555+f\frac{4.8693}{0.60760}\right)^2 = 3.72657\times 10^4$		
	$k = 4.504$				$f = 0.676$		
	Probable error of $\frac{\Delta P}{\mu Q} = \pm 0.07\%$				Probable error of $\frac{\epsilon^3 A}{(1-\epsilon)^2 L} = \pm 0.375\%$		
	Probable error of $S_0 = \pm 0.2\%$				Probable error of k in % is $\sqrt{(0.07)^2+(0.375)^2+(0.4)^2} = 0.55\%$		
	Mean $k = 4.500 \pm 0.023$				Mean $f = 0.667$		

the time for oil to fill a 500-cc volumetric flask. Q was then calculated in cc/sec.

The viscosity of air was obtained from the equation

$$\mu_\theta = \mu_{20} - 4.93\times 10^{-7}(20-\theta),$$

where $\mu_{20} = 181.92\times 10^{-6}$ poises, as given by Bearden.[7] θ = temperature in degrees C.

In order to determine and correct for errors due to the tube wall surface, a single tube C_1 and a multiple tube assembly C_2 were used. The two tubes, single and multiple, were of approximately the same length and volume, though the latter had about 4.67 times the wall surface of the former. By the use of both tubes a correction factor f for the wall surface was obtained. This factor was used as follows:

$$S_0^* = S_0 + fS/(1-\epsilon) \qquad (5)$$

so that when weighted by f the tube-wall surface would be directly additive to the glass-bead surface. S = surface of tube wall per cc of tube volume. The value of ΔP used was so small that the bracketed factor of (2) was negligible (~ 1.003). Equations (1), (3) and (5) were combined to give the form,

$$kS_0^{*2} = \frac{\Delta P}{\mu Q}\frac{\epsilon^3 A}{(1-\epsilon)^2 L}. \qquad (6)$$

The glass particles used were obtained from Parker Brothers, Ozone Park, New York. In order to select particles which were very nearly spherical, they were slowly poured on a slightly inclined glass plane, and only those which traversed the full length of the plane were retained. An ample supply of particles to fill the tubes was obtained. For measuring S_0, random samples of this supply were collected through a 0.6-cm hole in a 45×60-cm aluminum plate over which the complete supply of round

[7] J. A. Bearden, Phys. Rev. **56**, 1023–1030 (1939).

TABLE IV. *Data for flow of air through glass wool. Area of tube = 3.125 cm²; density of glass = 2.416 g/cc; mean fiber diameter = 7.80×10⁻⁴ cm; standard deviation for fiber diameter = 0.90×10⁻⁴ cm.*

Mass of Glass G	L CM	ϵ	S_0 CM	ΔP DYNES/CM²	μ POISES	Q CC/SEC.	k
			For fibers perpendicular to flow				
3.132	2.155	0.8075	5.25×10^{3}	892	182.6×10^{-6}	0.594	6.15
				933	182.8×10^{-6}	0.610	6.26
				945	183.2×10^{-6}	0.618	6.23
							Mean = 6.21
4.249	2.85	0.8025	5.02×10^{3}	1360	186.01×10^{-6}	0.716	5.87
				1351	186.01×10^{-6}	0.707	5.93
				1321	186.01×10^{-6}	0.703	5.82
							Mean = 5.87
							Mean for fibers perpendicular to flow 6.04
			For fibers parallel to flow				
10.395	10.28	0.8661	5.27×10^{3}	964	185.5×10^{-6}	0.703	2.94
				1024	185.9×10^{-6}	0.726	3.02
				986	186.0×10^{-6}	0.721	2.92
							Mean = 2.96
7.163	5.21	0.8179	4.92×10^{-3}	1026	185.57×10^{-6}	0.705	3.21
				1040	185.67×10^{-6}	0.720	3.18
				1037	185.81×10^{-6}	0.722	3.17
							Mean = 3.19
							Mean for fibers parallel to flow 3.07

particles was allowed to pass. Sub-samples of these random samples were then collected in like manner until the sub-samples each contained only one or two thousand particles. These particles then were counted and weighed. Mass determinations were corrected for air-buoyancy. Thus, the density of the glass particles being known, the diameter of the particle of mean weight was found. As this is the root mean cube, $(\Sigma D^3/N)^{\frac{1}{3}}$, of the particle diameters, it does not give S_0 directly, since

$$S_0=\frac{\Sigma\pi D^2}{\Sigma\pi D^3/6}=\frac{6\Sigma D^2}{\Sigma D^3}. \tag{7}$$

Hence, images of 4643 particles were projected by a projection microscope and their diameters measured. From these measurements the factor $(6\Sigma D^2/\Sigma D^3)(\Sigma D^3/N)^{\frac{1}{3}}$ was obtained. It was then divided by the root mean cube diameter as found by weight, to give the value of S_0. This process eliminated the value of the microscope magnification from the calculations.

In addition to the careful measurement on flow through the bed of particles, relatively rough measurements were made on the flow of air through beds of glass wool. The cases of fibers aligned parallel to the tube axis and of fibers aligned perpendicular to the tube axis were considered. A smaller tube was used with the glass wool, and as the fibers were rather fine, no correction was made for tube-wall effects. The glass wool used was Corning glass wool No. 008. As it was impossible to mix and sample the glass fibers properly, values of S_0 were taken for each mass used. This consisted of measuring with microscope and camera lucida the diameters of 100 fibers taken from each mass. Since the fibers were very nearly circular in cross section, $S_0=4\Sigma d/\Sigma d^2$. To array the fibers perpendicular to the direction of flow, sheets of the fiber mass were cut in small sections and stacked into the cylinder. A piston then compressed these sheets to the proper degree of porosity. For the alignment parallel to tube axis the fibers were parallelized by taking sheets of the fibers and elongating greatly in one direction. A compact bundle of such fibers was then urged into the cylinder. The desired orientation, of course, was not completely realized in either case. Flow measurements were then made in a manner similar to that for the particles.

RESULTS

Table I gives the constants of the apparatus used for the bed of particles. Table II gives the data for the particles. Table III gives data obtained for air flow through the bed of particles. These data, along with preliminary data, were

taken over a period of several months, hence it is believed that systematic errors were small. Probable errors indicated are calculated from random variations of the quantities involved and are the fiducial limits at the 50 percent level as given by Student's t distribution for small samples. By using Eq. (6) on first the single and then the multiple tube and solving simultaneously, it was possible to determine both k and f. It is to be noted that the wall-correction factor f, found to be 0.667 in this case, no doubt depends, among other things, upon the type of packing against the wall. Hence, this factor would not be applicable to all conditions.

Table IV gives data for flow of air through glass wool. It is readily observed that although there is some variation in these determinations, they give definitely different values of k for the different orientations.

Summary

It is shown that in expressing the permeability of a porous medium as a function having the form $K=\epsilon^3 A/kS_0^2(1-\epsilon)^2$, the value k must take different values for different orientations of the exposed surfaces. In particular where the surfaces are oriented at random, $k=4.50\pm0.02$, while if they are parallel to the direction of flow, $k\sim6.0$, and if the porous medium is composed of circular cylinders perpendicular to the flow, then $k\sim3.0$. It is recognized that the value of 4.50 differs from Carman's value of 5.0 by much more than the error of the experiment. One also notes that the work of Fowler and Hertel on textile fibers which were largely perpendicular to the direction of flow gives a value of $k=5.55$ in our notation, which is consistent with $k\sim6$ for complete perpendicularity. It should be remarked that these values of k apply to fairly compact media. In some unpublished work on textile fibers it has been found that for higher porosities ($\epsilon>0.9$) the conditions of flow become somewhat different. The study of flow through plugs of high porosity is being continued, and the authors plan to present the results of this study in a later paper.

Spark Gaps with Short Time Lag

Joseph Slepian and W. E. Berkey
Westinghouse Research Laboratories, East Pittsburgh, Pennsylvania

(Received August 22, 1940)

Short spark gaps (order of one mm) in air at atmospheric pressure, unless specially radiated, show large spark lag when tested at little above the sparking potential. In engineering literature this property is measured by the impulse ratio, i.e., the ratio of the voltage at which breakdown occurs under a voltage surge rising at a specified rate (about 50 kilovolts per microsecond), to the voltage at which breakdown occurs with slowly increasing impressed 60-cycle voltage. The spark lag shows statistical variations, and its mean has been shown to be nearly equal to the mean time for emission of an electron from the cathode, prior to the spark. The electron current from the cathode prior to the spark is greatly increased by the presence of a pointed projection on the cathode, so that the mean spark lag at a given voltage is greatly reduced. However, if a single pointed projection is used, of sufficient size to reduce the spark lag at a given voltage, it also reduces the 60-cycle sparking potential, so that the impulse ratio, which is the quantity important in engineering applications, is not reduced. By using a very large number of extremely small pointed projections on the cathode, the spark lag can be reduced without appreciable lowering of the 60-cycle sparking potentials. Thus impulse ratios little greater than unity can be obtained. Small particles of carborundum, rutile, alumina and porcelain, of various sizes were attached to the cathodes of spark gaps, and the impulse ratios tested. Minimum impulse ratios were obtained when the particle linear dimensions were between 2×10^{-3} and 15×10^{-3} cm.

Introduction

THE breakdown voltage of short enclosed spark gaps is known to be high and variable, when tested on rapidly rising surge voltage waves. A time delay in breakdown of even one microsecond on such a wave would allow thousands of volts to appear across the terminals of such a gap before breakdown occurs. It is therefore of vital importance that spark gaps used in protective devices shall have the shortest possible time delay of breakdown.

The statistical distribution of spark lags has

been found experimentally under a given test condition to be[1]

$$n = n_0 \epsilon^{-t/T},$$

where n_0 is the total number of tests, n the number with spark lag greater than t, and T is the average spark lag.

The tests used to determine this time lag equation were made with a rectangular test wave with crest voltages only a few percent higher than the static breakdown, the time lag being the time between the application of potential until the spark occurrence. In the tests described here the time lag is determined by measurement of the breakdown voltage on a known surge front rise. The time lag is then the time the rising surge exceeds the 60-cycle crest breakdown. The test surge used rose rapidly to a high overvoltage so that extremely short lags were obtained.

The formation of a discharge with short lag between electrodes of a spark gap is dependent on starting electrons being present at or near the cathode surface at the right time and place to initiate the discharge. The normal air ionizing processes do not usually supply enough electrons to provide a satisfactory short average time lag of breakdown in spark gaps with spacing in the order of 1 to 2 millimeters such as those used in lightning arrester applications. It is customary to encase such gaps in porcelain housings and this still further reduces the ionizing activity between the electrodes. Ultraviolet,[2] radioactive,[2] and other,[3,4] radiations have been used to shorten the breakdown lag in spark gaps.

TABLE I. *Effect on the breakdown of single porcelain chip on cathode surface.*

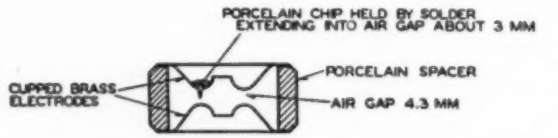

GAP	60-CYCLE BREAKDOWNS	IMPULSE BREAKDOWNS*	AV. IMPULSE RATIO
No Chip	(1) 10.8 kv r.m.s. (2) 11.1 (3) 11.1 (4) 11.2 Av. 11.05 Av. 15.65 kv crest	(1) 28.0 kv (2) 26.5 (3) 20.6 (4) 23.9 (5) 19.75 (6) 20.4 (7) 20.0 (8) 21.7 Av. 22.6 kv	$\frac{22.6}{15.65} = 1.45$
Single Porcelain Chip on	(1) 7.9 kv r.m.s. (2) 8.6 (3) 6.5 (4) 6.2 (5) 6.35 (6) 6.3 (7) 6.3 (8) 6.9 Av. 6.88 kv r.m.s. Av. 9.72 kv crest	(1) 15.0 kv (2) 15.85 (3) 15.2 (4) 14.55 (5) 15.2 (6) 14.55 (7) 15.0 Av. 15.05 kv	$\frac{15.05}{9.72} = 1.55$

* Surge rising to 55 kv at Av. rate of 50 kv/μ sec.

[1] A. Tilles, Phys. Rev. **46**, 1015 (1934).

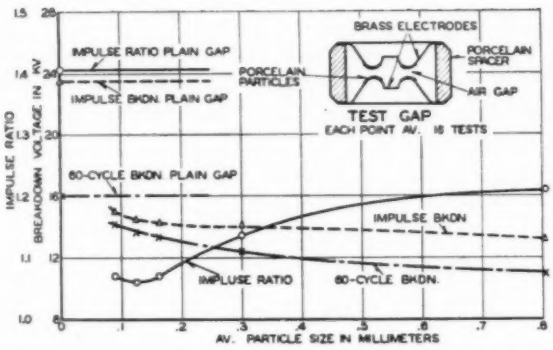

FIG. 1. Breakdown characteristics of gaps with sized porcelain particles on electrodes.

The time delay of a given spark gap operating in air at atmospheric pressure has been shown by Strigel[5] to correspond very closely to the time for emission of one electron from the cathode. Thus if an average time lag of 10^{-8} second is desired then an initial current of 10^8 electrons per second is necessary. The dark or initial current preceding breakdown which determines the spark lag is usually due to photoelectric activity of some radiation.[3] At very high overvoltages high field electron emission may become important. The method of shortening the spark lag described in this paper is to place projections on the surface of the cathode so that field distortions will increase the iniatory electron current from the cathode and provide a minimum spark lag.

In comparing the operation of spark gaps it is convenient to use "impulse ratio," which is defined as the ratio of impulse breakdown voltage obtained on a specified test wave front

[2] L. B. Loeb, Rev. Mod. Phys. **8**, 284 (1936).
[3] W. E. Berkey, Elec. Eng. p. 429–33, August, 1940.
[4] H. Raether, Zeits. f. Physik **110**, 611 (1938).
[5] R. Strigel, Wiss. Veröff a.d. Siemens-Konzern **11**, No. 2, 52–74 (1932).

to the 60-cycle crest breakdown voltage. In the results to be described the impulse test wave rose to 55 kv at the average rate of 50 kv per microsecond. The average slope is determined by the slope of a straight line between the 10 percent and 90 percent points on the wave front. Breakdown voltages varied from $\frac{1}{3}$ to $\frac{1}{2}$ the crest surge voltage. The time lag of a typical gap tested under these conditions with impulse ratio found to be 1.2 and with a 60-cycle crest breakdown of 10 kv, is then approximately 4×10^{-8} second.

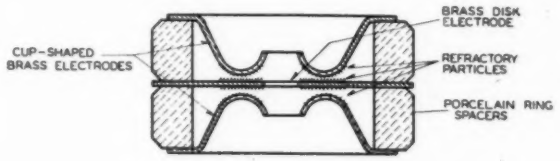

FIG. 2. Double test gap structure.

RESULTS

When a single refractory particle of relatively large size is placed on the cathode of a gap and tested, it is found that the 60-cycle breakdown voltage is lowered, presumably because of space charge and field distortion arising from the electron current from the particle with the accompanying ionization. This is indicated in the data of Table I, in which it was found that a single large porcelain chip reduced both the 60-cycle and impulse sparking voltage. On impulse tests however the field distortion due to space charges apparently did not have time to appear and the observed reduction is to be attributed to a plentiful supply of electrons which reduces the spark lag so that the impulse breakdown with the porcelain chip is practically equal to the 60-cycle spark overvoltage without the chip. It is observed that the impulse flashover voltages are more consistent with the chip than without it. These results suggested that it might be possible to minimize the decrease in 60-cycle breakdown while retaining the improved impulse flashover properties, by decreasing the size of the projection and providing many small ion points on the cathode.

Particles of wet-process porcelain were made by crushing and screening between two definite screen sizes. The average diameter of the particle is taken as the average between the two screen openings. The curves in Fig. 1 show the average electrical breakdown values obtained as a function of the particle size. The test procedure was to make eight impulse breakdown records on the cathode-ray oscillograph immediately followed by eight 60-cycle breakdowns on a 30-kv maximum testing transformer. Averages were used to determine the impulse ratio. Two gaps were tested and results averaged for each point.

The particles were bonded to the electrodes by first painting a thin coating of shellac or water-glass on them in the sparking areas. When the bond was partially dry each electrode was pressed on a pile of refractory grains and poorly held grains dislodged by jarring. In this way a uniform one layer covering was obtained. The electrodes were then heat treated to harden up the bond.

A double gap assembly is sketched in Fig. 2. All following tests were made on this type of gap. The refractory particles are shown bonded to the electrode surfaces. The disk electrode was coated on both sides.

Particles of silicon carbide on the electrodes of double gaps gave the results found in Fig. 3. Silicon carbide differs from porcelain mainly in conductivity. The electrical resistivity of silicon carbide is in the order of one ohm-cm. The breakdown voltages decreased much more rapidly with increase in particle size than with porcelain. Plain gaps with untreated electrodes were tested at the same time and are shown as reference lines in all the curves.

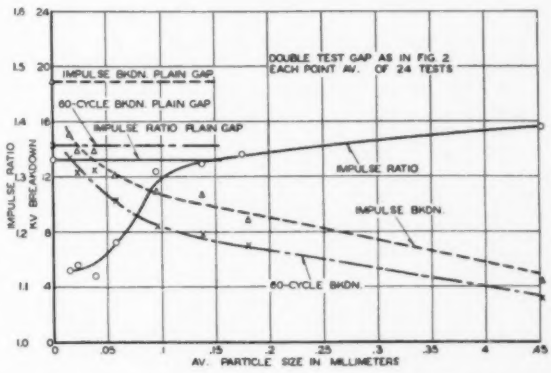
DOUBLE TEST GAP AS IN FIG. 2 EACH POINT AV. OF 24 TESTS
IMPULSE BKDN. PLAIN GAP
60-CYCLE BKDN. PLAIN GAP
IMPULSE RATIO PLAIN GAP
IMPULSE RATIO
IMPULSE BKDN.
60-CYCLE BKDN.
IMPULSE RATIO
KV BREAKDOWN
AV. PARTICLE SIZE IN MILLIMETERS

FIG. 3. Breakdown characteristics of gaps with sized silicon particles on electrodes.

Rutile particles with dielectric constant of 80

were tested next as electrode coatings. The impulse ratio fell off quite rapidly with reducing particle size as shown in Fig. 4.

The curves in Fig. 5 show the results obtained with alumina particles. What appears to be a minimum on the impulse ratio curve was found at particle size about 0.07 mm. Inspection of the grains with a microscope showed that the alumina particles were more rounded and had less sharp cleavage edges than any of the other particles. The test data with alumina were quite erratic.

Conclusion

The time lag of a spark gap can be materially shortened by placing small, sharp-edged, refractory particles on the cathode surface. Particles of porcelain, silicon carbide, rutile and alumina were tested in practical spark gap structures. Low impulse ratios were obtained for each material tested but at different sized grains.

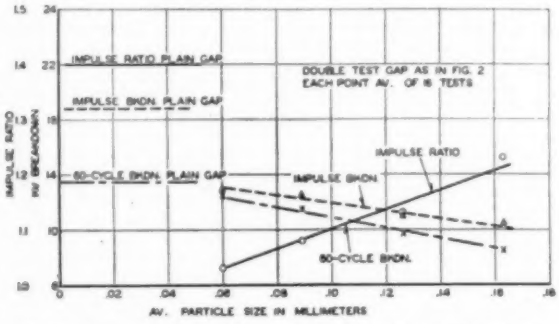
IMPULSE RATIO PLAIN GAP
IMPULSE BKDN. PLAIN GAP
60-CYCLE BKDN. PLAIN GAP
DOUBLE TEST GAP AS IN FIG. 2
EACH POINT AV. OF 18 TESTS
IMPULSE RATIO
IMPULSE BKDN.
60-CYCLE BKDN.
IMPULSE RATIO / 60-CYCLE BREAKDOWN
AV. PARTICLE SIZE IN MILLIMETERS

Fig. 4. Breakdown characteristics with sized rutile particles on electrodes.

If a single large chip is placed on the cathode, then the 60-cycle breakdown is lowered. When many smaller grains are placed on the electrodes in the high field areas, the 60-cycle breakdown voltage is lowered only moderately, and the impulse breakdown takes place with short lag.

Under the test conditions it seems probable that one electron from the cathode initates the discharge. The high impulse ratios obtained with plain gaps are due to an insufficiency of initiatory electrons from the cathode. When many small sharp points are placed on the cathode a large total number of initiatory electrons are supplied but spread over a large area. This insures a short lag on impulse breakdown with only small decrease in 60-cycle breakdown.

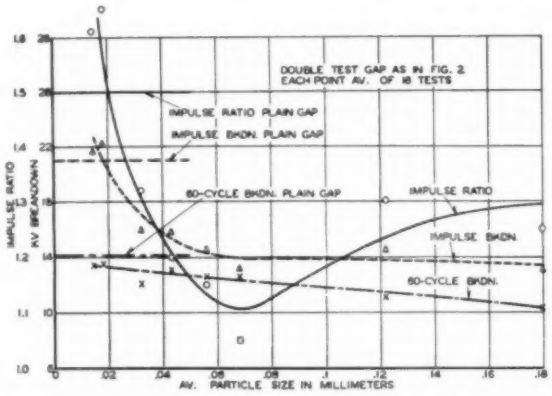
DOUBLE TEST GAP AS IN FIG. 2
EACH POINT AV. OF 18 TESTS
IMPULSE RATIO PLAIN GAP
IMPULSE BKDN. PLAIN GAP
60-CYCLE BKDN. PLAIN GAP
IMPULSE RATIO
IMPULSE BKDN.
60-CYCLE BKDN.
IMPULSE RATIO / 60-CYCLE BREAKDOWN
AV. PARTICLE SIZE IN MILLIMETERS

Fig. 5. Breakdown characteristics of gaps with sized alumina particles on electrodes.

IT is true that science often has been perverted to the work of death and destruction. It is also true that art has often been made the servant of propaganda, and that literature, when its expression is controlled by a dictatorship, may degrade rather than ennoble the human mind. But that does not argue for loss of faith in science, art or literature.—David Sarnoff in "Science and Security"

The Thermoplastic Behavior of Linear and Three-Dimensional Polymers

S. S. KISTLER
Norton Company Research Laboratories, Worcester, Massachusetts
(Received May 31, 1940)

IN the literature on synthetic resins, it is common to find them divided roughly into fusible and infusible products. A brief examination of the resins referred to reveals that this differentiation is generally very loosely applied and that often some substances—e.g., polyvinyl acetate—are classed as fusible, whereas there is no temperature below the decomposition point at which it will become fluid. To the resin chemist, however, the distinction has had meaning and has referred qualitatively to a large difference in thermoplasticity of resins.

In general, the linear polymers have been classed as fusible or thermoplastic and those that have been referred to as infusible have, in general, been three-dimensional or cross linked. In view of the large difference in type of binding between the molecules in these two classes of resins it is very logical to expect such a tremendous difference as is indicated by the terms fusible and infusible. It is even not at all unlikely that the logical expectation of difference due to structure has been responsible for the widespread use of the terms. However, in our attempt to become more specific and detailed in our thinking it is desirable to reconsider the application of these terms and to try to picture the mechanism which leads to large physical differences in high polymers.

STRENGTH OF FORCES BETWEEN MOLECULES

An examination of the chemical composition of a large number of polymers demonstrates strikingly the close relationship between molecular structure and physical properties. Those compounds that are most thermoplastic and the most readily deformed are, in general, not only the linear type but in addition are composed of chains with relatively nonpolar groups scattered along their lengths. Such substances as polyisobutylene, polybutadiene, rubber, polyvinyl acetate, polystyrene and polyvinyl chloride are all highly thermoplastic but show increasing softening temperatures roughly in the order listed. Undoubtedly this difference in softening temperature can be associated with the difference in composition of the linear molecules.

Table I, taken from Meyer and Mark,[1] lists radicals such as may occur along polymer chains and gives the relative strengths of attraction between these groups. A glance at this table helps one to understand the fact that if long molecules have scattered at intervals throughout their lengths such different radicals as CH_3, Cl or COOH, greatly different forces exist between the molecules themselves and, therefore, there are large differences in the ease of deformation of the masses, that is, the ease with which one molecule can slide over another. It is undoubtedly due to such differences in the secondary forces between these substituent groups that the series of polymers referred to above owes the differences in physical properties.

For example, rubber is very easily deformed, relaxes readily under persistent strain, and softens rapidly with rise in temperature. On the other hand, polyvinyl chloride is stiff at room temperature and will rupture before any extensive amount of deformation occurs. The temperature has to be raised to well above 100°C before it is readily deformable. From the table, it will be observed that whereas for a hydrocarbon group such as CH_3, the side group in rubber, the cohesive strength is only 1780, for Cl it amounts to 3400. It is, therefore, easy to see that with such high forces between the chlorine atoms, long chains of vinyl chloride should so

TABLE I.

GROUP	COHESION CAL./MOL.	GROUP	COHESION CAL./MOL.
$-CH_3$	1780	$-CHO$	4700
$=CH_2$	1780	$-COOH$	8970
$-CH_2-$	990	$-COOCH_3$	5600
$=CH-$	990	$-NH_2$	3530
$-O-$	1630	$-Cl$	3400
$-OH$	7250	$-CONH_2$	13200
$=CO$	4270	$-CONH-$	10600

[1] Meyer and Mark, *Der Aufbau der Hochpolymeren Organischen Naturstoffe* (Leipzig, 1930), p. 27.

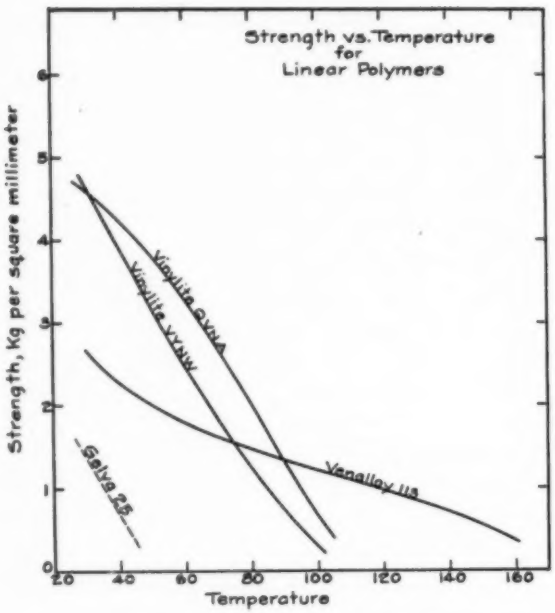

FIG. 1. The variation of strength with temperature of linear polymers.

attract each other that relatively large forces will be necessary to displace them, compared with the forces required to displace rubber or polybutadiene molecules.

Another factor is also quite important which does not appear in Table I, namely the volume occupied by the side groups. This will be noted particularly in comparing polyvinyl acetate with polyvinyl chloride. Although the cohesive strength of acetate groups is actually larger than chlorine atoms, the bulk of the acetate radical is so large compared to the chlorine atom that it is difficult for vinyl acetate chains to fit so closely to each other and, therefore, the mechanical force required to move one chain with respect to the next is greatly reduced. This reduction in cohesive forces between the vinyl acetate molecules is observed in thermoplasticity of the polymer. At temperatures above 40°C polyvinyl acetate is readily stretched to seven or eight times its original length, and if it is not held too long it will recover practically completely. It therefore resembles rubber more closely than it does polyvinyl chloride. On the other hand, if the forces of attraction between the polyvinyl chloride molecules are reduced by the incorporation of a plasticizer, it also becomes rubbery in character.

When one compares the strength of the secondary bonds between even the most polar groups with the strength of primary carbon bonds, it is obvious that the former are extremely weak and that a few primary bonds connecting chains would be much more effective in determining the physical properties than many secondary bonds. This type of reasoning is undoubtedly responsible for much of the loose use of the terms fusible and infusible, and for the general impression that high strength in resins is associated with cross linking.

It was one of the objects of this present investigation to examine the strengths of linear and three-dimensional polymers and to attempt to correlate the results obtained with chemical structure. Figure 1 shows the variation in tensile strength with temperature for a series of linear polymers differing from each other in the character of side groups along the main chains. The actual values recorded are so dependent upon measuring conditions that they should not be taken as of absolute significance but only for comparative results. These specimens were dumbbell-shaped and were broken in an Olsen machine equipped with a hot chamber that could be maintained at the specified temperature ±0.5°C. The standard procedure was to stress the sample at the rate of 6900 lb./square inch per minute except at temperatures of 100° and above when one-tenth of this rate was used.

The very large influence of the substituent groups is at once apparent by comparing, for example, polyvinyl acetate (Gelva) with polyvinyl chloride (Vinylite QYNA) or vinylidine dichloride (Venalloy). The last compound in particular shows a retention of strength to very much higher temperatures than the others and even at 160°C still retains appreciable strength. Vinylite VYNW is a copolymer of 95 percent vinyl chloride with 5 percent vinyl acetate.

Figure 2 shows the same type of measurements on typical three-dimensional polymers. Here the striking difference is the tendency for the strength to rise with rising temperature to some maximum value and then to drop off rapidly. This rise in strength with increase in temperature is quite contrary to what would be expected, but has a very simple explanation. The three-dimensional polymers in general are very brittle at low

temperatures, and it is extremely difficult to distribute stresses uniformly over the cross section of the test piece, so that at the lower temperatures unequal stress distribution leads to rupture of a portion of the cross section before the remainder has been stressed to its ultimate tensile strength. As soon as a crack starts, the forces are more unevenly distributed than before and the piece immediately breaks. At the higher temperatures the extension at rupture is somewhat greater and it becomes more possible for the stresses to be equalized. This increase in uniformity of stress distribution produces a continual increase in the apparent tensile strength, until the decrease in strength due to rise in temperature becomes of equal importance, when a maximum will be reached. At subsequent higher temperatures the strength will drop off very rapidly because of the thermal effect.

The striking similarity between Figs. 1 and 2 at first is puzzling, because of the fact that in Fig. 2 the primary forces attaching molecules to each other must be of an entirely different order of magnitude than the secondary forces in Fig. 1. It should be possible for molecules in Fig. 1 to slide over each other, and for rupturing to occur eventually by plastic deformation and necking down of the specimen. That the temperature coefficient for strength is approximately as high for three-dimensional polymers as for the linear polymers would indicate that the primary valency bonds are of relatively small importance in determining this coefficient, and, therefore, that the strength recorded is principally that due to secondary forces. In fact, had the strengths for the linear polymers been correctly calculated to the actual cross section at rupture, there would have been even less distinction between the two types. What the figures do not show is the large extension at rupture for most of the linear, and the very small extension for the three-dimensionsl polymers, which is probably the most striking difference between these two classes of resins.

If the bonds being ruptured were principally primary, one would expect the softening temperature of three-dimensional plastics certainly to be as high as glass and possibly even as high as fused quartz. That the softening temperature may not be any higher than for linear polymers in which there are strong secondary forces between the substituent groups indicates that the mechanism of rupture must be such as to bring great stresses to bear onto a few of the primary bonds at a time, thus preventing any large number of them from distributing the stresses between them and taking the principal part of the applied load.

That this can be so is quite clear from observations of the physical behavior of the test specimen during application of stress. The linear polymers in general stretch noticeably before rupture and some of them stretch to many times their original length. It is thus possible for an orientation of the molecules to occur and for stresses to be distributed among a very large number of molecules. On the other hand, the three-dimensional specimens in general stretch very little, particularly at the lower temperatures. Undoubtedly the molecules are much folded and bent and when the tensile stress is applied the secondary forces yield, permitting the stress to be carried largely by such primary bonds as may be attached to fairly large groups with little opportunity for yielding. When these primary bonds are ruptured, the only forces remaining in these regions to prevent complete rupture are the secondary. Molecules, or sections of molecules, therefore, can slide

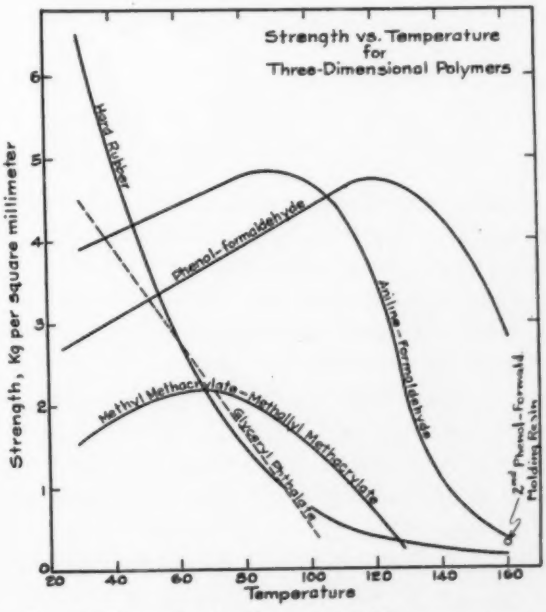

FIG. 2. The variation of strength with temperature of three-dimensional polymers.

over each other locally until other primary bonds prevent movement and are ruptured in succession.

The picture is somewhat as though one tied together here and there loops of a tangled mass of thread, then soaked the mass in heavy tar and applied tension to the ends. Here and there within the mass most of the tension would be localized on one or two threads where they were tied together. These would rupture quickly and the force required to stretch the mass would be largely that required to slide the threads over each other in the viscous tar. The forces required to produce viscous flow in the tar represent the secondary forces between chains while the knots between the loops represent the primary bonds. It is easy to imagine that such a tangle of thread would show little more tensile strength due to the knots than it would have shown if these knots had not been tied.

Even in the case of the very highly cured phenol-formaldehyde resin it is to be noted that at 160°, the maximum temperature to which the heating device would go, the temperature coefficient is as high as for some of the linear resins. Also there is a point on the graph at 160° representing another well-cured phenol-formaldehyde resin that is probably superior in strength and heat resistance to most of the molded articles on the market, and yet it showed lower strength at this temperature than polyvinylidine dichloride.

The Process of Flow in Plastics Under Stress

Henry Eyring[2] has called our attention to the possibility of obtaining activation energies for the process of flow in viscous materials. By treating viscous flow as an activated process it is possible to arrive at an equation relating rate of flow to force and activation energy. It therefore seems desirable to survey the plastic polymers and see if the calculated activation energies of flow and the "viscous volumes" have important correlations with other physical properties.

The detailed logic upon which the derivation of the conclusions depends is given by Eyring and others.[3] We shall give here a brief derivation of the equation for viscous flow, in view of the fact that former derivations published have stressed approximations rather than the accurate formulation, and strangely enough these approximations have been very little easier to use than the accurate equation, and have led to some errors. In general, probably, the errors of approximation are not large but it is conceivable that at times they may reach considerable magnitude, and the slightly greater ease of manipulation of the approximation is not worth the loss in accuracy.

Following Eyring, assume that atomic groups within the plastic are so bound together that they move as units. These groups may or may not be identified with molecular units. In a plastic composed of long chains it is likely that any one group is made up of portions of several molecules that happen to be closely associated or intertwined. Each group rests in a potential low and is surrounded by energy barriers, so that only occasionally does it possess enough energy to move over a barrier to a neighboring low. When there are no unbalanced external forces on the plastic, the frequency of such jumps can be represented by k' in the equation

$$k' = Ke^{-E/kT}, \tag{1}$$

where K is a constant at constant temperature, E is the activation energy required for the average jump, k is Boltzmann's constant and T is the absolute temperature.

If, now, a shearing stress is applied to the plastic, all jumps in the direction of the stress will be aided and those in the reverse direction retarded by it. If the atomic group has a projected area in the plane of shear, a, and the distance moved on the average at each jump is λ, the shearing stress being f dynes per square centimeter, the energy contribution of the stress will be $a\lambda f/2$. The factor $\frac{1}{2}$ is introduced since the group will only have to move approximately $\lambda/2$ in order to surmount the barrier.

The number of jumps forward per second will

[2] Henry Eyring, J. Chem. Phys. **4**, 283 (1936).

[3] R. H. Ewell and H. Eyring, J. Chem. Phys. **5**, 726 (1937); H. Eyring and J. O. Hirschfelder, J. Phys. Chem. **41**, 249 (1937); R. H. Ewell, J. App. Phys. **9**, 252 (1938); F. Eirich and R. Simha, J. Chem. Phys. **7**, 116 (1939); D. Frisch and H. Eyring, J. App. Phys. **11**, 75 (1940); Also see H. R. Lillie, J. Am. Ceramic Soc. **16**, 619 (1933).

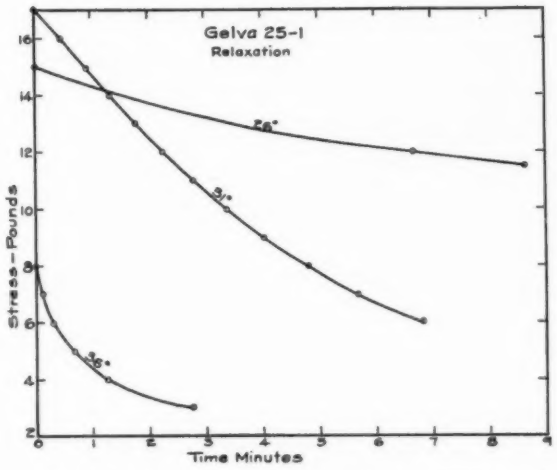

FIG. 3. The relaxation of polyvinyl acetate at three dimensions.

now be

$$k_f = Ke^{-(E-a\lambda f/2)/kT}, \tag{2}$$

and the jumps against the stress

$$k_b = Ke^{-(E+a\lambda f/2)/kT}. \tag{3}$$

Since it is the rate of progression due to the shearing stress that we are interested in, we subtract (3) from (2) and obtain

$$k_f - k_b = Ke^{-\frac{E}{kT}}(e^{a\lambda f/2kT} - e^{-a\lambda f/2kT}), \tag{4}$$

which can be put in the form

$$k_f - k_b = 2k' \sinh a\lambda f/2kT.$$

The velocity of an atomic group under shearing stress will then be

$$V = 2k'\lambda \sinh a\lambda f/2kT.$$

Now the viscosity is defined as

$$\eta = f\lambda_1/V,$$

where λ_1 is the distance between moving planes in a direction normal to the plane of shear. Thus

$$\eta = \frac{f\lambda_1}{2k'\lambda \sinh a\lambda f/2kT} = \frac{\Delta f}{\sinh Bf/T}. \tag{5}$$

It will be noted that the product $a\lambda$ has the dimensions of a volume. It is the product of the projected area of the atomic group in the plane of shear and the distance the group moves in the direction of shear. Therefore, it should be emphasized that it is not the volume of the moving atomic group. It has no other significance than the definition gives it, but since the area must have a relationship to the volume of the moving group, this volume, $a\lambda$, which we shall call the "viscous volume" also has some relationship to the volume of the moving group so that in general it is to be expected that when the "viscous volume" is large the volume of the moving group will also be large. This may not necessarily always be the case, since the distance moved for one group may be quite different from that for another. It would be desirable to calculate the actual volume of the moving group itself but since this is impossible at the moment we shall have to be content with a calculation of the "viscous volume."

It will be seen from Eq. (5) that the viscosity of a plastic should not be a linear function of the applied force except at such small shearing stress that there is a negligible contribution to the energy of the atomic group as it surmounts a barrier. In other words, plastics in general should exhibit non-Newtonian flow at stresses of the order of magnitude that are usually used in stretching or rupturing specimens, e.g., 10^6 dynes per square centimeter or greater. As an illustration, Gelva 25 (polyvinyl acetate) at an elongation of 300 percent shows a change of viscosity from 1.7×10^{10} to 4×10^9 poises with a change of shearing stress from 2.4×10^7 to 2.5×10^7 dynes per square centimeter, a change of only 4 percent. Similarly, the viscosity of dried rubber latex at an elongation of 290 percent changes from 2.2×10^{10} to 2.5×10^9 poises with a change in shearing stress from 7.3 to 8.2×10^6, 12 percent.

VISCOSITIES FROM RELAXATION CURVES

Using the test equipment that had been used for tensile strength measurements it was most convenient to measure the viscosity by rate of relaxation of stressed specimens at a given temperature. Figure 3 shows the large effect of temperature upon the rate of relaxation of vinyl acetate. From the slopes of these curves it is comparatively easy to calculate the viscosities using the equation:

$$\eta = Fl/2AS,$$

where F is the stress on the specimen, l its

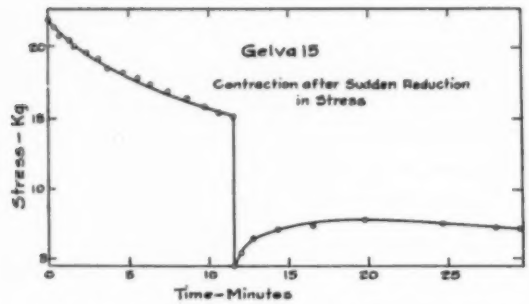

FIG. 4. The relaxation of polyvinyl acetate showing contraction after sudden reduction of stress.

length, A its cross-sectional area, and S is the velocity of separation of its ends. By determining the viscosities under two different loads at the same temperature, and at one other temperature, it is not difficult to calculate both the heat of activation and the "viscous volume" for a plastic. Table II shows the results so obtained for several vinyl acetates and at different percentages of elongation. The results are rather erratic and it was eventually decided that measurement of these quantities by calculation from the relaxation curves was not reliable due to elastico-viscous effects, the very large effect of differences in molecular orientation when successive measurements are made on the same sample, and the influence of the history of the sample.

Figure 4 shows a relaxation curve for polyvinyl acetate. The initial portion shows relaxation from a fairly high stress for a period of twelve minutes at the end of which time the stress was suddenly dropped from 33 lb. (15 kg) to 10 lb. (4.5 kg) whereupon the relaxation curve was continued. It will be noted that instead of relaxing there was a steady increase of stress for considerable time after the rapid drop, which shows that elastic recovery is occurring against high internal viscosity. It is only after a comparatively long time has elapsed that the normal shape of the relaxation curve is resumed.

When one stretches a specimen of polyvinyl acetate, orientation of the molecules occurs, with unraveling of the many entanglements that undoubtedly exist in the completely relaxed molecules. However, the internal friction is so high that the elastic forces tending to restore the original shape are largely masked, and only as time elapses is it possible for the specimen to retract. If rapid retraction is allowed to occur for a brief period and the specimen is then prevented from retracting further, the force required to prevent further contraction rises gradually due to relaxation of the viscous resistance in the specimen, and if it were not for slow slippage of the molecules over each other the elastic force would approach some value asymptotically. Also, there are undoubtedly occurring internal equalizations of stresses that had been produced by rapid distortion of the piece. In local sections the molecular configurations may be such as to permit deformation more readily than in some other sections so that comparatively large elements of volume may be moved with respect to each other, the distortion of structure being relatively large between them while within each mass the distortion may be comparatively small. As the new external form is maintained for a period of time the more highly deformed portions may contract at the expense of the sections that showed higher viscous resistance, and such changes may occur over considerable periods of time.

TABLE II.

POLYMER	MEASURING CONDITIONS	PERCENT STRETCH	TEMP.	λa, A^3	E, CAL.	REMARKS
1. Gelva 15–1	Relaxation	104–121	28.5	21,000	—	
2. Gelva 15–1	Relaxation	393–406	28.5	5,900	—	After a period at constant load.
3. Gelva 15–1	Relaxation	637–640	28.5	17,000	—	
4. Gelva 15–1	Relaxation	421–425	28.5, 37.5	—	69,000	Neglecting λa
5. Gelva 15–1	Relaxation	421–425	28.5, 37.5	—	73,000	Assuming $\lambda a = 5900$
6. Gelva 15–1	Relaxation	421–425	28.5, 37.5	—	89,000	Assuming $\lambda a = 17{,}000$
7. Gelva 25	Relaxation	*ca.* 105	26, 31	14,800	71,000	
8. Gelva 45	Relaxation	780–786	44	4,900	—	

Viscosities from Stretch at Constant Load

It then became necessary to test the plastics being studied under conditions that could be more readily duplicated and that might yield more comparable results. Undoubtedly the best conditions would be under constant stress per unit cross-sectional area, but in view of the fact that relatively large extensions occur, and the cross section is changing continually with extension, no machine is at present available for stressing under such conditions, and it was necessary to resort to stress under constant load on the specimen. Figure 5 shows the way elongation at constant load changes with the time.

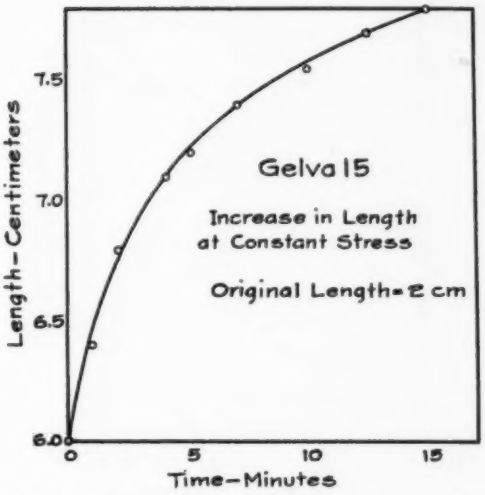

Fig. 5. The extension of polyvinyl acetate under constant load.

In the present measurements where constant load was applied, it must be remembered that the degree of orientation is increasing with time and that the values obtained for both the activation energy and the "viscous volume" will undoubtedly be influenced by this fact.

The procedure finally adopted in order to make the measurements as reproducible as possible, and make results with one plastic comparable to those with another, was to cut three test specimens from the same molded block and plot the elongation of each specimen against time. Two specimens were measured at the same temperature but under applied loads differing by 25 to 100 percent. The third specimen was then stressed at one of the former loads and at a temperature from 5° to 10° different from the initial. From the plots of these three curves it is possible to calculate the viscosity at precisely the same percentage elongation for each specimen, and from these figures calculate the two quantities desired.

It is to be noted that the activation energy cannot be calculated from the difference in viscosity at two temperatures alone but is a function also of the "viscous volume." This fact is illustrated by the calculations recorded in Table II, 4–6, for activation energy, neglecting in the first place the "viscous volume," second, assuming this volume to be 5900A^3, and in the third place assuming it to be 17,000A^3.

Table III gives the results for polyvinyl acetate of several molecular weights, and for three other thermoplastic resins, when measured by the foregoing procedure. It will be noted that the results are much less erratic than they were when the calculations were made from relaxation curves.

Table III.

Polymer	Measuring Conditions	Percent Stretch	Temp.	λa, A^3	E, Cal.	Remarks
9. Gelva 7	*C.L. 1.2–1.8$\times 10^7$ dynes/cm^2	129	35, 39.5	5,100	86,000	
10. Gelva 25	*C.L. 3–5 $\times 10^7$ dynes/cm^2	300	25, 35	9,200	54,000	
11. Gelva 25	*C.L. 6–10 $\times 10^7$ dynes/cm^2	600	35, 40	4,800	84,000	
12. Gelva 45	*C.L. 16–20 $\times 10^7$ dynes/cm^2	780–801	44	1,700	—	Successive observations on same piece.
13. Gelva 45	*C.L. 2.5–6 $\times 10^7$ dynes/cm^2	373	30, 35	8,400	64,000	
14. Plexiglas	*C.L. 1–2 $\times 10^7$ dynes/cm^2	136	82, 87	49,000	122,000	Röhm and Haas
15. Cellulose acetate	*C.L. 2–2.8$\times 10^7$ dynes/cm^2	112	80, 86	37,000	117,000	$\frac{1}{8}$" sheet from duPont
16. Formvar 15–95	*C.L. 1.6–2 $\times 10^7$ dynes/cm^2	137	110, 115	47,000	170,000	Shawinigan Chemicals Co.

* C.L. refers to constant load on the test specimen.

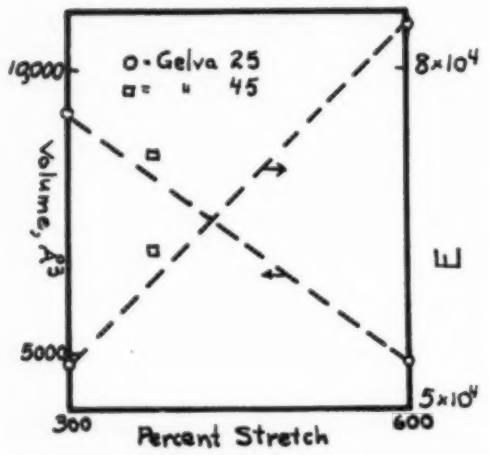

FIG. 6. Variation of "viscous volume" and activation energy for polyvinyl acetate at different elongations.

In turning attention to the polyvinyl acetates, there is a regular decrease in "viscous volume" and a steady increase in the activation energy with increase in percent of stretch. It will be noted that there is apparently little, if any, influence upon either the "viscous volume" or the activation energy due to variations in the molecular weight of the polyvinyl acetate at weights as large as, or larger than, Gelva 25. The results have been represented graphically in Fig. 6 in which it will be seen that the values for Gelva 45 lie between those given for Gelva 25, and while there may be some influence due to molecular weight this is apparently minor. This fact precludes the possibility that the atomic group that moves as a unit in these plastics during viscous flow can be identified as the molecule unless molecular weights for different vinyl acetates are constant and the differences in the viscosities of the solutions are due to other causes.

The fact that the values for Gelva 7 are out of line with the others is not surprising since there must be some minimum molecular weight beneath which a reduction in length of the chains will influence both the "viscous volume" and the activation energy. That the activation energy for the low molecular weight compound is higher than for the longer chains is at first surprising, but might be explained by the greater ease with which the small molecules can line up with each other and, therefore, approach closer to crystallization. The disturbance of a semicrystalline structure due to movement of one atomic or molecular group with respect to another would require greater energy than if orientation is entirely random.

In order to see if successive observations could be made on the same sample at such a high extension as 800 percent, the "viscous volume" was calculated for the Gelva 45 between 780 and 801 percent stretch. Here it seemed that approximately a steady state had been arrived at, but unless there is a much more rapid change in "viscous volume" in going from 600 percent to 800 percent than there is in going from 300 to 600 percent, this value of 1700A³ is probably low. (See 12, Table III.)

Other attempts were made to measure Gelva 45 by the constant load method at 800 percent stretch but apparently the ability to stretch this far is intimately connected with the molding conditions when the original slab is formed, since subsequent slabs would rupture before this extension was obtained. Undoubtedly, it would be simple to find the proper molding procedure to obtain this extensibility but time was lacking for this work.

TABLE IV.

Polymer	Measuring Conditions	Percent Stretch	Temp.	λa, A³	E, Cal
17. Dried rubber latex	C.L. 0.36–0.68×10⁷ dynes/cm²	275	25, 31	215,000	26,000
18. Dried rubber latex	C.L. 0.64–1.08×10⁷ dynes/cm²	440	25, 31	148,000	32,000
19. Dried rubber latex	C.L. 1.04–1.64×10⁷ dynes/cm²	575	25, 31	106,000	38,000
20. Vistanex high polymer	Relaxation	*ca.* 750	30, 35	50,000	24,000
21. Perbunan	Relaxation	780–840	25, 35	55,000	36,000
22. Vistanex high polymer	C.L. 1.20–1.39×10⁷ dynes/cm²	1000		25,000	27,000
23. Perbunan	C.L. 1.31–1.64×10⁷ dynes/cm²	800		58,000	24,000
24. Rubber (Smallwood)				3,500	10,200

Referring again to Table III it is interesting to note that Plexiglas and cellulose acetate have very similar "viscous volumes" and activation energies, which is also suggested by the fact that the softening temperatures for these two products were within two degrees of each other. The very high activation energies found for these two plastics and also for Formvar 15–95 are concordant with the extremely rapid rate at which softening occurs when the temperature is raised.

It is also interesting to note that the "viscous volumes" for these plastics are of another order of magnitude from those measured for vinyl acetate. This large difference undoubtedly is responsible for some of the large differences in physical behavior of these plastics, although it is difficult to do more than speculate on the origin of this difference. It seems plausible that it is associated with the polar forces between chains, and the greater ease of entanglement and the greater resistance offered to displacement in the less thermoplastic materials.

That the "viscous volume" should decrease with increase in stretch is quite logical because of the fact that clumps are being disentangled and orientation is occurring which should tend to decrease the large discontinuities that undoubtedly occur in a resin as it is formed. The "Locher Stellen" are elongated and represent smaller portions of the cross section and probably have less influence on differential movements as orientation occurs. Also it is in harmony with our picture that the activation energy increases with increase in stretch. Forces between chains that are oriented parallel with each other must be greater than when they lie at random.

Incidentally, it may be remarked that Poisson's ratio is 0.5 within experimental error for all of the polymers studied.

Rubber-Like Polymers

Table IV and Fig. 7 represent the results from measurements at constant load on rubber-like polymers. Here the most striking differences from other plastics are the very large "viscous volume" for the dried rubber latex and the uniformly smaller activation energies for these elastic polymers. In this table are also included

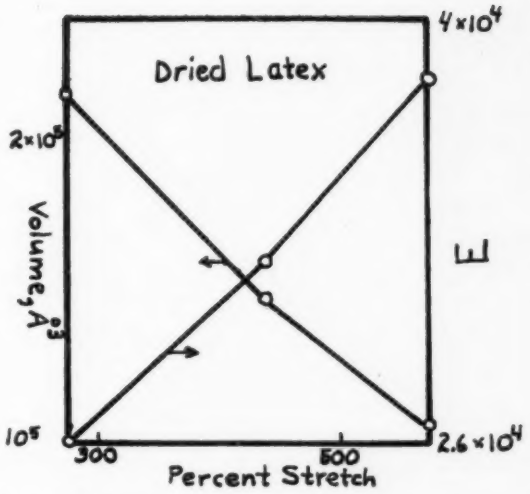

Fig. 7. Variation of "viscous volume" and activation energy for latex rubber at different elongations.

the values reported by Smallwood[4] calculated from the data of Mooney on milled rubber.

The tremendous difference between the "viscous volumes" for dried latex and for milled rubber is undoubtedly important and connotes a very large difference in structure. The rubber latex particles retain their identity on drying and such a mass is unusually nonhomogeneous even for a plastic. This lack of homogeneity will permit large masses to move with respect to each other and force the plastic deformation to occur between these masses of entangled rubber molecules. The milling operation undoubtedly breaks down the clumps and, therefore, reduces the size of the atomic or molecular group that moves in viscous deformation.

It is a bit surprising that the activation energy is not smaller than 10,000 calories when the viscous volume is as small as 3500A³.

It is probable that some of the high extensibility and high degree of recovery of unvulcanized dried rubber latex is due to the large "viscous volume." These dense clusters of molecules or portions of molecules undoubtedly can be physically deformed but require considerable stresses to produce plastic deformation. In fact much of the difference between milled and unmilled rubber may be due to the disruption of these clusters, and breaking of chains may be only a secondary effect, possibly necessary in

[4] Hugh M. Smallwood, J. App. Phys. 8, 505 (1937).

order to disentangle the molecules in these masses.

It is a well-known fact, for which there has been no explanation, that rubber cannot be broken down on the mill in the absence of oxygen. These measurements offer a convincing explanation of this phenomenon. The energy required to move one cluster by another may go as high as 40,000 calories, or perhaps slightly more at the extreme elongations. On the other hand, the energy required to rupture a carbon to carbon bond is 160,000 calories. Therefore it is impossible to bring such stresses to bear upon a single rubber molecule by plastic deformation of the mass to rupture the primary bond. If we imagine a single rubber molecule bridging the gap between two clusters that are moving with respect to each other, and can assume that such unusual circumstances arise that all of the viscous drag experienced by these clusters is opposed by this single molecule, long before such stresses are built up as could rupture the carbon to carbon bond these groups must be pulled from their positions of rest in their respective shearing planes, and only when the chain is weakened by oxidation is it possible for sufficient stresses to accumulate to pull it in two.

It is yet too early in this study of the activated processes accompanying viscous flow to say what correlations will be found between the quantities calculated above and physical properties of plastics, but it is reasonable to assume that many plastic phenomena can be explained in terms of these recent concepts.

For example, solvent and nonsolvent plasticizers show a large difference in their affects on plastics. It is quite logical to expect that this difference is due to the plasticizer in one case distributing uniformly throughout the mass, while in the other case concentrating in the regions between the denser clusters. It is, therefore, to be expected, though at present we have no data to verify the assumption, that a plastic softened with a nonsolvent plasticizer will show a much larger "viscous volume" on deformation than will a plastic softened by a solvent plasticizer. It is to be expected in the former case that elastic recovery would be much better with a given amount of plasticizer than in the latter.

Also, in two cases where the activation energies are the same but the "viscous volumes" are widely different, the internal viscosity of the one with the high "viscous volume" will be much less and its speed of retraction after elastic displacement will be much greater.

What further applications there will be for these plastic measurements and the accompanying calculated values cannot at the moment be predicted, but the work is going forward and it is hoped can be further extended by devising apparatus to stretch specimens under constant load per unit of cross section.

It should be emphasized here that in the above measurements conditions were not favorable for arriving at a "steady state" and therefore the quantitative interpretation of the results is not easy. We do not yet know what relations there are between viscosities, activation energies and "viscous volumes" measured during elastic displacement and during flow at constant orientation.

Summary

An examination has been made into the differences between linear and three-dimensional polymers. Thermoplasticity of the linear polymers is shown to have an intimate connection with the character of the side groups on the long chain molecules. It has also been shown that the ultimate tensile strength of three-dimensional polymers is dependent primarily upon secondary forces and has little connection with the degree of cross linking. The cross linking mainly influences the amount of extension under load and the amount of plastic deformation.

Calculations have been made of the activation energies and "viscous volumes" accompanying flow in plastics, and it has been shown that these values differ widely for different types of polymers. These values have been correlated to a limited extent with the physical properties of plastics, and in particular an explanation has been offered of the observed fact that rubber cannot be "broken down" on a mill in the absence of oxygen.

Changes in the Absorption Spectrum of Pb and Ni Films at Low Temperatures*

CHARLES F. SQUIRE†
Department of Chemistry, The Johns Hopkins University, Baltimore, Maryland
(Received July 13, 1940)

The temperature dependence (298°K to 80°K) of the absorption spectrum of Ag, Cu, Cd, Al, Sn, Sb, Pb, and Ni has been studied. Only Pb and Ni showed a relative change; Pb films transmit more ultraviolet light at 80°K than at 298°K, Ni films transmit less visible light at 80°K than at 298°K.

INTRODUCTION

THEORETICAL reasoning concerning the electronic behavior of metals has been based on a variety of thermal, electrical, magnetic and optical studies.[1] In the optical experiments the work of Sabine[2] and that of Wood[3] on thin metallic films has been most fruitful. We have made metallic films of Ag, Cu, Cd, Al, Sn, Sb, Pb and Ni, and studied the spectrum of the light transmitted through these films at 298°K to 80°K. The experiments were performed with the purpose of observing possible changes in the position or intensity of absorption bands (i.e., regions of heavy absorption) on lowering the temperature.

EXPERIMENTAL

The metal films were prepared by evaporation from a tungsten wire filament in a vacuum. The metals were deposited on quartz or Pyrex which had previously been thoroughly cleaned. The films were sufficiently thick (1μ) that their specific resistivity was that of the bulk metal. The metals were all of high tested purity. It should be emphasized that in nearly all work on the optical properties of metals, there is considerable doubt as to the crystalline structure of that portion of the metal which interacts with the light—i.e., in reflection or absorption.

Light from a hydrogen discharge tube passed through the metal film which was held by the cryostat and then into a Hilger E-31 quartz spectrograph. The exposure times were quite long (20 minutes) and the light intensity was held constant by a variable resistance. The cryostat was equipped with thermocouples and a gas thermometer; thermal equilibrium was insured by metallic contact with Wood's metal. The films were in high vacuum during the studies so that upon lowering the temperature, no moisture or gas could condense on the metallic surface.

Figure 1 shows the spectrum after having passed through a heavy film of Ag. The upper exposure was taken at 80°K and the lower one when the film was at 298°K. The pure H_2 spectrum extends across the entire plate and is not shown here. No change could be observed on the plate even with a sensitive densitometer. Similar results, showing no change in the spectrum of the transmitted light under identical conditions, save that of temperature, were obtained for all the other metals studied except Pb and Ni.

Figure 2 shows the same kind of study made on Pb and it is clear that the lowering of the temperature has the effect of increasing the transmission in the ultraviolet. The observed change was reversible—i.e., the original spectrum returned after warming the film back up to 298°K. The results of Pb were readily reproduced.

The change observed in the absorption spectrum of Ni films upon lowering the temperature was in the intensity with which the film absorbed

FIG. 1. Ag transmission at 80°K and at 298°K.

* Presented before the International Science Conference, Paris (1937) at the symposium of Professor A. Cotton. This work is part of a Doctorate Dissertation, Department of Chemistry, The Johns Hopkins University.

† Now at the Massachusetts Institute of Technology, Cambridge, Massachusetts.

[1] N. F. Mott and H. Jones, *Properties of Metals and Alloys* (Oxford University Press, 1936).

[2] R. B. Sabine, Phys. Rev. **55**, 1064 (1939).

[3] R. W. Wood, Phys. Rev. **44**, 353 (1933).

in the visible region. Densitometer studies on the spectrographic plates showed the effect—i.e., heavier absorption of visible light at 80°K than at 298°K. This work was held up for some time so that these results on Ni could be repeated in another manner. By means of a monochromator, light of approximately the same wave-length was sent through the metal film and then allowed to fall on a photo-cell. For the ultraviolet region a quartz Na-cathode tube was used. A Vance meter[4] was used to amplify the photo-current. The increased absorption in the visible region at low temperatures for Ni is brought out in Table I. The readings on Ag are included for comparison. The amplifier readings give only relative values; thus, the large change for Ni is really a change of only several percent on an absolute intensity scale. The reflected light from the Ni film showed no relative change on the amplifier corresponding to the change observed in the transmission.

TABLE I. *Photoelectric current (amplified) due to nearly monochromatic light which has passed through films of* (*a*) Ni *and* (*b*) Ag.

	Ni		Ag		
Temperature	298°K	80°K	298°K	80°K	
5800A	40.0	30.5	Heavy Absorption		
Ultraviolet	42.5	41.0	20.0	19.5	Microamp.

DISCUSSION

Germer[5] has recently shown by electron diffraction studies that metal films do have a crystalline pattern even down to a very thin film. This leads one to believe that an interpretation of these results may be inferred from the electron theory of metals. According to Mott,[1] the absorption of light in the visible region by Ni is due in large part to internal photoelectric transitions of electrons belonging to the $3-d$ band. It may possibly be that the changes in Ni observed here are due to a change in the number of electrons in the $3-d$ band upon lowering the temperature. Pb has a very large expansion coefficient in the range of temperatures investigated; such a large change in interatomic distance should affect the relative positions of electron energy bands. It seems impossible to give further details because of insufficient knowledge about these energy levels. It would be very interesting to make similar studies on metals like Ge and Hf where definite transition effects have been observed.

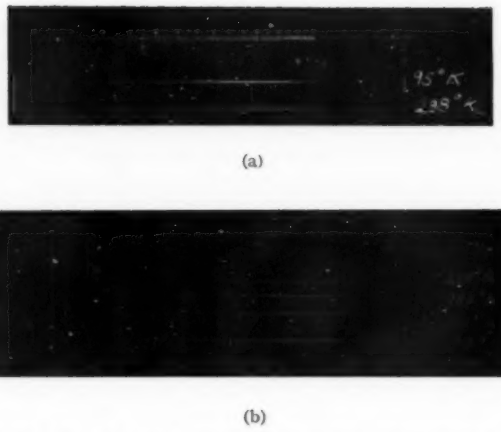

(a)

(b)

FIG. 2 (a) and (b). Pb transmission at various temperatures.

[4] A. W. Vance, Rev. Sci. Inst. **7**, 489 (1936).
[5] L. H. Germer, Phys. Rev. **56**, 58 (1939).

In the *Journal of Applied Physics* for January

Symposium on the Physics of Rubber

Theory of the Cyclotron

ROBERT R. WILSON*
Radiation Laboratory, University of California, Berkeley, California
(Received August 9, 1940)

The processes of formation of the initial ions in the cyclotron are reviewed, after which the various processes by which the ions are lost from resonance are considered. A theory of the loss of ions by collision or by electron capture is given and is compared with measurements made on the variation of the high energy beam current with gas pressure: satisfactory agreement is found. The inhomogeneity of the magnetic field of the 60-inch Berkeley cyclotron has been measured, and an analysis of the electric and magnetic focusing in that cyclotron is made. Rose's work on the loss of ions resulting from their getting out of phase with the radiofrequency voltage is applied to the calculation of V_0, the voltage necessary to apply to the dees just to get a beam. As an example, the value of V_0 is computed for the 60-inch cyclotron, and is found to be in good agreement with the directly measured value. The wandering of the ion paths is reviewed and is applied to the calculation of the inhomogeneity of the energy of emergent beam. Measurements made on the homogeneity of the energy of the protons from the 37-inch cyclotron are compared to the calculations. Finally, the question of shimming the magnetic field of a cyclotron is considered. It is suggested that the magnetic field be made to decrease from the center with a constant dH/dr. For this shape of magnetic field, analytic expressions are derived for the magnitudes of dH/dr and V_0, and methods for attaining such a field are suggested.

1. INTRODUCTION

SUPERFICIALLY, the theory of the cyclotron is very simple. An ion of charge e and mass M is formed at the center of the cyclotron and is accelerated by a radiofrequency voltage between the dees. The magnetic field H bends the ion's path with an angular velocity $\omega = eH/Mc$; if the frequency of the oscillating voltage is $\omega/2\pi$, the ion is said to be in resonance and is continuously accelerated so that its path spirals out with ever-increasing radius of curvature. Finally, at a radius R, the ion is withdrawn by means of an electric deflection field, and its energy has then become

$$W = e(H\omega/2c)R^2, \qquad (1.1)$$

if H is in e.m.u. and e is in e.s.u. (cf. Appendix I).

If we are interested in the intensity and homogeneity in energy of the emergent ion beam, we must investigate the processes of formation of the ions and then the various processes by which the ions are lost from resonance or have wandered so that they cannot be deflected to the target region. A complete theory should be able to account for the ions lost, it should be able to specify the best shape of the magnetic field, and it should be able to predict the necessary magnitudes of such factors as the dee voltage which would be required for larger contemplated cyclotrons. This paper constitutes a review of what has already been done in this regard[1–4] together with the results of some further calculations and measurements.

2. FORMATION OF IONS

The manner of formation of the initial ions is important, as it affects both the intensity and the homogeneity of the high energy beam. Two types of ion sources are ordinarily used: the filament type and the arc type. In the usual arrangement of the filament type of ion source, a filament is located under a shield in which a wide slot is cut to permit the electrons to pass up along the lines of magnetic force between the dees and so ionize by collision the gas in the central region of the cyclotron. An emission voltage between the filament and shield accelerates the electron from the shielded region. After an electron leaves the shielded region, its subsequent path is conditioned almost entirely by the large electric field of the dees. In general, the filament will be closer to one dee than the other, and consequently the electrons will be able to leave the filament region only when the voltage of the near dee is positive. It has been shown[5] that electrons which leave

* Now at Princeton University, Princeton, New Jersey.

[1] M. E. Rose, Phys. Rev. **53**, 392 (1938).
[2] R. R. Wilson, Phys. Rev. **53**, 410 (1938).
[3] L. H. Thomas, Phys. Rev. **54**, 580 (1938).
[4] E. M. McMillan, unpublished.
[5] R. R. Wilson, Phys. Rev. **56**, 459 (1939).

the filament when the voltage of the near dee is positive and becoming more positive are caught by the dee field, and that they oscillate up and down in the gap between the dees several times until the dee voltage falls to the value at which they started. Then the electrons fly off with considerable energy to strike either the cooling plate above or the filament structure below. This type of motion is shown in Fig. 1. At the same time that the electrons are oscillating up and down, they are executing cycloidal motion in the horizontal plane and move off in a direction perpendicular to the electric and magnetic field with an average velocity in this direction of cE/H. This sidewise motion can amount to several centimeters and thus considerably spreads out the region of initial ionization. Because the oscillating electrons go slower in the neighborhood of the median plane, there is a considerable enhancement of the density of ionization in that region, as is shown in Fig. 2. Electrons which are emitted during the phase when the near dee is positive and becoming less positive cross the magnetic gap only once, as is shown in Fig. 1, but the electrons emitted in the previous phase will still be oscillating and contributing to the ionization during this phase. Summarizing, the oscillations of the electrons increase the intensity of the ionization and tend to concentrate it toward the median plane, but considerably spread it out horizontally.

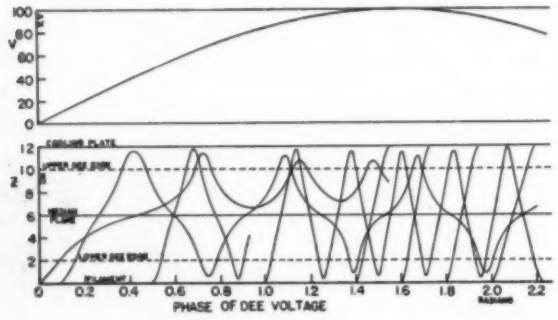

FIG. 1. In the lower curve is plotted the height of an electron above the filament as a function of the phase of the dee voltage when the voltage of the nearest dee to the filament is positive. In the upper curve is plotted the voltage between dees at the phase indicated on the lower graph. An electron starting at zero phase is seen to oscillate about the position of the upper dee edge. An electron which is emitted at an initial phase of 1.0 radian is seen to oscillate back and forth across the median plane and finally return to the filament after the dee voltage has dropped below the value it had when the electron was emitted—in this case after the phase has reached 2.1 radians. Electrons starting after an initial phase of $\pi/2$ radians, i.e., after the near dee voltage starts to become less positive, are seen to cross directly to the cooling plate.

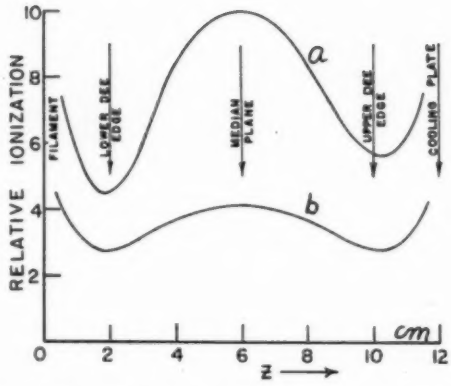

FIG. 2. The relative ionizing power of an electron is plotted as a function of its height above the filament. Curve *a* is for a typical oscillating electron emitted when the phase is about 0.3 radian. Curve *b* is for an electron emitted when the phase is about 2.0 radians, i.e., an electron which crosses directly to the cooling plate. In each case the ionizing power is seen to be increased near the median plane and decreased near the positions of the dee edges.

The arc type of ion source as developed by Livingston *et al.*[6] and modified by McMillan and Salisbury[7] is eminently more satisfactory than the filament type ion source in that the ions are produced in a very small region at the center of the cyclotron. Furthermore, the ambient pressure of the accelerating chamber is much smaller, and perhaps the relative abundance of singly charged ions is increased, thus producing less load on the oscillators and a smaller loss of ions due to collisions with the gas molecules.

3. Loss of Ions at Low Energies

The magnitude of the current of ions available for acceleration is of the order of milliamperes.[5] The high energy beam currents that are observed are of the order of tenths of milliamperes. Because of this disparity, it is of interest to find out how and where the initial ions are lost during the process of acceleration.

The first way that ions can be lost from resonance is by their capturing an electron or, in a smaller measure, by being scattered through a sufficiently large angle by a collision with the gas.

[6] M. Stanley Livingston, M. G. Holloway and C. P. Baker, Rev. Sci. Inst. **10**, 63 (1939).

[7] E. McMillan and W. W. Salisbury, Phys. Rev. **56**, 836 (1939).

To separate this loss from other types of losses which take place at higher energies, we can suppose that a current i' would reach the target or collector if there were no gas to impede the ions. Then with gas in the cyclotron, as there actually is, each ion may capture an electron or make a collision which will cause it to be lost from the beam. For a fixed dee voltage, the probability of these processes should increase linearly with the gas pressure p. We are then led to the usual collision type of formula

$$i=i'e^{-bp}, \tag{3.1}$$

where b depends on the dee voltage, the magnetic field, the geometry of the dees, the nature of the ion being accelerated, and the units in which p is measured.

In the case where a filament type of ion source is used, we can find experimentally to what degree ions are lost by electron capture and collisions. For such a case, i' is proportional to the initial ionization[4] which in turn is proportional to p,

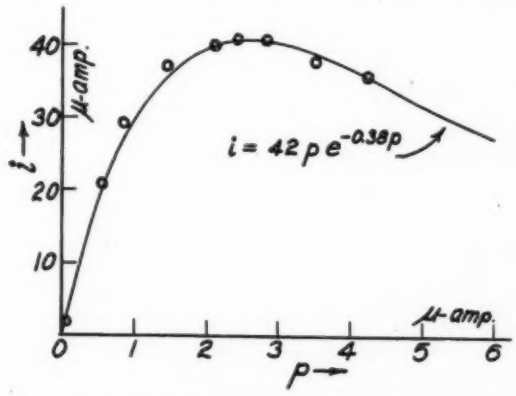

FIG. 3. The current of 8-Mev deuterons to the target of the 37-inch Berkeley cyclotron plotted as a function of the pressure of deuterium in the accelerating chamber—all other variables kept constant. The pressure is measured in terms of positive ion current in an ionization gauge.

other variables remaining constant. Eq. (3.1) can then be written:

$$i=ape^{-bp}, \tag{3.2}$$

where a depends on the filament variables and the dee voltage. The validity of Eq. (3.2) in describing the variation of beam current with pressure, keeping other variables constant, is demonstrated in Fig. 3. The data for the curve were taken by Professor E. M. McMillan for deuterons accelerated in the 37-inch Berkeley cyclotron.* The constant b is directly related to the optimum pressure p_{max}. Thus maximizing (3.2) with respect to changes of p yields the condition

$$p_{max}=1/b. \tag{3.3}$$

In Fig. 3 a curve given by (3.2) has been adjusted to the experimental points at the maximum value of current, and it is seen that elsewhere the experimental points agree to within the accuracy of the measurements.

The question arises concerning the degree that the circulating ions themselves produce more ions which can in turn be accelerated to high energy. If such were happening, the production of ions would depend on p^2 and (3.2) would take on the form

$$i=(ap+a'p^2)e^{-bp}. \tag{3.4}$$

That such an equation can in no way be fitted to the data, except with $a'\leqq 0$, is an indication that secondary production of ions is not appreciable. However, at a sufficiently high pressure a general glow discharge, which depends on the cyclotron being in resonance, does develop between the dees. This gives rise to a diffuse sort of circulating current which can be detected using a probe, but of which only a very small amount can get through the deflector system. Thus, while the diffuse circulating current can be of the same order of magnitude as the filament dependent circulating beam, the part of it that reaches the target chamber amounts to only a few percent of the beam obtained when the filament is on. Rough probe measurements indicate that the diffuse circulating current varies with p as given by (3.4).

Henderson and White[8] have published a curve of helium ion current as a function of the helium

* The pressures are given in terms of μa of positive ion current measured at an ionization gauge on the pump line. As was determined by calibration against a McLeod gauge attached directly to the accelerating chamber or tank, one μa at the ion gauge corresponded to a pressure of about 2.7×10^{-4} mm Hg in the tank for deuterium and to a pressure of about 1.2×10^{-4} mm Hg for air. During the measurements, the gas pressure was varied by changing the flow of gas into the tank, so that, as the pumping speed does not change with the pressure in this range, the ratio between the tank pressure and the pressure at the ion gauge stayed constant. When the pressure is varied by changing the pumping speed, as by partially closing a gate to the pumps, the tank pressure and the ion gauge pressure will not be proportional.

[8] M. C. Henderson and M. G. White, Rev. Sci. Inst. **9**, 19 (1938).

pressure for the Princeton cyclotron. Their curve can also be fitted by Eq. (3.2) to within the accuracy indicated by their plotted points. Protons would be expected to behave like deuterons, but no reliable data have been obtained for proton beams as yet.

It is of practical interest to examine the dependence of the beam on the background pressure of air in the cyclotron. To take account of the air, we have only to multiply (3.2) by the factor $\exp(-b'p_b)$, where p_b is the background pressure of air and b' is similar to b of (3.2). By letting air into the cyclotron by means of a variable leak and by noting the effect of this on the beam current, it was verified that the beam current actually did fall off as $\exp(-b'p_b)$.*

The effect of dee voltage on the loss of ions by electron capture or by collisions is not simple. Inasmuch as the collision cross section varies inversely with the square of the energy, and, as the probability of electron capture decreases about the same way, most of the ions will be lost at very low energy. In the case of an arc source, the main loss, if any, will occur as the ions just leave the source. In the case of the filament type of ion source, the main loss will occur during the first few revolutions. During these first revolutions, the ions do not penetrate into the dees, but move in the approximately uniform sinusoidal electric field between the dees. This motion can easily be calculated. The magnetic field H is in the z direction, and the electric field X is in the x direction which is perpendicular to z and varies with time as:

$$X = X_0 \cos(\omega t + \alpha), \tag{3.5}$$

where X_0 is the peak field and is considered uniform, ω has the resonance value eH/mc, and α is the phase at which the ion is produced. The equations of motion are:

$$\begin{aligned} m\ddot{x} &= eX_0 \cos(\omega t + \alpha) - He\dot{y}, \\ m\ddot{y} &= He\dot{x}, \end{aligned} \tag{3.6}$$

where y is perpendicular to x and z. The solution of these equations for ions starting from rest at the origin and at the phase α is:

$$\begin{aligned} x &= \frac{eX_0}{2m\omega^2}[\omega t \sin(\omega t + \alpha) - \sin\alpha \sin\omega t], \\ y &= \frac{eX_0}{2m\omega^2}[\sin\omega t - \omega t \cos(\omega t + \alpha) \\ &\qquad - \sin\alpha \cos\omega t - 2\sin\alpha]. \end{aligned} \tag{3.7}$$

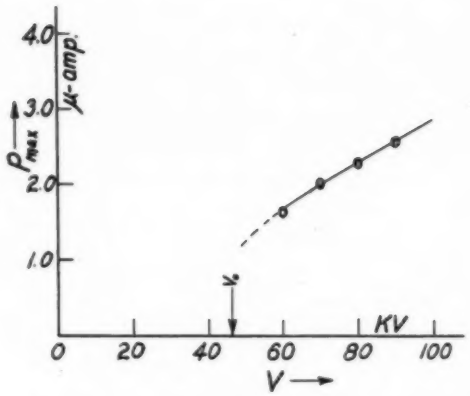

FIG. 4. The optimum pressure p_{max} plotted as a function of the radiofrequency voltage V.

It has been shown by electrolytic tray measurements that for ratios of dee separation to dee height less than 0.5, the electric field between dees is nearly independent of the dee separation. Hence the field X_0 will be proportional to V/h, where h is now the height of the dees.

If one knew how the probability of electron capture varies with energy, Eq. (3.6) would furnish the necessary information to calculate the coefficient b in (3.2). It can be seen from inspection of (3.6) that b will be a function of X_0 or V/h, H, and the nature of the gas. For a resonance magnetic field throughout the paths of the ions, we can see that b will be given by

$$b = kh/HV, \tag{3.8}$$

where k is a constant dependent on the nature of the gas and the ion being accelerated. This expression is so because the average number of terms, or the distance traveled, while the energy of the ion is small, will vary inversely with X_0 and H.

Eq. (3.3) now becomes

$$i \equiv ape^{-(kh/HV)p}. \tag{3.9}$$

* The constant b' was evaluated to be about 0.2 per μa of ion current at the ionization gauge, or if p is measured in mm Hg, b' becomes about 1.6×10^3 per mm Hg. This is for deuterons in the 37-inch cyclotron with the dee voltage at 75 kv.

Since a in this expression is dependent in an as yet unknown way on V, we cannot test the equation directly. However, we have from (3.3) that

$$p_{\max}=HV/kh. \tag{3.10}$$

This equation can be tested experimentally, and some values of $p_{\max}$ were measured as a function of V for a deuteron beam in the 37-inch cyclotron. As seen in Fig. 4, the points roughly indicate a linear relationship of $p_{\max}$ with V. It is probably better to regard the data of Fig. 4 as an experimental evaluation of the variation of b with V.

The above discussion, remember, was for a resonance magnetic field so that all the ion paths, regardless of α, would be lengthened or shortened in the same ratio as V varied. Actually the magnetic field does not have the resonance value throughout, but the radial inhomogeneity and the relativistic increase of mass causes some of the ions to get out of phase with the dee voltage. Thus, as will be seen later, at the threshold value of V, the value of voltage V_0 necessary to give any beam at all at the target chamber, only the ions starting nearly 90° behind in phase can get out. These ions must obviously make many more turns at low energy than does an ion nearly in phase, so that one would expect b to become correspondingly larger at V_0. However, for values sufficiently far above V_0, most of the ions that start at any initial phase get out, and one would then expect Eq. (3.10) to hold. The experimental data of Fig. 4 were taken at values of V considerably above V_0.

4. Electric Focusing

The initial focusing or defocusing of ions is complicated because the ions travel in an electric field which varies rapidly with time and position. It is possible to set up a formidable general equation of motion which is valid near the origin, but as yet a solution has not been obtained. For ions in phase with the velocity, a graphical analysis has been made for the initial focusing which indicates that there will be a severe defocusing that will last for the first few revolutions.[2] In the case of a filament type of ion source, some of the ions formed near the top or bottom edges of the dees are surely lost because of this initial defocusing.

After an ion has made several revolutions and has attained enough energy to penetrate into the field-free region within the dees, the focusing can be handled analytically. The electric focusing can be considered as consisting of two factors. The predominant factor for ions out of phase with the dee voltage is due to the relative change of the electric field during the acceleration of an ion. This was first shown by Rose.[1] The other factor[1, 2] which is only appreciable for ions nearly in phase, depends on the change in the energy of an ion in being accelerated. It is convenient to think of focusing in terms of an average vertical force. Thus, during each acceleration an ion gets a change in its vertical velocity. This change in vertical velocity per acceleration or per half-period of dee oscillation represents an average vertical acceleration, and the acceleration divided by the mass of the ion represents an average vertical force acting on the ion. This force f_e can be approximately expressed by the equation:

$$f_e=\left(\frac{eV\sin\alpha}{\pi r^2}-\frac{2ecV^2\cos^2\alpha}{3\pi hH\omega r^3}\right)z, \tag{4.1}$$

which holds for $r>2h$, where h is the height of the dees (cf., Appendix II). The first term within the brackets represents the out-of-phase focusing, and the second term represents the in-phase focusing.

For values of α negative or zero, f_e is a restoring force directed vertically toward the median plane and proportional to z; thus an ion moving with constant r and α would oscillate about the central plane with constant amplitude and period. The quantity in the brackets of (4.1) represents the force constant of the oscillation; and, as r and α change, the period and amplitude of the oscillation will also change. It is well known that if the force constant, $\partial f/\partial z$, of an oscillator changes slowly in comparison with the period, as it does in this case, a condition is that the action variable remains constant. In the case of a linear oscillator, this requires that U_vT_v, the energy of vertical oscillation times the period of vertical oscillation, be a constant. This can be written:

$$U_vT_v=2\pi^2M(A^2/T_v)=\text{constant}, \tag{4.2}$$

where A is the amplitude of oscillation. If we neglect the in-phase focusing term of (4.1), be-

cause it is much smaller than the out-of-phase focusing for most of the ions, we can write:

$$T_v = 2\pi\left(\frac{M}{\partial f/\partial z}\right)^{\frac{1}{2}} \tag{4.3}$$

$$= 2\pi\left(\frac{Hr^2}{c\omega V \sin\alpha}\right)^{\frac{1}{2}}, \tag{4.4}$$

so that (4.2) can be manipulated into

$$A_v = q\left(\frac{Hr^2}{V\sin\alpha}\right)^{\frac{1}{4}}, \tag{4.5}$$

where q is to be an adjusted constant.

Equations (4.3) and (4.4) show how the period and amplitude vary with $r/\sin\alpha$ in a uniform magnetic field. It is seen that for a resonance field (α constant), there will be a slow defocusing since the amplitude of oscillation increases as $r^{\frac{1}{4}}$. Actually the magnetic field is neither uniform nor at the resonance value. Thus, $\sin\alpha$ can change in such a way that there can be focusing or bad defocusing. Rose has considered the effects of variously shaped magnetic fields on this type of focusing and the reader is referred to Rose's paper for the details.

5. Magnetic Focusing

The usual magnetic field in the cyclotron can be considered azimuthally homogeneous and symmetrical about the median plane. The lines of magnetic force are not always entirely in the z direction but may bow outwards, especially near the edges. We can consider the magnetic field as broken into two components: a large vertical component H_z which keeps the ions in a circular horizontal path, and a very small radial component H_r, As the ions—if their paths are reasonably central—move perpendicular to H_r, the vertical force on them will be

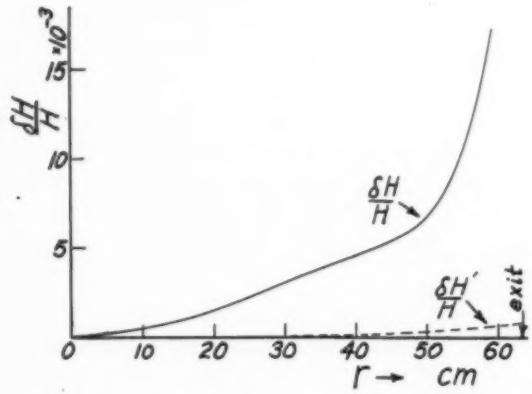

Fig. 5. The radial inhomogeneity of the 60-inch Berkeley cyclotron. The quantity $\delta H/H$, as measured with air in the cyclotron, is plotted against the radius r. $\delta H = H - H_c$, where H is the magnetic field and H_c is the magnetic field of the center of the magnet. The quantity $\delta H'/H$ is the calculated correction due to the distortion produced in the magnetic field by evacuating the chamber. The correction is to be added.

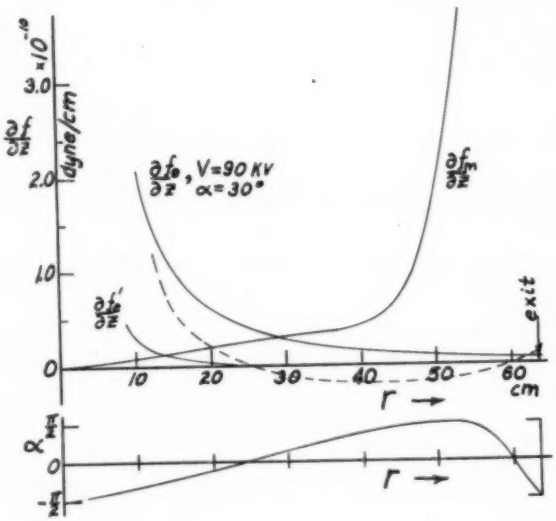

Fig. 6. The electric and magnetic focusing in the 60" cyclotron. $\partial f_e/\partial z$ is the "out-of-phase" focusing for $\alpha = -30°$, $V = 90$ kv; $\partial f_e'/\partial z$ is the "in-phase" focusing, $V = 90$ kv; and $\partial f_m/\partial z$ is the magnetic focusing. The dotted curve corresponds more nearly to the actual electric focusing and is for an ion with the phase as given in the curve below.

$$f_m = H_r e v/c. \tag{5.1}$$

Now H_r is closely given by

$$H_r = z\partial H_r/\partial z, \tag{5.2}$$

and since curl $H = 0$ in the gap, and assuming $H_z = H$,

$$H_r = z\partial H/\partial r. \tag{5.3}$$

Substituting (5.2) and $v = r\omega$ into (5.1) we get

$$f_m = \frac{e\omega}{c} r \frac{\partial H}{\partial r} z. \tag{5.4}$$

If $\partial H/\partial r$ is negative (i.e., field decreasing with r) the magnetic force causes strong focusing, especially at large values of r. On the other hand,

if $\partial H/\partial r$ becomes positive, it can give rise to a serious defocusing. For negative $\partial H/\partial r$, we see that f_m represents a restoring force towards the median plane and proportional to z so that the ions will oscillate about the median plane. Their period of oscillation is:

$$T_v = 2\pi\left(\frac{c\omega^2 r}{H}\frac{\partial H}{\partial r}\right)^{-\frac{1}{2}} \tag{5.5}$$

and, as r changes slowly in comparison to T_v, we can use (4.2), so that the amplitude becomes

$$A_m = q'\left(\frac{r}{H}\frac{\partial H}{\partial r}\right)^{-\frac{1}{4}}, \tag{5.6}$$

when q' is to be an adjusted constant.

It is interesting to compare the magnetic and electric focusing. In Fig. 5 the magnetic field of the 60-inch Berkeley cyclotron, shimmed for deuteron resonance, is plotted as a function of r. From this, $\partial f_m/\partial z$ as a function of r is plotted in Fig. 6. Also in Fig. 6 is plotted $\partial f_e/\partial z$ as given by (4.1) for a deuteron 30° behind in phase and with $V=90{,}000$ volts.

The magnetic field as measured with air in the accelerating region must be corrected to obtain the true magnetic field which results when the accelerating region is evacuated. This is because of the bending of the lids of the chamber due to the air pressure. The correction to be added is appreciable for a large cyclotron and is approximately given by

$$\delta H'/H = (d/\sigma)(r^2/r_0^2), \tag{5.7}$$

where d is the deflection at the center of the lids, σ is one-half the magnetic gap, and r_0 is the radius of the lids. The deflection d can be measured or calculated.

6. Loss of Ions Due to Resonance Requirements

Usually a cyclotron magnetic field shows a sharp, radially symmetric decrease in the vicinity of the exit slit such as is shown in Fig. 5. This decrease in the field strength causes the ions to revolve with a slower angular velocity and so to tend to get out of phase with the voltage. The relativistic increase of mass also decreases the angular velocity. Rose and Bethe first pointed out that, for a given value of the dee voltage, the relativistic increase of mass imposes an upper limit on the energy obtainable; if the magnetic field is increased at large radii to compensate for the increase of mass, the magnetic lines will bow inward and a serious magnetic defocusing will be introduced. This result is true for a radially symmetrical magnetic field. Thomas has shown that a variation of the magnetic field with polar angle can produce a focusing effect and at the same time preserve resonance and stability. Lawrence has suggested the use of foils or grids across the faces of the dees to improve the electric focusing and thus increase the energy obtainable for a given dee voltage (cf., Appendix II). However, so far it has been practical to increase the upper limit by increasing the dee voltage.

For a complete discussion of the resonance condition and its effects on focusing, the reader is referred to Rose's admirable paper.[1] An application of the equations of focusing and of resonance condition to the case of the 60-inch cyclotron will be illustrative of the magnitude of the various effects. The change in the phase due to the relativistic effect and the inhomogeneity in

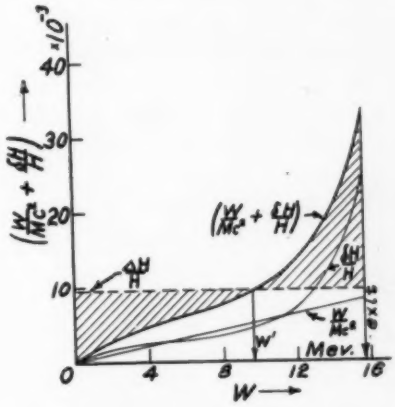

FIG 7.

the magnetic field can be expressed by an equation which was first derived by Rose:[1]

$$\Delta \sin\alpha = \frac{\pi}{eV}\int_0^W\left(\frac{W}{M_0c^2}+\frac{\delta H}{H}+\frac{\Delta H}{H}\right)dW, \tag{6.1}$$

where $\delta H = H - H_e$ and $\Delta H = H_e - H_0$. H_e is the magnetic field strength at the center and H_0 is the resonant value of the field strength at low energy.

We can apply this to calculate V_0, the voltage

necessary to give a beam. The most favorable case will be for an ion whose phase varies from $-\pi/2$ radians to $\pi/2$ radians and back to $-\pi/2$ radians, that is, for an ion that starts behind in phase $-\pi/2$ radians and in a magnetic field slightly greater at the center than the resonance value. The ion will then gain in phase until it is $\pi/2$ radians ahead in phase. At this point the magnetic field becomes less than the resonance field, due to the relativistic change in mass and the edge effect decrease of the magnetic field, so that the ion will start to lose in phase until its phase again gets behind by $\pi/2$ radians just as the ion reaches the deflector. Of course, at or slightly above V_0, the operator adjusts the magnetic field strength at the center (i.e., ΔH) such that the phase of the ions varies nearly as stated above.

In Fig. 7, $(W/M_0c^2+\delta H/H)$ for the sixty-inch cyclotron is plotted as a function of the energy of the ions, the data for calculating δH having been taken from Fig. 5. Now for the case outlined above $\Delta \sin \alpha = 2$ while the ion is gaining in phase and $\Delta \sin \alpha = -2$ while the ion is losing in phase. Then to find V_0, the procedure is to determine a line parallel to the W axis, as the dotted one shown in Fig. 7, such that the area below the line and above the curve before the line and the curve intersect is the same as the area above the line and below the curve after the intersection. The ordinate of the dotted line is the average ordinate of the curve, and it corresponds to the value of $\Delta H/H$ which is adjusted by the operator. The two areas are each proportional to $\Delta \sin \alpha$, and it follows from (6.1) that V_0 will be given by

$$V_0=\frac{\pi}{2e}\left[\frac{\Delta H}{H}W'-\int_0^{W'}\left(\frac{W}{M_0c^2}+\frac{\delta H}{H}\right)dW\right], \quad (6.2)$$

where W' is the value of W at which the dotted line and the curve intersect, and the quantity in the brackets corresponds to the areas measured. The value of V_0 calculated from the data of Fig. 7 by numerical integration gives 95 kv. This is in good agreement with the directly measured value of 90 kv inasmuch as both values are accurate to about five percent. The value of V_0 calculated from (6.2) should be considered as a lower limit inasmuch as the extreme values of α which were used assumed that no electric defocusing takes place when the phase is positive. Furthermore, the ions might not be able to start behind in phase by as much as $\pi/2$ radians, as then they might not clear the ion source. It is also possible that the ions might not be able to get into the deflector when they are behind in phase $\pi/2$ radians as was assumed. It will be shown later, however, that even an ion behind in phase $\pi/2$ radians can be deflected.

Concerning the electric defocusing when α is positive, we can see in Fig. 6 that the magnetic focusing due to the shims will predominate over the electric defocusing. Thus below the focusing curves in Fig. 6 is plotted the phase of an ion which starts behind in phase $\pi/2$ radians and is accelerated by a dee voltage of V_0. The dashed curve in Fig. 6 represents the electric focusing for such an ion. The total focusing, $\partial f/\partial z$, is the sum of the electric and magnetic focusing. This sum reaches a minimum at a radius of about 30 cm. As the amplitude of oscillation of the ions about the median plane is inversely proportional to the fourth root of $\partial f/\partial z$ we can see that the beam will diverge for about the first 30 cm and will converge beyond this radius. The beam will converge very sharply after a radius of about 50 cm where the steep edge effect decrease of the magnetic field begins.

7. Homogeneity of the Energy of the Beam

A number of factors contribute to the inhomogeneity of the energy of the emergent beam of ions. As is seen from (1), the energy of an ion in the beam is proportional to R^2, where R is the final radius of curvature of the ion's path. For ions arriving at the deflector, R can vary because:

(1) The initial ionization is spread over a considerable region for the case of a filament ion source (§2).

(2) For the case of the arc source, the centers of rotation can be displaced because of the initial acceleration by the feelers. This displacement will vary with the initial phase of the ion, so that the centers of rotation will be spread over a region near the center instead of a point.

(3) If the center of rotation is not located midway between the dees, the ion can creep along the dee gap. This motion is a result of the effect

of the electric field and was first pointed out by McMillan.[4] The equations which describe the effect have been worked out by Thomas.[3]

(4) If the dee voltage varies over the length of the dees because of their inductance, the ion paths will creep along the dee gap and toward the end where the voltage is smaller. McMillan and Salisbury[9] have considered this effect in some detail.

(5) A slight nonparallelism of the magnet pole faces of the lids of the cyclotron chamber will produce a linear gradient in the strength of the magnetic field which will cause the ion paths to wander in a direction perpendicular to the direction of the field gradient. Thomas and McMillan have worked out the equations for this effect.

(6) The first four effects above cause the centers to spread out along the dee gap. As this direction is perpendicular to the direction of a line drawn between the center of the cyclotron and the lip of the deflector, the spreading out would not be expected to affect seriously R or the energy of the beam. However, the rather sharp radial decrease in the magnetic field due to the edge effect causes off-center ion paths to precess about the magnetic center. This effect becomes very appreciable for large values of r; thus, if the path center of an ion has become displaced a distance l from the magnetic center for any reason at low energies, the precession which occurs at high energy will cause the path center to move around the magnetic center in a circle of radius l. It turns out that the path center can move around its circle of precession several times, depending on the phase, before the ion reaches the deflector. Thus, if the path centers of all the ions are spread out in a line at low energies, this line of centers will be spread into a disk shaped region at high energy. Accordingly, any displacement of the path centers in any direction can seriously spread out the values of R for the ions and so cause considerable inhomogeneity of the beam reaching the deflector lip. Of course the deflector is somewhat selective of the energy of the ions which can pass through it.

Let us consider the magnitude of the various effects for the case of protons in the 37-inch Berkeley cyclotron for which some energy measurements have been made. A filament type ion source is used; the filament is about four cm long and the motion of the oscillating electrons (§2) along the dees can further spread the initial ionization out about four more cm. Consequently we can think of the initial ionization as spread into a vertical sheet about eight cm long. There will be a negligible displacement of the path centers due to the first acceleration because an ion spirals around in the field between the dees several times before actually penetrating into the field-free space within the dees. This motion is given by (3.7), and it is seen that the path remains more or less centered.

Usually the filament is not exactly centered between the dees, but is off center as much as one cm. The average displacement of the path center per revolution due to this is given by:*

$$\frac{\delta y}{\delta n}=l\frac{Ve}{W}\sin\left(\frac{\omega_0-\omega}{\omega_0}\pi+\alpha\right), \qquad (7.1)$$

where l is the displacement of the path center from midway between the dees, $\omega_0=eH/M_0c$, and α is the phase of the ion (cf., Appendix III). Integrating over all the revolutions, assuming a resonance magnetic field, i.e., $\omega=\omega_0$, gives an idea of the order of magnitude of the total effect, Δy:

$$\Delta y=\frac{l}{2}\tan\alpha\log\frac{W}{2V\cos\alpha}. \qquad (7.2)$$

For a proton in the 37-inch cyclotron out of phase by 30° and off center by one cm, (7.2) gives a total motion along the dees of about one cm.

For most of the cyclotrons now built, the dee voltage is supplied much nearer to one end of the dee gap than to the other. Because of the inductance of the dees, the voltage is then higher at the far end. McMillan and Salisbury have derived the following approximate equation for the creep of path centers along the dee gap caused by this voltage gradient—assuming the dee voltage to be applied at the extreme end of the dee gap:

$$\Delta y=9R^2/\lambda^2, \qquad (7.3)$$

[9] Unpublished.

* This equation is similar to an equation given by Thomas (reference 3); however, it differs by a factor of ω, which he seems to have forgotten in the process of averaging over a revolution.

where R is the radius of the dees and λ is the wave-length of the dee voltage. For the 37-inch cyclotron, Δy only amounts to about one-half of a mm.

The wandering of ion paths due to the non-parallelism of the magnetic gap is given by the following formula which has been derived by both Thomas and McMillan:

$$\delta\xi/\delta n=\frac{\pi r^2}{H}\frac{dH}{d\eta}, \tag{7.4}$$

where $\delta\xi/\delta n$ is the average displacement of the path center per revolution due to a linear gradient of the magnetic field strength, $dH/d\eta$, in the η direction. The displacement is perpendicular to the η direction. Assuming a resonance field, and integrating with respect to r gives for the total displacement,

$$\Delta\xi=\frac{\pi WR^2}{4Ve\cos\alpha}\frac{1}{H}\frac{dH}{d\eta}. \tag{7.5}$$

If we assume that the 37-inch cyclotron chamber lids are parallel to within one-thousandth of an inch over-all, $\Delta\xi$ could amount to about one mm for an ion out of phase by 30°.

Finally we come to the path wandering because of radial inhomogeneity of the magnetic field. The radial inhomogeneity can be caused by radially symmetric shims or by warping of the lids of the cyclotron chamber as a result of the pressure difference and of the magnetic attraction of the pole faces. However, the predominant radial inhomogeneity is caused by the edge effect. The magnetic field can be expressed very nearly by an equation of the form

$$H=H_0(1-ae^{-\pi(r_0-r)/\sigma}), \tag{7.6}$$

where r_0 is the pole face radius, σ is half the magnetic gap, and a is a constant. Now an ion moving in a radially symmetric field and in an orbit whose path center does not coincide with the magnetic center will precess about the center. If the average path center is off the magnetic center by a distance l, the path center will move around a circle of radius l a distance δS per revolution given roughly by

$$\frac{\delta S}{\delta n}=\frac{\pi^2 lra}{\sigma}e^{-\pi(r_0-r)/\sigma} \tag{7.7}$$

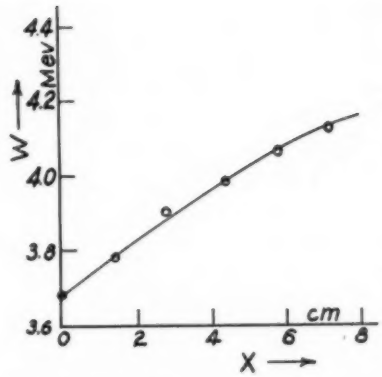

FIG. 8. The energy of the proton beam from the 37-inch Berkeley cyclotron at various positions in the beam. The variable x is measured horizontally from the inside edge of the beam and transversely to the direction of the beam.

(cf., Appendix IV). The direction of δS will be the same as the direction that the ion moves when it is farthest from the magnetic center. The magnitude of $\delta S/\delta n$ only becomes appreciable at large values of r. Let us again assume that the ion remains in resonance and then integrate (7.7) with respect to r to get an idea of the total wandering ΔS: we get approximately,

$$\Delta S=\frac{\pi W}{eV\cos\alpha}ae^{-\pi(r_0-r)/\sigma}. \tag{7.8}$$

In the case of the 37-inch cyclotron, a and σ are roughly 0.6 and 7.5 cm while r_0 is about 46 cm. For an ion whose path is off center by one cm, $\delta S/\delta n$ is about one cm per revolution at the value of r, where the ions are withdrawn. For protons and the same conditions, the total wandering ΔS around the circle of radius one cm is about 3 cm for an ion in phase throughout the acceleration. This represents about one complete revolution. Ions off center by any value of l would also make about one revolution as ΔS is proportional to l. As the ions are not all in phase, especially at large values of r, most of the path centers probably make several complete revolutions around the circle of precession.

We can now apply these results to the homogeneity of the energy of the beam. We have seen that at low energies the path centers tend to spread out along the gap and that this spreading can amount to about six cm at least—most of the spread being due to the manner of formation of the initial ions. Then at high energy the linear

spread of path centers is smeared more or less uniformly into a disk or cylinder-like region concentric with the magnetic center.

Thus for the case considered and considering the geometry of the dees, we would expect the values of r for ions arriving at the deflector to vary from about 32 to 39 cm. This would correspond to an energy variation of from 3.0 to 4.2 Mev for ions arriving at the deflector. Now the beam that arrives at the target chamber is spread out horizontally about 10 cm, and the energy on the side of the beam toward the cyclotron is lower than that on the side away from the cyclotron. The energy distribution in this beam from one side to the other was measured by obstructing the beam with a piece of molybdenum in which a series of vertical slits were cut at intervals of about two cm. The average range and direction of the ions coming through each slit was measured and the results are shown in Fig. 8. It is seen that the average energy at each slit varies from 3.7 to 4.2 Mev. This variation is less than the calculated variation, and probably is a result of the selective action of the deflector. By the use of a number of defining slits placed in the magnetic field of the cyclotron, the energy of the beam can be made as uniform as one pleases—sacrificing intensity for uniformity, of course.

Probe measurement[10] on the circulation current of deuterons in the 37-inch cyclotron indicates that the path centers are spread out about 12 cm. This is in agreement with the above discussion. Because of this large spread of the path centers, it is not difficult to understand that the circulating current is about ten times as large as the deflected current. As most of the inhomogeneity of energy is introduced by the manner of formation of the ions, one would expect an arc source to yield a beam considerably more uniform in energy than that given by a filament type source.

The wandering due to the radial decrease in the magnetic field produces an opening up of the successive ion paths beyond that produced by the acceleration of the dee voltage. Lawrence and Cooksey[11] first pointed out that this opening up of the ion paths is a desirable characteristic inasmuch as it facilitates the deflection of the ions from the accelerating region. It has been shown above how the ion path centers move around the magnetic center on a circle of precession of radius l. If the path center is moving around this cirele in such a way that it is approaching the deflector, then the successive ion paths will be opened up by a distance nearly that given by (7.7). For an ion path off center about one cm, this opening up can amount to about one cm. If the path center is receding from the deflector, of course the effect is then in the opposite direction; and it is probable that such an ion would first strike the dees elsewhere before being deflected, although if the circle of precession is small, there may be some possibility that the path center would continue around the circle of precession and be deflected before striking the dees.

The reality of the above effect is best illustrated by the horizontal distribution of induced radioactivity on a probe. This was measured for a probe which had been bombarded by deuterons in the 37-inch cyclotron.[10] It was found that the activity extended 1.2 cm from the leading edge of the probe, whereas the opening up of the successive ion paths corresponding to the change in radius of path produced by being accelerated twice by the maximum dee voltage would amount to less than 0.5 cm. Another example is that the optimum width of the deflector channel at the leading end is about one cm instead of 0.5 cm. As cyclotrons are built to higher and higher energies, the opening up of the successive paths by the wandering will be of increased importance if the beam is to be deflected.

8. Shimming

Shimming can be defined as the art of placing configurations of iron in the gap between the magnet pole faces in such a manner as to increase the current of high energy ions. The shimming is ordinarily done in the gaps between the lids of the cyclotron chamber and the pole faces of the magnet. The usual procedure of shimming has been the highly empirical one of placing various arrangements of piles of circular iron plates in the shimming gaps and noting the effect on the

[10] R. R. Wilson and M. D. Kamen, Phys. Rev. **54**, 1031 (1938).
[11] E. O. Lawrence and D. Cooksey, Phys. Rev. **50**, 1131 (1936).

intensity of the beam. This has turned out to be a lengthy and laborious process, although a successful one in the end. On the other hand, it is felt that it is possible to shape the magnetic field in advance such that one can be assured that a beam of high energy ions will be obtained if a specified dee voltage, which can be calculated, is applied.

The question of the shape of the field is a delicate one, and will probably vary from one cyclotron to another depending on the available amount of dee voltage as well as the energy and current desired. Perhaps some general considerations can be noted. Near the center of the cyclotron the ions will be behind in phase and there will be electric focusing as given by (4.1). The beam will diverge vertically but not seriously in this region, and it is not essential to provide magnetic focusing. At an intermediate radius, perhaps one-third of the final radius, the phase of the ions becomes positive, so that there is strong electric defocusing. Over the region where the phase is positive, it is indispensable, if the cyclotron is to work near its limit of energy, that magnetic focusing be provided. Beyond this region, the electric focusing will be small in comparison to the vertical forces due to natural inhomogeneities of the magnetic field, and it will be necessary to provide some sort of positive magnetic focusing to keep the ions near the median plane. The magnitude of the magnetic field gradient to provide the magnetic focusing will depend on the dee voltage and the position of the region where ions have positive phase. Of course, it cannot be emphasized too strongly that it is necessary to maintain the direction of the magnetic lines of force accurately perpendicular to the median plane where they cross it. The ions will strongly tend to oscillate about the position where the lines of force are vertical;* and if this position departs very far above or below the median plane, the oscillating ions will strike the dees and be lost. As the position where the lines of magnetic force become vertical is very sensitive to small dissymmetries in the iron, one of the major problems of shimming is to maintain the lines vertical at the median plane.

A simple magnetic field that is suggested is a radially symmetric one with a constant and negative radial gradient. The magnitude of the gradient will depend on the magnitude of the electric defocusing during the region where the phase of the ions is positive. As the magnetic focusing force is proportional to rdH/dr, such a field will produce a slowly converging beam ($\sim r^{-\frac{1}{2}}$) after the magnetic focusing predominates over the electric focusing. Following the procedure of Section 6, it is possible to calculate for the above magnetic field the minimum dee voltage V_0 and the corresponding dH/dr just to get a beam. One obtains:

$$V_0 = (0.22/e)(W_1^2/M_0c^2), \tag{8.1}$$

and

$$dH/dr = 0.14HW_1/RM_0c^2, \tag{8.2}$$

where W_1 and R are the final energy and radius (cf. Appendix V). The wandering in such a field can be given by

$$\delta S/\delta n = \pi l r dH/Hdr, \tag{8.3}$$

where l and S are as in (7.7), and this wandering is negligible. Of course, it would not be necessary to maintain the gradient near the center. Rose has carefully analyzed other shapes of the magnetic field, especially with the view of obtaining maximum energy for a given dee voltage.[1]

Having selected the desired shape of the field, one would proceed to change the natural magnetic field which obtains between the pole faces of the usual cyclotron magnet into the specified field. A good start would be the insertion of the internal ring shims calculated by Rose.[12] These shims correct the sharp decrease in the field near the edge of the pole pieces. It has been found by Henderson *et al.*,[13] that the thickness of the shims should be twice that calculated by Rose. It might be desirable to have the magnetic field drop off steeply at the radius where the ions just arrive at the deflector. This would facilitate the deflection of the ions due to the opening up of the successive paths, but at the expense of an increased V_0.

Assuming an initially homogeneous magnetic field, one would insert concentric circular plates of various sizes until the desired shape of field

* By vertical is meant perpendicular to the median plane.

[12] M. E. Rose, Phys. Rev. **53**, 715 (1938).

[13] Henderson, King, Risser, Yearian and Howe, J. Frank. Inst. **228**, 563 (1939).

is obtained. For small cyclotrons, the plates can be inserted in a shimming gap outside of the cyclotron chamber; but because of the shielding effect of the lids, the external shims are large in comparison to the size required if the shims were placed within the chamber. As cyclotrons are built larger, the external shims will become so cumbersome that it will be preferable, if not necessary, to place the shims within the chamber. It will be natural to place them between the copper cooling plate and the lids. An approximation to the constant gradient field discussed above could be obtained by beveling the inside surfaces of the lids from the center out at an angle β given by

$$\beta=(2\sigma/H)(dH/dr), \tag{8.4}$$

where σ is one-half the magnetic gap.

One of the important problems concerning the cyclotron that is yet to be solved is the analytic prediction of the shape of the shims or pole faces necessary to produce a specified configuration of the field. Until this problem is solved it will be necessary to proceed to build up the field empirically with the assistance of the intuition and sensitive magnetic field measuring instruments. One must bear in mind the change produced in the magnetic field due to the distortion of the lids introduced by evacuating the chamber. Furthermore, different shimming is required at different field strength due to the saturation of the iron and the difference in the distortion of the lids caused by the magnetic field.

There are two instruments that would be invaluable in this work. One, to measure dH/dr accurately, might consist of two coils connected in series with each other and a ballistic galvanometer. The coils, of many turns, should be of opposite sense in the magnetic field so that variations of H with time will balance out. Then one coil is kept fixed near the center, and the other coil is jerked from the center to various radii as the throw of the galvanometer is noticed. The other instrument is to insure that the lines of force become vertical at the median plane. It would consist of a needle fastened to a mirror and some sort of an optical system. As the system must be absolute, one suggestion is to have the needle and mirror consist of a highly polished (perhaps plated) and accurately machined rectangular steel bar or plate. In any case, one could check the absolute accuracy by reversing the needle. The sensitivity of the instrument will be dictated by the magnitude of dH/dr as given by (8.2) if the linear gradient field is used. Because curl $H=0$ in the gap, we have

$$d\varphi/dz=(1/H)(dH/dr), \tag{8.5}$$

where φ is the angle between the lines of force and the vertical. Of course, as is seen from the above equation, the optical instrument is sufficient by itself as it also gives dH/dr. However, experience has shown that the search coil method is more rapid and convenient.

It is a pleasure to express my gratitude to Professor Ernest O. Lawrence for his encouragement of this work. I am also grateful to Professor Edwin M. McMillan for his permission to use some of his unpublished results. Acknowledgment is made to the Research Corporation for financial support in this project.

Appendix I

The energy equation

$$W=\tfrac{1}{2}Mv^2, \tag{1a}$$

$$v=r\omega, \tag{2a}$$

$$M\omega r=Hev/c, \tag{3a}$$

$$\omega=eH/Mc. \tag{4a}$$

Combining (1a), (2a), (4a) and at the exit slit $r=R$ we get:

$$W=eH\omega R^2/2c. \tag{1.1}$$

Appendix II

Electric focusing

The average vertical force, f_e, per acceleration is

$$f_e=\frac{1}{\Delta t}\int_t^{t+\Delta t} Zedt, \tag{1b}$$

where Z is the z component of the electric field between dees, and the integral is from the field-free region of one dee to the field-free region of the other dee. Then as $\delta t=\pi/\omega$ and taking $t_0=0$, we get

$$f_e=\frac{\omega}{\pi}\int_0^{\omega/\pi} Zedt. \tag{2b}$$

Near the median plane we may write

$$Z=z\partial Z/\partial z, \tag{3b}$$

and because of Laplace's equation

$$Z=-z\partial X/\partial x, \tag{4b}$$

and as the voltage is sinusoidal,

$$Z=-z\frac{\partial X_0}{\partial x}\cos(\omega t+\alpha). \tag{5b}$$

Now as the ion crosses the dee gap

$$dt\cong dx/v_x, \tag{6b}$$

and using (4b), (7b) and (8b) we get

$$f_e=-\frac{\omega e}{\pi}\int\frac{z}{v_x}\frac{\partial X_0}{\partial x}\cos(\omega t+\alpha)dx, \tag{7b}$$

and as the change in z in crossing the gap is small

$$f_e=-\frac{\omega ez}{\pi}\int\frac{\cos(\omega t+\alpha)}{v_x}dX_0: \tag{8b}$$

after integration by parts, this integral can be manipulated into the form

$$f_e=-\frac{\omega ez}{\pi}\left[\frac{\sin\alpha}{v_x r}\int X_0dx+\frac{e\cos^2\alpha}{mv_x^3}\int X_0^2dx\right]. \tag{9b}$$

Now $\int X_0dx$ across the gap is V. $\int X_0^2dx$ across the gap depends on the geometry of the dees, but for ratios of dee separation to dee height less than about one-half, the field between the dees is nearly independent of the geometry. In this case, as evaluated graphically, $X_0^2dx\cong\frac{2}{3}V^2/h$, where h is the dee height. Then using (2a)

$$f_e=\left[\frac{eV\sin\alpha}{\pi r^2}-\frac{2ecV^2\cos^2\alpha}{3\pi hH\omega r^3}\right]z. \tag{4.1}$$

In case a foil or a set of grids covers the face of the dee toward which the ions are traveling (as has been suggested by Professor Lawrence), the integral of (7b) is only carried to the face of the foil. This corresponds to carrying the integral halfway across the gap if there were no foil. When this is done, one obtains for the average force per acceleration

$$f_e'=-\frac{\omega ez}{\pi}\left[\frac{X_1}{v_x}\cos\alpha+\frac{V}{rv_x}\sin\alpha\right], \tag{10b}$$

where X_1 is the peak value of the electric field at the face of the foil and is given by*

$$X_1=\frac{2V}{h[1+\frac{1}{2}(d/h)^2]}, \tag{11b}$$

where d is the separation of the dees. Then if the dees are close together, and neglecting the second term of (10b) as it is small, we get

$$f_e'=-\frac{2Ve}{\pi hr}\cos\alpha. \tag{12b}$$

This type of focusing is much larger than that given by (16), and is always positive focusing. Thus, by the utilization of foils or grids across the dee faces, one can obtain an appreciable reduction in the voltage necessary to give a beam of a certain energy. Professor Edwin McMillan has made extensive calculations of this effect, which are to be published soon.

Appendix III

Creep of ion paths along the dees

Suppose the ion path center is located on the average a distance l from the plane midway between the dees. As the ion crosses the gap, the radius vector will make an average angle θ with respect to a line parallel to the gap and of magnitude l/r. At each crossing of the gap by the ion, it follows from (1) that

$$dr=rdW/2W \tag{1c}$$

or

$$\delta r=(erV/2W)\cos(\omega t+\alpha). \tag{2c}$$

Let us assume that $t=0$ at a certain crossing. The path center is shifted along the gap by an amount

$$\delta y=\delta r\cos\theta \tag{3c}$$

$$=(erV/2W)\cos\alpha\cos\theta. \tag{4c}$$

* I am indebted to Dr. L. R. Walker for the calculation of the value of X_1.

After the ion makes a half of a revolution, the dee voltage will be

$$V_0 \cos\left(\pi+\frac{\omega_0-\omega}{\omega_0}\pi+\alpha\right),$$

where ω is the angular velocity of the dee voltage and ω_0 is the resonance angular velocity as given by (4a). The radius vector of the ion must pass through an additional angle, 2θ, however, before the ion crosses the gap again, at which time the dee voltage has become

$$V_0 \cos\left(\pi+\frac{\omega_0-\omega}{\omega_0}+\alpha+2\theta\right).$$

The path center will now be shifted along the dee gap by

$$\delta y=-\frac{e(r+\Delta r)}{2W}\cos\left(\frac{\omega_0-\omega}{\omega_0}\pi+\alpha+2\theta\right)\cos\theta \quad (5c)$$

or a total creep per revolution of approximately

$$\frac{\delta y}{\delta n}=\frac{erV}{2W}\Big[\cos\alpha - \cos\left(\frac{\omega_0-\omega}{\omega_0}\pi+\alpha+2\theta\right)\cos\theta\Big]. \quad (6c)$$

This neglects the effect of Δr in (5c) which merely causes the centers to oscillate back and forth about the average center but without a resultant creep. Expanding the cosine term of (6c) and neglecting $\cos\theta$, as θ is small, gives:

$$\frac{\delta y}{\delta n}=\frac{erV}{2W}\sin\left(\frac{\omega_0-\omega}{\omega_0}\pi+\alpha\right)\sin 2\theta \quad (7c)$$

and as $\theta=l/r$,

$$\frac{\delta y}{\delta n}=\frac{eVl}{W}\sin\left[\frac{\omega_0-\omega}{\omega_0}\pi+\alpha\right]. \quad (7.1)$$

Appendix IV

Path wandering caused by radial decrease of the magnetic field

It has been shown by P. Villard[14] that an ion off center in a radially homogeneous magnetic field will precess about the magnetic center. Thus the average position of the path center, if off from the magnetic center by a distance l, will move around a circle of radius l. Let us calculate the distance $\delta s/\delta n$ that the path center advances around this circle each revolution. As McMillan[4] has shown, $\delta s/\delta n$ is perpendicular to l and is given by

$$\frac{\delta s}{\delta n}=\int_0^{2\pi}\cos\theta\, dr, \quad (1d)$$

where θ is the angle between the radius vector of the ion and the direction perpendicular to l. We have the relation

$$dr=-rdH/H, \quad (2d)$$

so

$$\frac{\delta s}{\delta n}=-\int_0^{2\pi} r\cos\theta\frac{dH}{H}. \quad (3d)$$

Now the magnetic field between the pole faces can be expressed as

$$H=H_0\left[1-a\exp\left(-\pi\frac{r_0-r'}{\sigma}\right)\right], \quad (4d)$$

where r' is the distance from the magnetic center, r_0 is the radius of the pole faces, σ is half of the magnetic gap, and a is a constant.* The value of r' for the ion is $r-l\sin\theta$. Substituting (4d) into (3d) gives

$$\frac{\delta s}{\delta n}=\int_0^{2\pi}\frac{\pi lr}{\sigma}\cos^2\theta \times\exp\left[-\pi\frac{(r_0-r-l\sin\theta)}{\sigma}\right]d\theta, \quad (5d)$$

which can be expanded into a series and then integrated to give

$$\frac{\delta s}{\delta n}=\frac{\pi^2 arl}{\sigma}\exp\left(-\frac{\pi(r_0-r)}{\sigma}\right)\times\left[1+\frac{\pi^2 l^2}{4\sigma^2}+\cdots\right]. \quad (7.7)$$

[14] P. Villard, J. de phys. et rad. **7**, 439 (1908).

* This equation is derived by Rose, reference 22, who gives the value of a as about $\frac{1}{4}$. However, because of the saturation of the iron, a differs considerably from this value, and it is best to determine it experimentally.

Appendix V

Shimming equations for a constant radial magnetic field gradient

We assume a constant radial field gradient $-dH/dr$, and we wish to calculate its magnitude such that there is always focusing and such that there is a minimum loss of ions by their getting out of phase. Thus we wish dH/dr to be just large enough so that the magnetic focusing as given by (5.4) predominates over any electric defocusing as given by (4.1). Equating (4.1) and (5.4) and neglecting the in-phase type of focusing in (4.1) gives the relation:

$$\frac{V\sin\alpha}{\pi r^2}=\frac{\omega}{c}\frac{dH}{dr}r \tag{1f}$$

or

$$\frac{1}{H}\frac{dH}{dr}=\frac{e}{2\pi}\frac{V\sin\alpha}{qW^{\frac{1}{2}}}, \tag{2f}$$

where we have eliminated r, using (1), and where

$$q=r/W^{\frac{1}{2}}. \tag{3f}$$

We wish to find the maximum value of $(1/H)(dH/dr)$ as given by (2f) for ions being accelerated with an initial dee voltage V_0 which is given by

$$V_0=\frac{\pi}{2e}\left[\frac{\Delta H}{H}W'-\int_0^{W'}\left(\frac{W}{M_0c^2}+\frac{\delta H}{H}\right)dW\right]. \tag{6.2}$$

Now

$$\delta H/H=(1/H)(dH/dr)r, \tag{4f}$$

and, as we saw in Section 6, $\Delta H/H$ is the average value of the integrand of (6.2), i.e.,

$$\frac{\Delta H}{H}=\frac{1}{W_1}\int_0^{W_1}\left(\frac{W}{M_0c^2}+q\frac{1}{H}\frac{dH}{dr}W^{\frac{1}{2}}\right)dW$$

$$=\frac{W_1}{2M_0c^2}+\frac{2}{3}q\frac{1}{H}\frac{dH}{dr}W_1^{\frac{1}{2}}, \tag{5f}$$

where W_1 is the final energy. W' is the energy at which the integrand of (1) becomes equal to $\Delta H/H$, i.e.,

$$\frac{W'}{M_0c^2}+q'\frac{dH}{Hdr}W'^{\frac{1}{2}}=\frac{W_1}{2M_0c^2}+\frac{2}{3}q\frac{1}{H}\frac{dH}{dr}W_1^{\frac{1}{2}}, \tag{6f}$$

and as $W'\cong W_1/2$, a second approximation to W' from solving (6f) is

$$W'=\frac{W_1}{2}-0.040q\frac{M_0c^2}{H}\frac{dH}{dr}W_1^{\frac{1}{2}}. \tag{7f}$$

Substituting these in (6.2) and integrating gives

$$V_0=\frac{\pi}{2e}\left[\frac{W_1^2}{8M_0c^2}+0.12q\frac{1}{H}\frac{dH}{dr}W_1^{\frac{1}{2}}\right]. \tag{8f}$$

Now for an ion starting behind in phase $\pi/2$ radians,

$$\sin\alpha=-1+\Delta\sin\alpha$$

$$=-1+\frac{\pi}{eV}\left[\frac{\Delta H}{H}W-\int_0^W\left(\frac{W}{M_0c^2}+q\frac{1}{H}\frac{dH}{dr}W^{\frac{1}{2}}\right)dW\right]$$

$$=-1+\frac{\pi}{eV}\left[\frac{\Delta H}{H}W-\frac{W^2}{2M_0c^2}-\frac{2}{3}q\frac{1}{H}\frac{dH}{dr}W^{\frac{1}{2}}\right]. \tag{9f}$$

Substituting (8f) and (9f) into (2f) and solving for $(1/H)(dH/dr)$ gives

$$\frac{1}{H}\frac{dH}{dr}=-\frac{W_1^{\frac{1}{2}}}{4qM_0c^2}\left[\frac{E^{-\frac{1}{2}}-\frac{1}{8}E^{-\frac{1}{2}}-E^{\frac{1}{2}}}{\frac{4}{3}-\frac{1}{3}E^{-\frac{1}{2}}+\frac{0.12}{4}E^{-\frac{1}{2}}}\right]_{\max}, \tag{10f}$$

where $E=W/W_1$. The function of E within the brackets was plotted against E and it exhibited a maximum value of 0.56 at $E=0.27$. This determines the value of $(1/H)(dH/dr)$ we are after, i.e.,

$$(1/H)(dH/dr)=0.14W_1/RM_0c^2, \tag{8.2}$$

and substituting this value into (8f) gives

$$V_0=(0.22/e)(W_1^2/M_0c^2). \tag{8.1}$$

For an arbitrary $(1/H)(dH/dr)$, from (8f) we get

$$V_0=\frac{\pi}{2e}\left[\frac{W_1^2}{8M_0c^2}+0.12\frac{R}{H}\frac{dH}{dr}W_1\right], \tag{11f}$$

where R is the final radius.

Electrolytic Polishing. II

W. C. Elmore
Department of Physics, Swarthmore College, Swarthmore, Pennsylvania
(Received August 14, 1940)

From the assumptions underlying the diffusion theory of electrolytic polishing two quantitative current-time relations are deduced and compared with the behavior of a copper-orthophosphoric acid cell. One equation relates the current through the cell to the time required for the growth of the concentration layer necessary for polishing. The other equation describes the fall in limiting current once the layer is formed. Both equations are in accord with the results of some simple experiments designed to test them. The present study removes some of the mystery in electrolytic polishing and permits a more intelligent use of it to be made.

THE electrolytic polishing of metals by the Jacquet method has a number of uses in the laboratory.[1, 2] Recently there have been described several important industrial applications.[3] In view of the attention being paid to the method it is of interest to have a clear notion of the mechanism responsible for the polishing effect. In an earlier account[4] the writer described experiments which favor an explanation based on ideas of diffusion. The present investigation has been carried out in order to test the assumptions of this theory.

A metal is electrolytically polished by making it the anode in a cell containing a suitable electrolyte. Polishing occurs when a sufficiently great concentration layer has been established at the metal surface. In general each kind of metal requires its own individual electrolyte.[5] It seems likely, however, that the mechanism responsible for polishing is essentially the same for the various metal-electrolyte combinations.

To account for electrolytic polishing on the basis of diffusion the following assumptions are required. (1) When current passes through the cell dissolved metal leaves the vicinity of the anode for the most part by diffusion and not by migration. This requires that the concentration gradient at the anode be proportional at all times to the current density. Thus, for a plane anode of area A located at $x=0$ the current is given by

$$i=-AFD(\partial c/\partial x)_{x=0}, \tag{1}$$

where F is the faraday, c is the concentration of metal in equivalents, and D is the coefficient of diffusion of dissolved metal, assumed to be a constant. (2) After the current has passed for a certain time t_0 the concentration at the anode surface reaches a maximum value c_m which represents the solubility limit of the metal in the electrolyte. (3) At times later than t_0, provided that no new anode reaction occurs, the current is limited according to Eq. (1) by the concentration gradient which exists at the anode. By a new anode reaction is meant either that the anode becomes passive, that a salt is precipitated or that the electrolyte is decomposed or chemically altered. Any of these reactions may be unfavorable for satisfactory polishing.

From these assumptions it follows that when a limiting current has been established, as shown by a characteristic plateau in the voltage-current curve, metal going into solution will diffuse from high points on the surface more rapidly than from depressions, since, near the former, steeper concentration gradients will exist. Consequently the surface will become progressively more smooth. According to this theory electrolytic polishing may be considered a physical rather than a chemical phenomenon. The choice of suitable electrolytes would seem to rest solely on avoiding an unfavorable anode reaction after the onset of limiting current. In practice this requires that the undesired reaction occur at a sufficiently elevated overvoltage.

The diffusion theory has been suggested by

[1] For metallographic applications see P. A. Jacquet, Bull. Soc. chim. France **3**, 705 (1936), and numerous other publications by Jacquet between 1935 and the present.
[2] For other applications see H. Lowery, H. Wilkinson and D. L. Smare, Phil. Mag. [7] **22**, 769 (1936); and J. M. Hughes and E. A. Coomes, Phys. Rev. **55**, 1138A (1939).
[3] For a summary see S. Tour, The Iron Age [21] **145**, 56 (1940); [22] **145**, 26 (1940).
[4] W. C. Elmore, J. App. Phys. **10**, 724 (1939).
[5] For a list of metal-electrolyte combinations see Metals and Alloys **11**, MA23 (1940), January.

two observations. (1) For a range of initial currents the anode polarization back e.m.f. has the same value at the onset of limiting current.[4] (2) A limiting current is necessary for polishing.[1] In order to place the theory on a firmer basis, certain current-time relations for the concentration layer will be calculated and compared with the behavior of a $Cu-H_3PO_4$ cell.

To discuss the growth of a concentration layer it is necessary to solve the diffusion equation

$$D(\partial^2 c/\partial x^2)=\partial c/\partial t, \tag{2}$$

subject to appropriate boundary conditions. This may be done by Fourier analysis using either series or integrals. Since in practice the cathode to anode distance is large compared with the thickness which the concentration layer attains during polishing,[1] solution by an infinite integral is to be preferred, or what amounts to the same thing, solution by the Heaviside operational method.[6]

Let us assume that the concentration of metal dissolved in the electrolyte is everywhere zero at time $t=0$, at which instant a steady current i_0 is established. It is desired to find the concentration of metal in solution at the anode as a function of time.[7] Writing $p=\partial/\partial t$, Eq. (2) has the formal solution

$$c(x, t)=e^{-x(p/D)^{\frac{1}{2}}}c(0, t). \tag{3}$$

On using Eq. (1), the following operational relation between current and concentration is found

$$c(0, t)=[1/AF(Dp)^{\frac{1}{2}}]i(t). \tag{4}$$

Placing $i(t)=i_0 1$, where 1 is the Heaviside unit function, it follows that

$$c(0, t)=(i_0/AFD^{\frac{1}{2}})p^{-\frac{1}{2}}1=[2i_0/AF(\pi D)^{\frac{1}{2}}]t^{\frac{1}{2}}. \tag{5}$$

Thus, when $c(0, t)=c_m$, defining the time t_0,

$$i_0 t_0^{\frac{1}{2}}=\tfrac{1}{2}c_m AF(\pi D)^{\frac{1}{2}}=\text{Const.} \tag{6}$$

Let us now consider the behavior of the current after the condition of limiting current is reached on the assumption that no new anode reaction occurs other than the formation of a hydroxyl ion double layer which gives rise to the overvoltage mentioned earlier in the paper.[8] Equation (4) must be solved with $c(0, t)$ given by

$$c(0, t)=[2i_0/AF(\pi D)^{\frac{1}{2}}][t^{\frac{1}{2}}1+(t_0^{\frac{1}{2}}-t^{\frac{1}{2}})1_{t_0}], \tag{7}$$

which states that the concentration at the anode grows according to Eq. (5) until $t=t_0$ and then remains constant. By using the transfer operator $\exp(-t_0 p)$, expanding $[1+(t/t_0)]^{\frac{1}{2}}$ by the binomial theorem, and replacing terms containing powers of t by their operational equivalents, Eq. (7) becomes

$$c(0, t)=(i_0/AFD^{\frac{1}{2}})\left\{p^{-\frac{1}{2}}-2(t_0/\pi)^{\frac{1}{2}}e^{-t_0 p}\left[\frac{1}{2}(t_0 p)^{-1}-\frac{1\cdot 1}{4}(t_0 p)^{-2}+\frac{1\cdot 1\cdot 3}{8}(t_0 p)^{-3}-\cdots\right]\right\}1, \tag{8}$$

which expresses the time dependence in operational form. To obtain $i(t)$ this equation must be multiplied by $AF(Dp)^{\frac{1}{2}}$ and the operational expression replaced by the equivalent time function. When this is done the infinite series can be identified as an inverse tangent, giving as a final result

$$i(t)=i_0 1-(2i_0/\pi)\tan^{-1}[(t-t_0)/t_0]^{\frac{1}{2}}1_{t_0}. \tag{9}$$

Hence the current, after remaining at the value i_0 until time t_0, drops according to the following law

$$i/i_0=1-(2/\pi)\tan^{-1}[(t-t_0)/t_0]^{\frac{1}{2}}=(2/\pi)\cot^{-1}[(t-t_0)/t_0]^{\frac{1}{2}}. \tag{10}$$

TABLE I. *Typical data taken with* $Cu-H_3PO_4$ *cell to test Eq. (6).*

Sp. Gr.	T°C	i_0 in Amp.	t_0 in Sec.	$i_0 t_0^{\frac{1}{2}}$
1.330	23.5	0.100	438	2.10
		.150	195	2.10
		.200	110	2.10
		.250	70.4	2.10
		.300	48.5	2.09
		.400	27.3	2.09
		.500	17.3	2.08
		.600	12.1	2.09
1.200	24.0			av. 2.72
1.300	24.0			av. 2.28
1.400	23.5			av. 1.68
1.500	24.0			av. 1.17
1.600	24.0			av. 0.76

[6] See, for instance, V. Bush, *Operational Circuit Analysis* (Wiley, 1929). Appendix C contains the necessary operational formulas.

[7] The solution of the diffusion equation for this case is well known; its application to electrolytic polishing is believed to be new.

[8] A small transient current (which can be neglected) is required to form the double layer.

Data to test Eq. (6) have been obtained with a $Cu-H_3PO_4$ cell. Uniform current density at the anode (of area 3.30 cm²) was insured by making it the bottom of a cylindrical cell.[4] The current i_0 was maintained at a steady value until it began to drop rapidly and the time required for the onset of this drop was interpreted as t_0. Table I summarizes data taken for several electrolyte concentrations, for each of which the prediction that $i_0 t_0^{\frac{1}{2}} = \text{Const.}$ is found to be well verified. Detailed data are given for one concentration and the average value of $i_0 t_0^{\frac{1}{2}}$ from equally consistent data is shown for the other concentrations. The decrease in the value of the constant with increased acid concentration is to be expected, for the solubility limit c_m of copper should be less when there is more acid present. If it is assumed that $D \doteqdot 10^{-6}$, then for $i_0 t_0^{\frac{1}{2}} = 2.1$ Eq. (6) gives $c_m \doteqdot 7.5$ equivalents/liter, a value which appears high, but not unreasonably so. An electrolyte of specific gravity as low as 1.200 does not polish satisfactorily, since a copper salt is precipitated on the anode after the concentration layer is formed.

To obtain data to test Eq. (10) an electric timer was turned on when the current i_0 was established. The current was again maintained at a steady value until it began to drop rapidly, at which instant the timer was stopped and simultaneously a source of time signals started. The cell voltage was then allowed to increase as the current dropped and current readings were taken at each time signal. Typical data thus secured with the $Cu-H_3PO_4$ cell are presented in Fig. 1. Oxygen liberation caused no trouble since an upper limit to the cell voltage was set by the two volts available from a storage cell. If the cell voltage was adjusted to keep it at all times below some lower value, for instance 1.8 volts, no significant changes in the results shown in Fig. 1 were found. This point is mentioned to illustrate the secondary role that voltage plays, i.e., the voltage need only be on the plateau of the voltage-current curve. The success of the experimental tests of Eqs. (6) and (10) indicates that the assumptions underlying the equations constitute an adequate basis for the diffusion theory of electrolytic polishing.

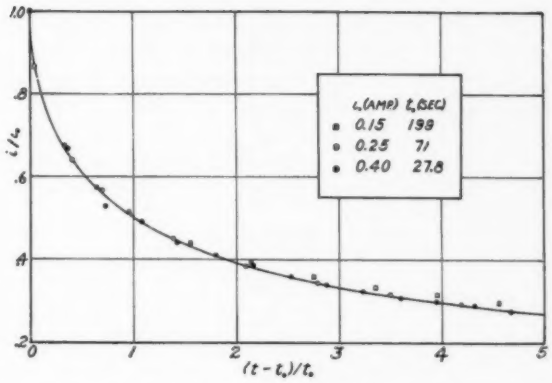

FIG. 1. Fall of limiting current with time. Curve calculated from Eq. (10); experimental points for copper anode in H_3PO_4, sp. gr. 1.330, $T = 24°C$.

A few practical conclusions may be drawn from the present study. For a given concentration of electrolyte polishing is effected with the least removal of metal if the concentration layer is formed with the largest practicable current. The gain in this respect may be estimated from Eq. (6). After the layer is formed, the current decreases according to Eq. (10). On account of resistance in the circuit the cell voltage will at the same time increase, the increase being taken up by a double layer at the anode. For successful polishing the potential of the double layer must not be allowed to exceed the overvoltage value for the next anode reaction, such as the liberation of oxygen, or the establishment of passivity. Electrolytes of very high acid concentration have a high resistivity, making adequate voltage control more difficult. Furthermore, the layer is quickly formed by a moderate current which then drops fairly rapidly so that the polishing process may be unduly prolonged. Electrolytes of fairly low acid concentration require a relatively long time for the layer to form, and hence for certain uses may not be satisfactory even though no difficulties of a chemical nature arise to prohibit their use. Between these two not very well defined limits there is a range of concentrations which should be useful.

A Graphical Method for Selecting Suitable Radiations for the Precision Determination of Noncubic Lattice Constants and for Indexing Back-Reflection Lines in Powder X-Ray Photograms

LOUIS A. CARAPELLA
Laboratory of Physical Metallurgy, Harvard University, Cambridge, Massachusetts

(Received August 18, 1940)

A simple method by which the proper radiation or combination of radiations may be selected for the precision determination of hexagonal, rhombohedral, and tetragonal lattice constants is described and illustrated in detail. The method involves the use of specially prepared charts. With a knowledge of the approximate lattice constants, positions of diffraction lines with $\theta > 60°$; i.e., back-reflection lines, can be predicted directly from the charts for any common radiation. From the number, distribution, and indices of back-reflection lines, a suitable target may be chosen for an accurate determination of lattice constants. Furthermore, the charts are useful for predicting positions of beta-lines, and for indexing without calculation back-reflection lines in powder x-ray photograms of hexagonal, rhombohedral, or tetragonal lattices.

INTRODUCTION

PRECISE determinations of hexagonal, rhombohedral and tetragonal lattice constants by extrapolation methods[1–3] require a minimum of three back-reflection lines with at least one line having $\theta > 72°$. A larger number of lines near complete back-reflection is generally desirable for higher accuracy. Moreover, if the indices of the lines are not selected with care, the two lattice constants of these systems may be determined with widely differing precision. This may be avoided by a proper choice of radiations.

Hitherto, there has been no simple and direct means by which number, positions and indices of back-reflection lines for a given lattice could be obtained from common radiations. Calculations of such information are, indeed, long and tedious, yet necessary if the proper choice is to be made. The accompanying charts, however, eliminate calculation and yield directly for any radiation the number, distribution and indices of back-reflection lines from the approximate lattice constants. A possible target may then be selected from the general distribution of lines, but it is important to note that good distribution does not necessarily determine both constants with high precision. Jette and Foote[4] have already considered this fact in detail and have shown that if the relative errors in the lattice constants, a_0 and c_0, are to be the same, the data from which they are derived, must satisfy the following equations:

(a) For hexagonal (or rhombohedral)[5] lattices:

$$\left(\frac{16}{9}\right)\left(\frac{c_0}{a_0}\right)^4 = \frac{C_A}{C_B}. \tag{1}$$

(b) For tetragonal lattices:

$$\left(\frac{c_0}{a_0}\right)^4 = \frac{C_A}{C_B}, \tag{2}$$

where a_0 and c_0 are lattice constants,[6] while C_A and C_B are minors of the indices elements in the determinants of the coefficients in the normal equations,[3, 4] and are defined thus:

(a) For hexagonal (or rhombohedral) lattices:

$$\frac{C_A}{C_B} = \frac{\begin{vmatrix} \sum(l^2)^2 & \sum(l^2)(\phi \sin 2\phi) \\ \sum(l^2)(\phi \sin 2\phi) & \sum(\phi \sin 2\phi)^2 \end{vmatrix}}{\begin{vmatrix} \sum(h^2+hk+k^2)^2 & \sum(h^2+hk+k^2)(\phi \sin 2\phi) \\ \sum(h^2+hk+k^2)(\phi \sin 2\phi) & \sum(\phi \sin 2\phi)^2 \end{vmatrix}}, \tag{3}$$

[1] A. J. Bradley and A. H. Jay, Proc. Phys. Soc. London **44**, 563 (1932).
[2] J. Weigle, Helv. Phys. Acta **7**, 46, 51 (1934).
[3] M. U. Cohen, Rev. Sci. Inst. **6**, 68 (1935); **7**, 155 (1936); Zeits. f. Krist. **94**, 288 (1936).
[4] E. R. Jette and F. Foote, J. Chem. Phys. **3**, 605 (1935).
[5] The space geometry of rhombohedral lattices is such that they may be expressed as hexagonal lattices by a simple transformation of crystallographic axes. Thus, for the sake of convenience, rhombohedral lattices shall be treated throughout as a subdivision of the hexagonal system. Of course, it must be remembered that such a transformation will give rise to certain characteristic vanishings.
[6] For preliminary consideration, the constants need not be known to more than three significant figures.

(b) for tetragonal lattices:

$$\frac{C_A}{C_B}=\frac{\begin{vmatrix}\sum(l^2)^2 & \sum(l^2)(\phi\sin 2\phi)\\ \sum(l^2)(\phi\sin 2\phi) & \sum(\phi\sin 2\phi)^2\end{vmatrix}}{\begin{vmatrix}\sum(h^2+k^2)^2 & \sum(h^2+k^2)(\phi\sin 2\phi)\\ \sum(h^2+k^2)(\phi\sin 2\phi) & \sum(\phi\sin 2\phi)^2\end{vmatrix}}, \tag{4}$$

where h, k, l are the Miller indices of any diffracting plane, and ϕ is the complement of the Bragg angle of diffraction (i.e., $\phi=\pi/2-\theta$). Thus, the method for selecting proper targets to determine a set of lattice constants with great accuracy and with equal precision involves the use of specially prepared charts and the above equations.

The charts are also useful for indexing back-reflection lines in powder patterns of hexagonal, rhombohedral, and tetragonal lattices without calculation provided the approximate lattice constants and the radiation are known. Moreover, beta-lines can be readily identified by means of the charts.

Construction of Charts

The fundamental equation of x-ray diffraction in any crystal lattice is given as:

$$d=\frac{\lambda}{2\sin\theta}\ \text{(Bragg law)}, \tag{5}$$

where d is the interplanar spacing, λ, the wave-length of the radiation used and θ, the angle of diffraction. Furthermore, it can be shown by space geometry that in hexagonal, rhombohedral and tetragonal lattices, d has the following relationships:

(a) For hexagonal (and rhombohedral)[5] lattices:

$$d/a_0=\frac{1}{\left[\frac{4}{3}(h^2+hk+k^2)+\frac{l^2}{(c_0)^2/(a_0)^2}\right]^{\frac{1}{2}}}. \tag{6}$$

(b) For tetragonal lattices:

$$d/a_0=\frac{1}{\left[h^2+k^2+\frac{l^2}{(c_0)^2/(a_0)^2}\right]^{\frac{1}{2}}}. \tag{7}$$

The charts shown in Figs. 1, 2, and 3, are actually a graphical representation of Eqs. (5), (6) and (7). Figures 1 and 2 deal with hexagonal (and rhombohedral), and Fig. 3 with tetragonal, lattices. In the lower portion of each chart—see Fig. 1, for example—is plotted Eq. (5), with d as a function of θ for common radiations. Shown also in the same portion is a plot of d/a_0 against d, on a common ordinate, for various values of a_0. The curves in the upper portion are representative of Eq. (6), for hexagonal and rhombohedral lattices, and Eq. (7) for tetragonal lattices, in which c_0/a_0 is plotted against d/a_0 (on a common abscissa, as the lower curves) for various values of h, k, l. To facilitate the use of the charts, the indices of rhombohedral lattices in Fig. 2 are indicated by the letter r, and those of tetragonal lattices, in Fig. 3, by b, and f, for body-, and face-centered types, respectively.

Applicability of Charts

In their final forms, the charts are useful for selecting suitable radiations for the precision determination of noncubic lattice constants. As an illustration, let us select the proper target which will give with equal precision a more precise value of the lattice constants of a hexagonal lattice having $a_0\approx 2.50$A and $c_0/a_0\approx 1.62$. We then proceed by means of the charts to consider the number, indices, and distribution of diffraction lines for each radiation. Let us, for example, start with cobalt $K\alpha$ radiation.[7] The number and indices of diffraction lines are quickly determined by drawing horizontal lines, such as AB and DE, from the extremities of the cobalt $K\alpha$ radiation curve until they intersect the proper lattice constant line ($a_0\approx 2.50$A), see Fig. 1. At points of intersection, vertical lines, BC and EF, are next drawn to intersect at F and C along the horizontal line representing $c_0/a_0\approx 1.62$. The number and indices of possible diffraction lines for cobalt

[7] The average value of wave-lengths of $K\alpha$ doublets has been used for all $K\alpha$ radiations.

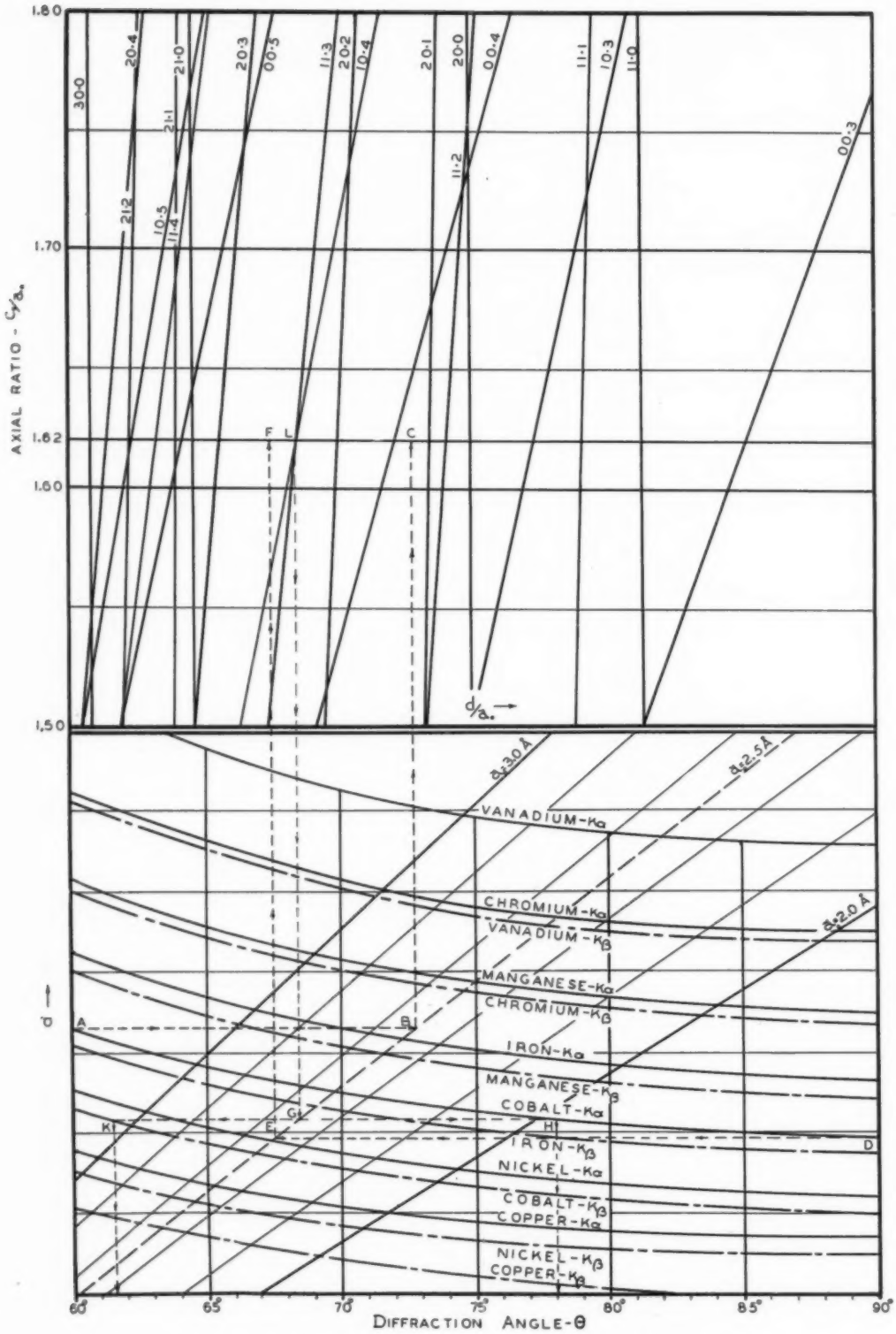

FIG. 1. Illustrating the use of a chart for hexagonal lattices.

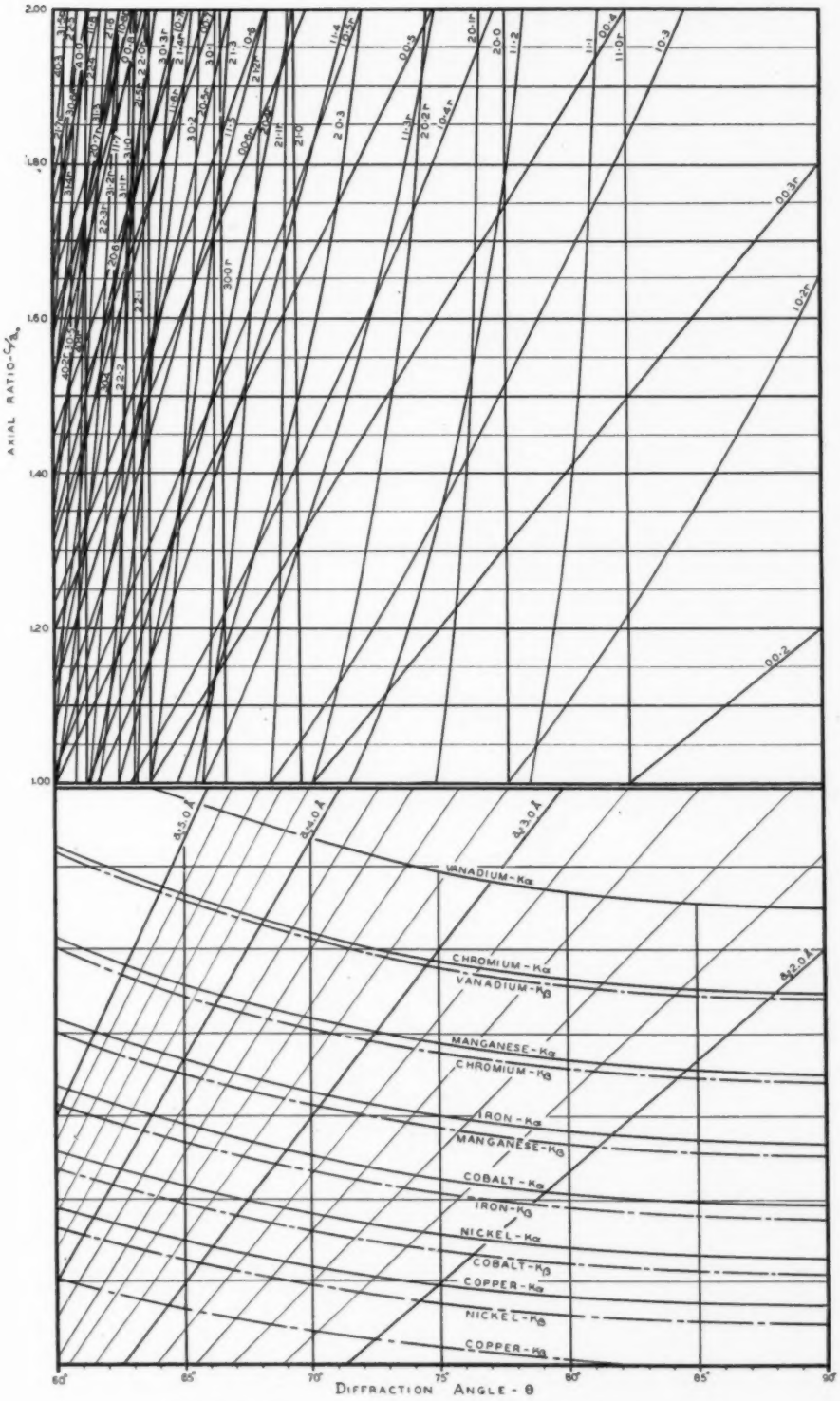

FIG. 2. Chart for hexagonal and rhombohedral lattices.
r = indices of rhombohedral lattices.

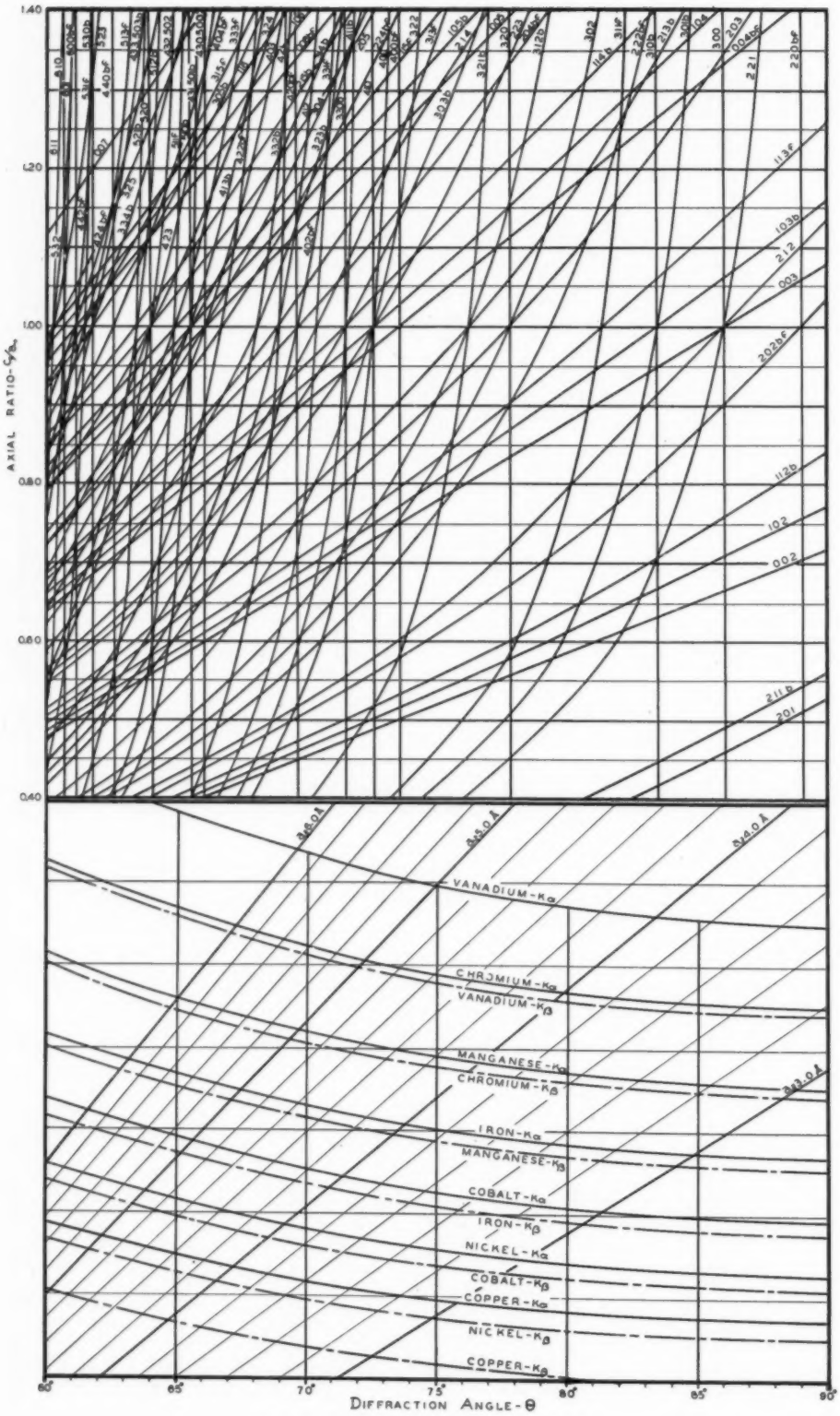

FIG. 3. Chart for tetragonal lattice.
b = indices of body-centered type;
f = indices of face-centered type.

$K\alpha$ radiation are then read from the indices curves which intersect the horizontal line between F and C. There are four lines in all, 11·3, 10·4, 20·2 and 00·4, respectively. The θ-values may be obtained for each diffraction by drawing a vertical line, such as LG, from the point of intersection made by the indices curve with the horizontal line, until it intersects the lattice-constant line. At the point G, another horizontal is drawn to meet the cobalt $K\alpha$ radiation curve at the angle of diffraction, $\theta=78.1°$ for 11·3 and 10·4 lines. In like manner, each radiation has been considered and the results are tabulated in Table I.

From the data compiled in Table I and Eqs. (1) and (3), it is possible to note the influence of each radiation or combination of radiations upon the precision with which each constant may be determined. The results are shown in Table II. By applying Eq. (1) to the above problem, we get:

$$C_A/C_B=\frac{16}{9}(1.62)^4=12.24. \qquad (8)$$

Rarely is the above equation ever satisfied, but excessive deviations from it may be eliminated by the proper selection of radiations. Cobalt radiation seems to be in reasonable agreement with Eq. (8). It has, however, one possible disadvantage in that the 10·4 and 11·3 lines may not be in absolute coincidence. A slight variation from coincidence may produce blurred lines which are not measurable with accuracy, and so for this reason cobalt may turn out to be undesirable. Copper radiation, however, has an excellent distribution of back-reflection lines and deviates none too seriously from Eq. (8), and, therefore, may be selected[8] as an alternative.

TABLE I. *Diffraction lines and their distribution for a hexagonal lattice with* $a_0\approx 2.50A$, $c_0/a_0\approx 1.62$.

	θ-VALUES IN DEGREES FOR COMMON $K\alpha$ RADIATIONS						
hk·l	VANADIUM	CHROMIUM	MANGANESE	IRON	COBALT	NICKEL	COPPER
00·3	67.7°						
11·0		65.7°					
11·1		73.2°	62.0°				
10·3			65.6°				
20·0			75.0°	63.0°			
11·2			81.2°	65.6°			
20·1				67.5°			
00·4				73.1°	62.2°		
20·2					69.0°		
10·4					78.1°	64.3°	
11·3					78.1°	64.3°	
20·3						78.4°	
21·0							70.1°
00·5							72.2°
21·1							73.7°
11·4							78.3°

TABLE II. *The influence of radiations on the precision of each lattice constant.*

RADIATIONS	NO. LINES	CA/CB (CALC.)	$\frac{CA}{12.24(C_B)}$	REMARKS*
Vanadium $K\alpha$ Chromium $K\alpha$	1 2	6.20‡	0.51‡	$a_0>c_0$
Manganese $K\alpha$	4	3.09	0.25	$a_0>c_0$
Iron $K\alpha$	4	52.58	4.30	$a_0<c_0$
Cobalt $K\alpha$	4	12.11	0.99	$a_0\approx c_0$
Nickel $K\alpha$	3	4.31	0.35	$a_0>c_0$
Copper $K\alpha$	4	16.83	1.38	$a_0\approx c_0$

* The relative precision with which the constants may be determined for a given radiation is shown in this column.
‡ The combination of vanadium and chromium radiations was chosen because neither radiation alone gives the minimum number of diffraction lines required for extrapolation methods; namely, three.

The indexing of back-reflection lines in noncubic powder pattern can also be done directly from the charts, providing the diffraction angle, radiation, and approximate lattice constants are known. For example, the indices of a line which appears at $\theta=78.1°$ in a hexagonal powder pattern taken with cobalt radiation and having the following lattice constants, $a_0\approx 2.50A$, $c_0\approx 4.05A$, and $c_0/a_0\approx 1.62$, are found to be 11·3 and 10·4. The solution, in brief, was obtained by drawing lines such as HG and GL, as shown in Fig. 1. The position of its beta-diffraction is found by simply drawing a horizontal line, such as KGH, until it intersects the cobalt $K\beta$ radiation curve at its angle of diffraction, $\theta=61.6°$.

The procedure thus far described, applies not only to hexagonal but also to rhombohedral and tetragonal lattices. For certain axial ratios, the tetragonal chart may also be used for cubic lattices; however, other simplified charts[9] are more recommendable for this purpose.

The author feels indebted to Professor Ralph R. Hultgren for many suggestions.

[8] Before making the final selection, some consideration should be given to the absorption characteristics of the material under investigation.
[9] L. A. Carapella, J. App. Phys. **11**, 510 (1940).

Introduction to the Problem of the Isochronous Hairspring

S. Goudsmit and Ming-chen Wang
Department of Physics, University of Michigan, Ann Arbor, Michigan
(Received August 31, 1940)

Deviations from isochronism for the system of hairspring and balance wheel are treated by a method due to Haag. The results are given a geometrical interpretation. It is shown that the deviations are related to the displacement of the end point of the hairspring in a set-up in which this end point is free to move keeping its tangent constant in direction. Such an arrangement can be realized with Bouasse's pendulum. For the so-called "helical" spring a more accurate solution than Phillips' has been found for the shape of the terminals. Extensive numerical calculations have been made for flat spiral springs, and a new simple terminal has been designed.

I. The Problem

1. Introduction

THE system of hairspring and balance wheel in use to regulate watches and chronometers does not perform an exact simple harmonic motion and the period of the vibrations depends upon the amplitude of the balance wheel. In watches this amplitude may vary from 270° to each side, immediately after winding, down to 150° at the time the watch has to be rewound. For the proper functioning of the watch it is necessary to reduce the lack of isochronism of the vibrations as much as possible.

One end of the hairspring is fastened to the axis of the balance wheel, the other end by means of the "stud" to the frame of the watch. If the balance wheel is turned out of its equilibrium position, a reaction force is set up in the two end points. The mathematical analysis of the problem shows that this reaction force is the cause of the deviations from isochronism. The simplest and most rigorous mathematical treatment of the problem has been given by J. Haag[1] of the Institut de Chronométrie at Besançon, France. Unfortunately this beautiful method appears to be described only in a very short note in the *Proceedings of the 3rd International Congress for Applied Mechanics*, which does not contain any reference to a more detailed publication. The present paper is based almost entirely on the method used in Haag's note and the mathematical part gives a detailed derivation of some of the formulas given there.

[1] J. Haag, *Proceedings of the 3rd International Congress for Applied Mechanics, II* (1931), pp. 96–98.

2. Method of Phillips

If the shape of the spring is designed so as to make the reaction force at the end points as small as possible the deviations from isochronism will be correspondingly small. This is, at least in principle, the approach to the problem as given in the famous classical article by Phillips.[2] For the spring of finite length fastened to balance axis and stud, the reaction force can never be made exactly zero, but by using a special shape for the end portions of the spring, the "terminals," this force can be reduced considerably.

3. Method of Résal and Caspari

It is also possible to design the shape of the hairspring so that the reaction force changes the period by an amount which is approximately independent of the amplitude. This is, in principle, the solution given by Résal and Caspari.[3] In this case the reaction force does not need to be small. The Phillips' type of solution, however, seems to be preferred in practical applications.

4. End point displacement of free-end spring

Bouasse has pointed out that perfect isochronism for a flat spring would result if the outer end point were not fixed at the stud, but were free to move in the plane of the spring, provided the direction of the tangent at that end point remained the same. This parallel displace-

[2] M. Phillips, Ann. des Mines, Mémoires 20, 1–107 (1861).

[3] See the excellent survey of the problem in *Pendule, Spiral, Diapason* by H. Bouasse, Vol. II, Chap. V (Delgrave, Paris, 1920). Unfortunately Bouasse does not give any references and we have been unable to locate the original articles by Résal and Caspari.

ment can, of course, not be realized in a watch, but it may be visualized by means of the large scale model, shown in Fig. 1. Bouasse proposes that the end point of the model spring be fastened to the end of a long rod which can move as a spherical pendulum. The end point will, indeed, move parallel with itself and, if the pendulum is well balanced by means of the counter weight at the top, it will not create a reaction force on the end of the spring. We shall call this arrangement a "free-end spring."

If the axis to which the inner end of the spring is fastened is turned over a certain angle, the outer end point will experience a displacement. This displacement is approximately proportional to the reaction force which would exist at the end point if it were fixed at the stud instead of free to move. The Phillips solution is therefore equivalent to designing a spring for which the free-end displacement is as small as possible.

This approach reduces the dynamical problem to a geometrical one. Furthermore a crude large scale model like that of Fig. 1 can actually be used to give some information about the end point displacement and the isochronism for various shapes (see Fig. 2); whereas measurements of the reaction forces and periods are more difficult to perform. We shall, in the following, obtain the dynamical properties of the actual spring with both ends fixed by studying the end point displacement of the same spring considered as a free-end spring.

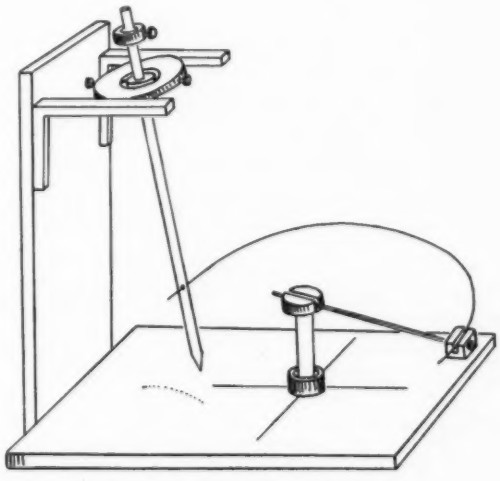

FIG. 1. Bouasse's pendulum.

II. Results and Applications

1. The "helical" spring

The calculations of Phillips deal with the so-called "helical" spring. As, however, the height of the helix is neglected, they are strictly valid only for a fictitious flat spring of several windings, all having exactly the same radius. Nevertheless the consideration of the idealized spring is useful as an illustration of the problem, because the calculations can be executed explicitly. Figure 3 shows the actual path of the end point for a "helical" spring of 10 windings and total length L. The line from the balance wheel axis to the end point in the rest position is chosen as the positive x axis. Figure 4 is for $10\frac{1}{4}$ windings.

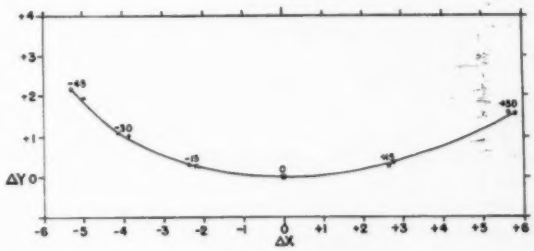

FIG. 2. End point displacement in cm for a semicircle of radius 15.5 cm; (●) calculated, (×) obtained by the model shown in Fig. 1. Numbers on curve indicate the angle of rotation of the balance wheel. Positive values mean unwinding and negative mean winding up.

The end point displacement is greatly reduced when the "terminals" of the spring are given a different shape fulfilling the first approximation calculated by Phillips. The magnitude of the displacement is roughly 20 times smaller, which reduces the deviation from isochronism by a factor of the order 400. If the terminals fulfill both the first and second approximations, the displacement will be about 300 times smaller.

2. Résal-Caspari solution for the helical spring

The mathematical treatment shows that the period of the vibrations of the fastened spring will be changed by an almost constant amount if the shape is such that for the free-end spring the ratio $(|\Delta|/\alpha)^2$ is a constant plus an odd function of α, where $|\Delta|$ is the magnitude of the end point displacement, and α the angle turned by the balance wheel. This is realized for a "helical" spring with $n+\frac{1}{4}$ and $n-\frac{1}{4}$ windings,

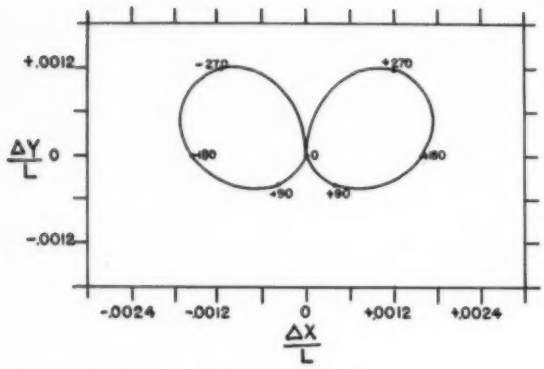

FIG. 3. End point displacement for "helical" spring of 10 windings (displacement decreases with the square of the number of windings), total length L.

according to Résal and Caspari, as we shall prove below.

3. Flat spiral spring

For the hairsprings used in watches the calculation must be done numerically. The terminals usually applied to a flat spiral are the same as those calculated by Phillips for a "helical" spring with the same radii as the inner and out-most windings. Figures 5 and 7 indicate the smaller end point displacement. A disadvantage is that the outer terminal has to be bent out of the plane of the spiral, because it comes nearer to the axis than the outer windings. This deflection is not considered in the calculation.

An ingenious solution has been proposed by Van den Broek,[4] who considers a spring which first winds outward and then spirals inward again: the two spirals unfortunately must lie in different planes. Figure 6 shows that this double spiral has indeed a small end point displacement.

Figures 5 and 7 indicate also the reduction in end point displacement for a new terminal. It is certainly as satisfactory as the Phillips' terminal and has the great advantage that it is completely in the same plane as the spiral. Its construction is shown in Fig. 8.

4. Center of gravity

The mathematical analysis shows that the deviation from isochronism depends not only upon the end point displacement Δ but also upon $d\Delta/d\alpha$. The deviation is in fact proportional to the product $\alpha|\Delta|d|\Delta|/d\alpha$ averaged over a period of the balance wheel. Considering Δ as a vector it is possible to show that $d\Delta/d\alpha$ is connected with the position of the center of gravity of the free-end spring. If the vector $\mathbf{G}$ indicates the position of the center of gravity as a function of the rotation angle we shall show later that the above-mentioned product can also be written as $\alpha|[\mathbf{G}\times\Delta]|$.

It is obviously advantageous to have the center

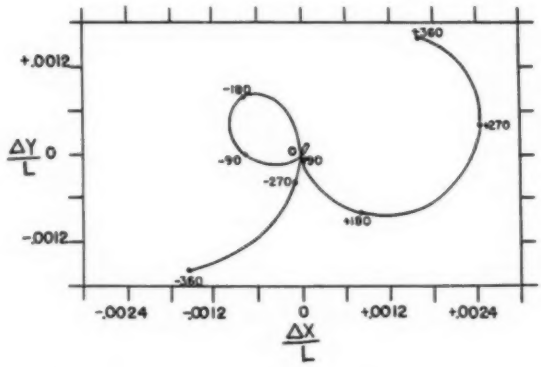

FIG. 4. End point displacement for "helical" spring of $10\frac{1}{4}$ windings, total length L.

of gravity as near as possible to the balance axis in order to make this product small. However, it is not necessarily best to place the balance axis at the center of gravity of the undistorted spring. This will certainly make the product small for small angles α, but for the usual large amplitudes $\alpha|[\mathbf{G}\times\Delta]|$ may become larger, as is the case for Archimedes spirals.

The vectors $\boldsymbol{\Delta}$ and especially $\mathbf{G}$ are rather complicated functions of the rotation angle α. The occurrence of a vector product adds to the complication. It is, therefore, advisable to disregard the interpretation in terms of the center of gravity of the free-end spring and to consider the much simpler quantities $|\Delta|$ and $d|\Delta|/d\alpha$. Figure 7 shows the change in $|\Delta|$ for an Archimedes spiral of 13.5 windings after addition of Phillips' terminals, and also for the new outer terminal.

III. MATHEMATICAL

1. Notation

We choose a coordinate system with its origin at the axis of the balance wheel. It is advan-

[4] J. A. Van den Broek, Trans. Am. Soc. Mech. Eng. **53**, APM page 247 (1931).

tageous, though not necessary, to take either the inner or the outer end point of the spring on the positive x axis. The shape of the spring is characterized by giving at each point the angle ψ which the tangent makes with the x axis as a function of s, the arc length, measured from the inner end point (Fig. 9). The formulas are simplified by combining the x and y coordinates into a complex number

$$z=x+iy.$$

In this notation we have for the equation of the spring

$$x(s)=x(0)+\int_0^s ds\cos\psi(s),$$

$$y(s)=y(0)+\int_0^s ds\sin\psi(s)$$

or

$$z(s)=z(0)+\int_0^s dse^{i\psi(s)}, \tag{1}$$

where $z(0)$ determines the position of the inner end point. Differentiation after the arc length s shall be indicated by a prime, thus

$$z'(s)=e^{i\psi(s)}. \tag{2}$$

The curvature $1/\rho$ at each point is given by

$$1/\rho=\psi'(s). \tag{3}$$

When the balance wheel is rotated over an angle α, the spring will be distorted and the new shape can be characterized by giving the change in $\psi(s)$. This change of angle for each element is denoted by $\phi(s)$. It depends upon the amount α the balance wheel is turned, and also upon the conditions at the end point. It will be a different function for the "free-end" spring and the spring

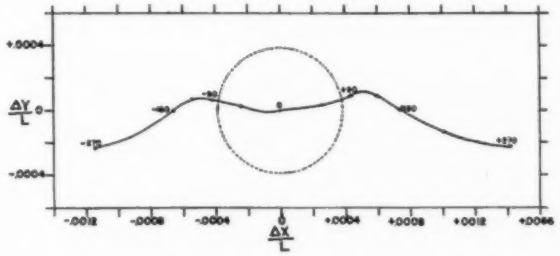

FIG. 5. End point displacement for Archimedes spiral of 13½ windings, inner radius 1, outer radius 2.35, length 45.2π. The dotted circle indicates the range of the end point path for this spiral plus Phillips' terminals, or an outer terminal as shown in Fig. 8.

fastened at the stud. The change in curvature of each element of the spring due to the distortion is given by

$$\text{change in curvature}=\phi'(s). \tag{4}$$

2. Elastic energy

If the deformation is within Hooke's law the energy stored in each element of a distorted spring is proportional to the square of the

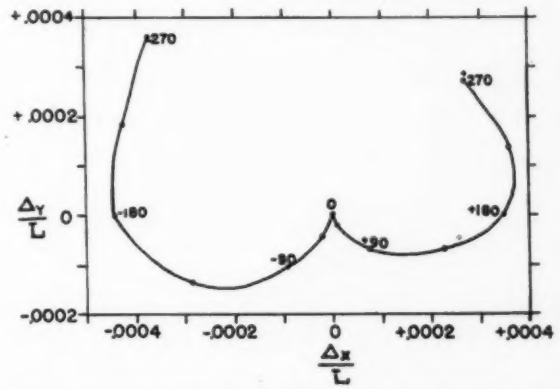

FIG. 6. End point displacement for Van den Broek double spiral of 6 windings in and out, inner radius 1, outer radius 2.2, total length $L=37.2\pi$.

change in curvature. The total potential energy V is therefore

$$V=\frac{k}{2}\int_0^L \phi'^2(s)ds. \tag{5}$$

The constant k depends upon the material of the spring and its cross section, L is the total length of the spring.

When the balance wheel is turned, the distorted shape of the spring will be such that the energy V is a minimum, subject to the proper conditions at the two end points. The determination of $\phi(s)$ is thus a standard problem of the calculus of variations.

3. The free-end spring

We denote by $z_f(s)$ and $\phi_f(s)$ the functions $z(s)$ and $\phi(s)$ of the "free-end" spring after distortion. When the balance wheel is turned over an angle α, the inner end point moves in a circle over the same arc, thus

$$z_f(0)=z(0)e^{i\alpha}. \tag{6}$$

The position of the outer end point is not prescribed. The free-end spring was defined such

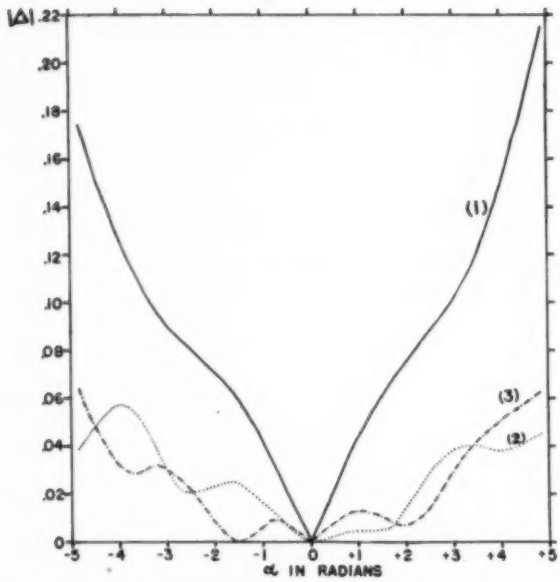

FIG. 7. Magnitude of end point displacement $|\Delta|$ as function of rotation angle α. (1) For Archimedes spiral, inner radius 1, outer radius 2.35, 13.5 windings, (2) with Phillips' terminals, (3) with new outer terminal of Fig. 8.

that the tangent at the outer end point remains the same as before the distortion. At the inner end point the tangent turns over the angle α, giving

$$\phi_f(L)=0, \tag{7}$$

$$\phi_f(0)=\alpha. \tag{8}$$

With these boundary conditions the minimum of the potential energy of Eq. (5) is simply determined by

$$\phi_f''(s)=0, \tag{9}$$

which has the solution

$$\phi_f(s)=-\alpha s/L+\alpha. \tag{10}$$

It also follows that

$$\phi_f'(s)=-\alpha/L. \tag{11}$$

The latter result means that for the free-end spring the change in curvature is the same everywhere along the spring and proportional to the angle of rotation α.

4. End point displacement

The end point displacement Δ is given by

$$\Delta=z_f(L)-z(L)=z(0)e^{i\alpha}+\int_0^L ds e^{i(\psi+\phi)}-z(L). \tag{12}$$

A partial integration, using Eqs. (2), (7), and (8) gives

$$\Delta=-i\int_0^L z(s)e^{i\phi(s)}\phi'(s)ds. \tag{13}$$

This relation is valid in general, not only for the free-end spring, because Eqs. (7) and (8) are also true for the fastened spring. Substituting $\phi_f(s)$ for the free-end spring, we find

$$\Delta=i\frac{\alpha}{L}e^{i\alpha}\int_0^L z(s)e^{-i\alpha s/L}ds. \tag{14}$$

This is the principal formula of the present paper. The problem consists in designing the undistorted spring, $z(s)$, so that this integral becomes as small as possible.

As an example we can take a "helical" spring of radius R, consisting of n complete windings and a partial winding of arc θ. Its equation is

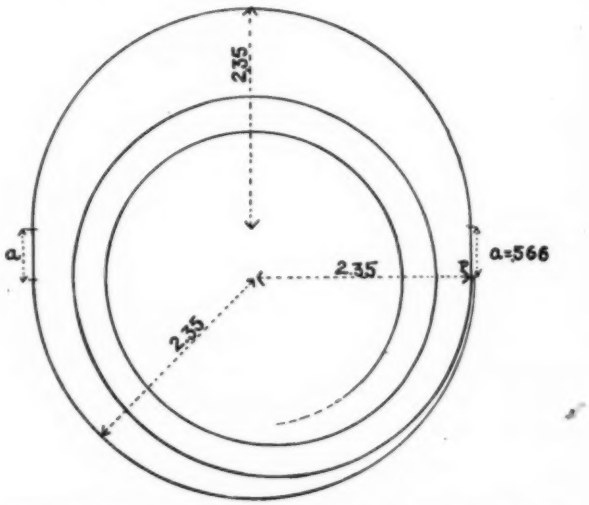

FIG. 8. Plane terminal, consisting of two semicircles joined by two straight portions a with dimension indicated. P is the point where it joins the main spiral.

$$z(s)=Re^{is/R};\quad L=(2\pi n+\theta)R. \tag{15}\ (16)$$

This yields for Δ

$$\Delta=\frac{R^2\alpha}{L-R\alpha}(e^{i\theta}-e^{i\alpha})\sim\frac{L\alpha}{4\pi^2n^2}(e^{i\theta}-e^{i\alpha}). \tag{17}$$

Figures 3 and 4 show some examples of this.

5. Terminals

We divide the spring of length L into three parts l_1, $L-l_1-l_2$, l_2 and take the "terminals"

l_1 and l_2 short compared to the total length L. We can consider the end point displacements due to each part separately. The contribution arising from the inner terminal l_1 is

$$\Delta_1 = i\frac{\alpha}{L}e^{i\alpha}\int_0^{l_1} z(s)e^{-i\alpha s/L}ds = i\frac{\alpha}{L}e^{i\alpha}e^{-i\alpha l_1/L}\int_0^{l_1} z(\sigma)e^{+i\alpha\sigma/L}d\sigma. \quad (18)$$

The latter integral results if we measure the arc length σ along this terminal in the opposite direction, $\sigma = l_1 - s$. Similarly the outer terminal l_2 contributes

$$\Delta_2 = i\frac{\alpha}{L}e^{i\alpha}\int_{L-l_2}^{L} z(s)e^{-i\alpha s/L}ds = i\frac{\alpha}{L}e^{i\alpha l_2/L}\int_0^{l_2} z(\sigma)e^{-i\alpha\sigma/L}d\sigma. \quad (19)$$

The second integral is obtained if the arc length σ is measured from the beginning of the terminal, $\sigma = s - L + l_2$. The terminals are supposed to be short compared to the total length, the exponentials in the integrands may be expanded in powers of α/L. The problem consists in choosing the shape of the terminals in such a way that Δ_1 and Δ_2 approximately cancel the contribution to the end point displacement caused by the main central portion of the spring.

6. Terminals for "helical" spring

Returning to the classical example we take for the central portion a "helical" spring. Its equation is conveniently taken as

$$z(s) = Re^{i(s-l_1)/R}. \quad (20)$$

The arc length over the helical part goes from l_1 to $L - l_2$ and we choose again n complete windings plus an arc θ

$$L - l_1 - l_2 = (2\pi n + \theta)R. \quad (21)$$

Its contribution to the end point displacement is

$$\Delta_c = i\frac{\alpha}{L}e^{i\alpha}\int_{l_1}^{L-l_2} z(s)e^{-i\alpha s/L}ds = \frac{R^2\alpha}{L - R\alpha}(e^{i\theta}\cdot e^{i\alpha l_2/L} - e^{i\alpha}\cdot e^{-i\alpha l_1/L}). \quad (22)$$

In order that $\Delta_1 + \Delta_2 + \Delta_c \sim 0$ we compare Eq. (22) with Eqs. (18) and (19) and set

$$e^{i\theta}R^2\alpha/(L - R\alpha) \sim -i\frac{\alpha}{L}\int_0^{l_2} z(\sigma)e^{-i\alpha\sigma/L}d\sigma, \quad (23)$$

$$R^2\alpha/(L - R\alpha) \sim i\frac{\alpha}{L}\int_0^{l_1} z(\sigma)e^{+i\alpha\sigma/L}d\sigma. \quad (24)$$

The factor $e^{i\theta}$ is immaterial, it merely means a rotation of the whole outer terminal over the angle θ, the incompleted winding. Disregarding this by taking $\theta = 0$, we see that Eqs. (23) and (24) are just complex conjugates. The two terminals are thus the same, except for a reflection with respect to the x axis. Expanding Eq. (24) in powers of α/L, the first term gives

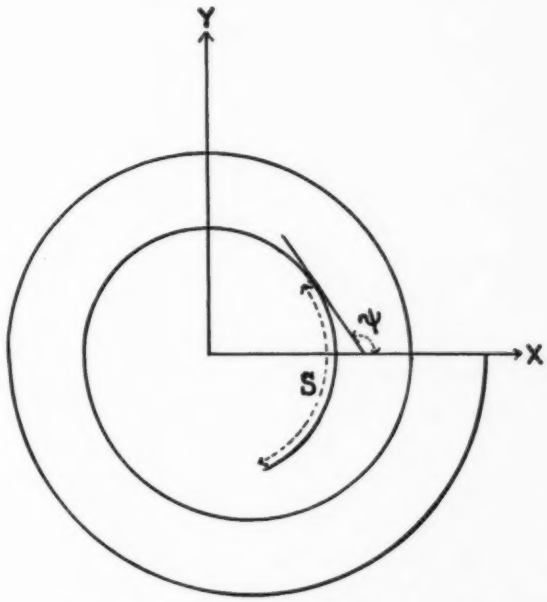

FIG. 9. Coordinates characterizing the spiral.

$$R^2 = i\int_0^l z(\sigma)d\sigma \quad (25)$$

or

$$R^2 = -\int_0^l y d\sigma; \quad (25a)$$

$$0 = \int_0^l x d\sigma. \quad (25b)$$

These are the famous conditions obtained by Phillips. They mean that the terminal must have

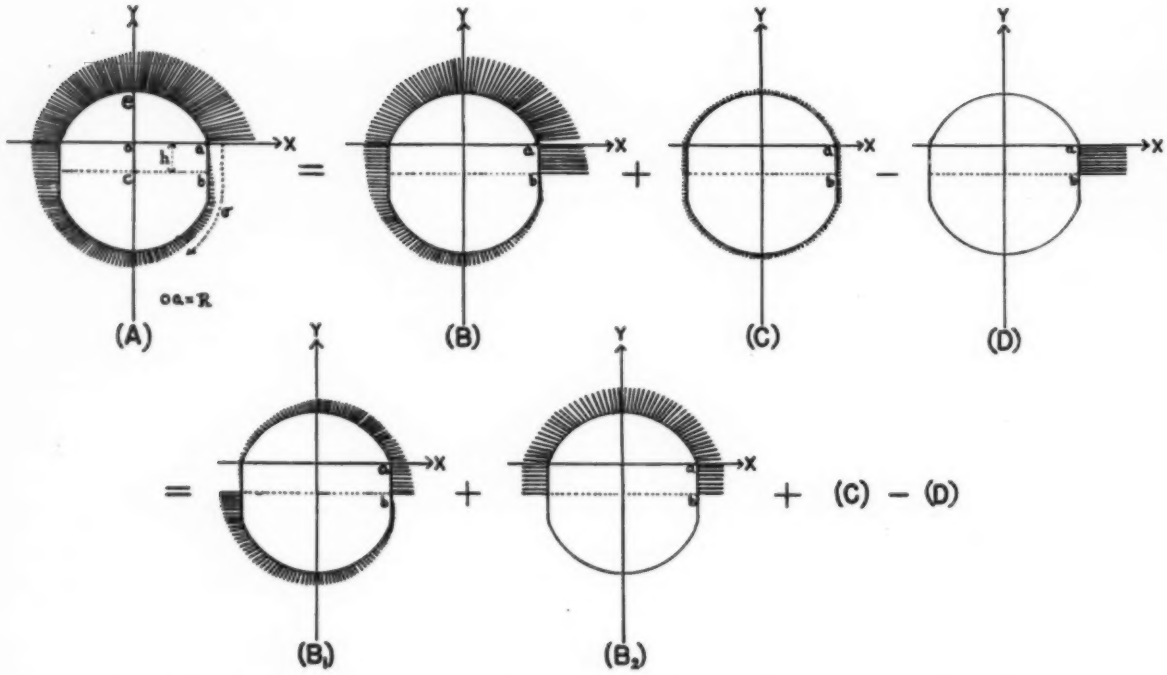

FIG. 10. The width of the shaded part is proportional to the fictitious density, and the solid line is the outline of the terminal. The x (or y) moment of the required distribution (A) is equal to the sum of x (or y) moments of (B_1), (B_2) and (C) minus that of (D). (A) Weighted terminal with starting point a to be analyzed; (B) similarly weighted terminal with starting point b, which is in turn analyzed into (B_1) and (B_2); (C) uniform strip of density h along the whole terminal; (D) uniform strip of density l along the portion ab only.

its center of gravity on the negative y axis, a distance R^2/l from the origin. As Phillips pointed out, one can satisfy these conditions in an infinite number of ways.

7. The second approximation

Comparing the coefficients of $(\alpha/L)^2$ in the expansion of Eq. (24) we find for the next requirement

$$R^3 = -\int_0^l \sigma z(\sigma) d\sigma \tag{26}$$

or

$$R^3 = -\int_0^l \sigma x d\sigma ; \tag{26a}$$

$$0 = \int_0^l \sigma y d\sigma . \tag{26b}$$

We must thus find a terminal fulfilling both Eqs. (25) and (26) and moreover

$$z(\sigma) = R \quad \text{for } \sigma = 0, \tag{27}$$

because the terminal has to fit onto the helical part of the spring. Haag[5] states that he has been unable to find a solution. However, here follows a solution found by one of us (Miss W.).

A terminal, as shown in Fig. 10(A), with the following specifications: (1) Symmetrical with respect to the y axis, (2) symmetrical with respect to a line through its center of gravity c perpendicular to the y axis, (3) with center of gravity at a distance of $h(=R^2/l)$ below the x axis, (4) with ab and its corresponding portions parallel to the y axis, will fulfill conditions (25a) (25b) and (26a) simultaneously. Since the form of ae and three similar arcs is not specified, one can adjust it to satisfy condition (26b).

Now conditions (25a) and (25b) are taken care of by specifications No. 3 and 1, respectively. The geometrical interpretation of condition (26a) is as follows. If we give each element of the terminal a fictitious density equal to its arc length σ from the point a, where it joins the main part of the spring, the x moment ($\sum_i x_i dm_i$) of this weighted terminal must be $-R^3$. Such a

[5] Cf. reference 1. See also F. Keelhoff, Mémoires de L'Académie Royale de Belgique **6**, (1922).

weighted terminal can be analyzed into several simple density distributions, as shown in Fig. 10, so that the x moment of the former can be obtained from those of the equivalent distributions.

By virtue of specifications No. 1 and 2 the x moment of the density distributions (B_1) (B_2) and (C) are all zero. (D) will give an x moment of amount $l \cdot h \cdot R$, therefore the net x moment of the original distribution (A) is the negative of (D), i.e., $-lhR$. Combining this with the condition $lh=R^2$, we have the x moment of the weighted terminal equal to $-R^3$.

As a simple example, one can assume the portions ae, etc., to be corners of a rectangle, which fit onto the straight parts ab, etc., to make the terminal a perfect rectangle of width $2R$ and height $2g$. We can adjust the length g in order to fulfill (26b). This gives for g the equation

$$g^4+4g^3R+4g^2R^2-17R^4/16=0 \qquad (28)$$

with the solution

$$g=0.425R. \qquad (29)$$

8. The Archimedes spiral

In polar coordinates, the equation of the Archimedes spiral is

$$r=a\theta. \qquad (30)$$

It follows that in our notation

$$z=a\theta e^{i\theta}. \qquad (31)$$

The hairsprings are not complete Archimedes spirals which begin at the origin, but several inner windings are omitted. Therefore, the angle does not start from 0, but begins at θ_0, which is usually of the order 15π. There may be from 10 to 15 windings in the spiral, thus θ goes up to about 50π. The arc length is given by

$$s=\tfrac{1}{2}a\left[\theta(1+\theta^2)^{\frac{1}{2}}+\log\{\theta+(1+\theta^2)^{\frac{1}{2}}\}\right]_{\theta_0}^{\theta} \sim\tfrac{1}{2}a(\theta^2-\theta_0^2). \qquad (32)$$

The latter approximation is certainly sufficient in view of the range of values of θ. For the end point displacement we obtain, using θ as the variable,

$$\Delta=\frac{\alpha}{L}ie^{i\alpha}\int_{\theta_0}^{\theta_L}a^2\theta^2e^{i\theta}e^{-(i\alpha a/2L)(\theta^2-\theta_0^2)}d\theta. \qquad (33)$$

This integral has to be evaluated numerically with the help of tables or asymptotic formulas for Fresnel integrals. Results are shown in Figs. 5 and 7.

9. Spring with fixed end point

We have studied above the end point displacement of the "free-end" spring and must now prove that this displacement is a measure of the reaction forces set up in the end points of the actual hairspring which is fastened to the stud. We denote by $z_a(s)$ and $\phi_a(s)$ the coordinates z and the function ϕ for the actual spring *after* rotation of the balance wheel over an angle α. We now have the additional requirement that the end point remain fixed

$$z_a(L)=z(L)=\text{constant} \qquad (34)$$

or in components

$$x_a(L)=x_a(0)+\int_0^L ds\cos(\psi+\phi_a)=\text{constant}, \qquad (35a)$$

$$y_a(L)=y_a(0)+\int_0^L ds\sin(\psi+\phi_a)=\text{constant}. \qquad (35b)$$

We must now find the minimum of the potential energy V, Eq. (5), subject to these constraints. Using Lagrange multipliers 2λ and 2μ which are proportional to the x component and y component of the reaction force caused by the constraint, the Euler-Lagrange equation now becomes

$$\phi_a''(s)+\lambda\sin(\psi+\phi_a)-\mu\cos(\psi+\phi_a)=0. \qquad (36)$$

This equation for $\phi_a(s)$ cannot, in general, be solved, but we can derive some useful conclusions from it. Anticipating that the distribution will differ little from that of the free-end spring we write

$$\phi_a(s)=\phi_f(s)+\epsilon(s)=-\alpha s/L+\alpha+\epsilon(s). \qquad (37)$$

This changes the differential equation into

$$\epsilon''(s)+\lambda y_a'-\mu x_a'=0 \qquad (38)$$

with the boundary values

$$\epsilon(0)=\epsilon(L)=0. \qquad (39)$$

Integrating once we get

$$\epsilon'(s)+\lambda y_a-\mu x_a=\text{constant}. \tag{40}$$

The constant is determined by integrating once more, now from 0 to L, using the boundary values for $\epsilon(s)$. We finally obtain

$$\epsilon'(s)=-\lambda(y_a-Y_a)+\mu(x_a-X_a) \tag{41}$$

with X_a and Y_a the coordinates of the center of gravity of the *distorted* spring, defined by

$$LX_a=\int_0^L x_a ds; \tag{42a}$$

$$LY_a=\int_0^L y_a ds. \tag{42b}$$

We must now connect this with the displacement Δ by observing that

$$\begin{aligned}\Delta&=z_f(L)-z(L)=z_f(L)-z_a(L)\\&=\int_0^L ds(e^{i\psi_f}-e^{i\psi_a})=\int_0^L ds e^{i\psi_a}(e^{-i\epsilon}-1)\\&=i\int_0^L z_a(s)e^{-i\epsilon}\epsilon' ds\sim i\int_0^L z_a(s)\epsilon' ds.\end{aligned} \tag{43}$$

The last line is obtained by partial integration and in the final approximate expression the exponential is replaced by unity. Next substituting Eq. (41) for ϵ' and writing the components, we obtain

$$\begin{aligned}\Delta_x&=\int[\lambda(y_a^2-y_aY_a)-\mu(x_ay_a-y_aX_a)]ds\\&=\lambda LA-\mu LF,\end{aligned} \tag{44a}$$

and

$$\Delta_y=-\lambda LF+\mu LB, \tag{44b}$$

where A, B, and F are the moments and products of inertia, with respect to the center of gravity of the distorted spring, defined as

$$LA=\int_0^L y_a^2 ds-LY_a^2; \tag{45a}$$

$$LB=\int_0^L x_a^2 ds-LX_a^2; \tag{45b}$$

$$LF=\int_0^L x_a y_a ds-LX_aY_a. \tag{45c}$$

We find at once for the square of the reaction force

$$\lambda^2+\mu^2=\frac{(B\Delta_x+F\Delta_y)^2+(F\Delta_x+A\Delta_y)^2}{L^2(AB-F^2)^2}. \tag{46}$$

Usually $A\sim B$ and $F=0$ so that a first approximation gives

$$\lambda^2+\mu^2\sim|\Delta|^2/A^2L^2. \tag{47}$$

This result proves that the reaction force is approximately proportional to the displacement Δ.

10. Deviation from isochronism

We finally consider the energy of the distorted spring with a fixed end point

$$\begin{aligned}V&=\frac{k}{2}\int_0^L \phi_a'^2(s)ds=\frac{k}{2}\int_0^L(\phi_f'+\epsilon')^2 ds\\&=\frac{k\alpha^2}{2L}+\frac{k}{2}\int_0^L\epsilon'^2 ds.\end{aligned} \tag{48}$$

The last result is obtained by using the known solution for ϕ_f, Eq. (10) and the boundary values for $\epsilon(s)$, Eq. (39). Substituting the formula for ϵ' found above we can write

$$\begin{aligned}V&=\frac{k\alpha^2}{2L}+\frac{k}{2}(B\Delta_x^2+A\Delta_y^2+2F\Delta_x\Delta_y)/L(AB-F^2)\\&\sim\frac{k\alpha^2}{2L}+\frac{k|\Delta|^2}{2LA}=\frac{k}{2L}(\alpha^2+\xi(\alpha)).\end{aligned} \tag{49}$$

The correction term, abbreviated $\xi(\alpha)$, causes the deviation from isochronism. The balance wheel is very much heavier than the hairspring and is alone responsible for the kinetic energy, which is thus proportional to $(d\alpha/dt)^2$. The equation of motion of the balance wheel has, therefore, the form

$$d^2\alpha/dt^2=-\omega^2(\alpha+\tfrac{1}{2}d\xi/d\alpha), \tag{50}$$

where $\omega=2\pi/T$, T being the period if the correction term were absent as in the free-end spring. Writing

$$\alpha\sim\alpha_0\sin\omega(1+\delta)t+\cdots, \tag{51}$$

we find by well-known methods the first approxi-

mation of δ, the fractional increase in frequency

$$\delta\sim\frac{1}{\alpha_0^2T}\int_0^T\frac{d\xi}{d\alpha}\alpha dt \sim\frac{2}{\alpha_0^2TA}\int_0^T|\Delta|\frac{d|\Delta|}{d\alpha}\alpha dt. \quad (52)$$

We shall not discuss this expression in detail but call attention to the fact that if $\xi(\alpha)$ is an odd function of α, the integral vanishes. However, $\xi(\alpha)$, being proportional to the square of $|\Delta(\alpha)|$, can never be a pure odd function of α. If the even part of ξ is α^2 only, δ will be some constant value independent of the amplitude α_0. Therefore if $|\Delta|^2/\alpha^2$ is a constant plus an odd function of α, the period will change by a constant amount. For example, in the case of a "helical" spring

$$\Delta\sim\alpha(e^{i\theta}-e^{i\alpha}), \quad (53)$$

which gives

$$|\Delta|^2/\alpha^2\sim[1-\cos(\alpha-\theta)]. \quad (54)$$

When $\theta=\pm\pi/2$, $\cos(\alpha-\theta)=\pm\sin\alpha$, and $|\Delta|^2/\alpha^2$ fulfills the requirement for constant change of period, which proves the theorem of Résal and Caspari.

Because $\xi(\alpha)$ is proportional to $|\Delta|^2$, the integral representing δ will be small if $|\Delta|$ is small, provided, however, that $d|\Delta|/d\alpha$ does not become too large. This confirms our point of view that the best way to achieve isochronism is by making the end point displacement Δ be as small as possible. This result can be connected with the motion of the center of gravity of the free-end spring. Using Eqs. (10) and (12) we obtain

$$\frac{d\Delta}{d\alpha}=iz(0)e^{i\alpha}+i\int_0^L e^{i\psi_f}ds-\frac{i}{L}\int_0^L se^{i\psi_f}ds =\frac{i}{L}\int_0^L z_f(s)ds=iG. \quad (55)$$

G is the complex coordinate of the center of gravity of the free-end spring and changes its position with different rotations α. We may now write for Eq. (52)

$$\delta=\frac{2}{\alpha_0^2TA}\int_0^T|[G\times\Delta]|\alpha dt. \quad (56)$$

It is obviously advantageous to have G as small as possible for all values of α. To have the center of gravity of the undistorted spring ($\alpha=0$) fall exactly on the axis is, however, not necessarily the best solution (except for small amplitudes), because G is a complicated function of α. We verified this numerically for a few examples.

Concentrator of Eddy Currents for Zonal Heating of Steel Parts

G. Babat and M. Losinsky
Leningrad, U.S.S.R.
(Received March 6, 1939)

INDUCTIVE heating of steel parts in high frequency electromagnetic fields now finds wide use for industrial purposes. This method of heating may be employed for annealing and normalizing steel, for welding, for peripheral alloying, etc. Inductive heating is of particular importance for the surface hardening of steel parts. This process has a number of advantages which may be stated briefly as follows:

(1) Since the metal heated is but a small percentage of the whole volume of the piece, defects of warping produced during the heating and hardening procedures are almost completely avoided.

(2) The high frequency equipment for hardening is characterized by enormous productivity, because heating the peripheral layer of the part to the hardening temperature takes only a few seconds.

(3) The cost of the thermal treatment is low.

(4) The work conditions are essentially improved.

In each individual case only some specific local surface areas of the given piece are to be hardened; e.g., in gears, the working surface only; in dies, the cutting edges; etc. In the majority of cases surface hardening is also zonal hardening.

The heater coil should be shaped so that it will induce eddy currents only in the local surface areas of the piece; i.e., those areas which are to be heated. Consequently the form of the heater coil will be determined by the shape of specific surface sections of the part. In the design of equipment for surface hardening, a most important step is the definition of the heater coil form. Any analytic computation of electromagnetic fields may be accomplished with more or less accuracy only for the simplest forms of heater coil; e.g., for the case of a wire stretched over an infinite plate.

The authors (in collaboration with W. S. Lukoshkow) have developed a model method by which pictures of high frequency magnetic fields may be taken. This method, which employs an electrolytical tank, makes possible the determination of distribution of peripheral current density in the case of parts with complicated shape. The method is based upon the following assumptions: With frequencies of the order of 10^4–10^6 cycles, the frequencies preferable for the purpose of surface hardening by inductive heating, the electromagnetic wave-length in air is 30 km to 300 meters. Since the largest heater coil dimensions are, in most cases, tenth centimeters, the radiation of electromagnetic power in the surrounding space is quite negligible, and the heater coil may be considered as a circuit element with concentrated self-induction; i.e., the angle of current may be considered the same along the whole length of the heater coil. The depth of penetration of electromagnetic waves into metal at these frequencies is a part of a millimeter, an insignificant percentage of the dimensions of the piece treated and of the heater coil. Moreover, since the electromagnetic process in metal is damped to the extent of only a wave-length, the magnetic field may be considered as zero in the whole space inside the metal.

Consequently we may consider the problem of magnetic field distribution in the space surrounding the heater coil and the piece heated as a problem of magnetostatics, assuming that both the piece and the heater coil are made of some hypothetical material with zero permeability. The magnetic force lines seem to "wash" the piece and the heater coil in the same manner as the air streams in an aerodynamic tube are washing the model of an aircraft wing.

The best analogy to the lines of the magnetic field will be given by current lines around the models of the heater coil and the part, if the models are made of dielectric and placed in an electrolytical tank so that they represent their respective situation in question. The models may be made of wood, ebonite, paraffin, or some other insulating material. If the heater coil and the part are small, it is desirable to magnify the

dimensions of the models. In order to find the magnetic field distribution in the space between heater coil and part, their models should be correspondingly situated in the electrolytical tank. Electrodes should be installed so that they correspond to equipotential surfaces of the magnetic field.[1] A.c. voltage is applied to the electrodes and the distribution of currents in the water around the models is determined by means of a probe wire. The electric field around the models E_t will correspond to the strength of the magnetic field H_t. The peripheral density[2] of eddy currents at the given local area of the heated-piece surface will be $H_t/4\pi$. In this way the picture of the distribution of eddy currents and of the heat they generate may be obtained on a model.

To the designer of inductive heating devices the electrolytical tank is a kind of aerodynamic tube which allows him quickly to "blow through" an experimental model of a heater coil. Without having to build the actual heater coil in nature and to execute costly experiments involving heating and investigation of steel parts, data may be obtained on the distribution of eddy current density and on the general effectiveness of a given form of heater coil.

It is important to emphasize that, when the depth of penetration of current in the materials of heater coil and piece is much less than their dimensions, then neither the resistivity ρ nor the permeability μ of the materials will affect the distribution of peripheral density of eddy currents. The distribution of magnetic field strength taken down in the electrolytical tank will be true both for the pieces made of steel and those made of copper. The values of ρ and μ will affect only the depth of penetration and the amount of heat generated by eddy currents in the peripheral layer of metal.

Figure 1 shows the distribution of the magnetic field and of the peripheral current density taken down on a model in an electrolytical tank. It is easier to give the heater coil the form desired in the case where it consists of a single turn. In order to minimize undesirable stray flux, the spacing between coil and piece should be no more than several millimeters. The voltage across the heater coil terminals should not exceed some hundred volts. As the hardening temperature is reached, thermionic emission starts from the surface of the piece treated. In the space between heater coil and piece, ionization may occur and breakdown is possible with heater coil voltages of the order of several kilovolts.

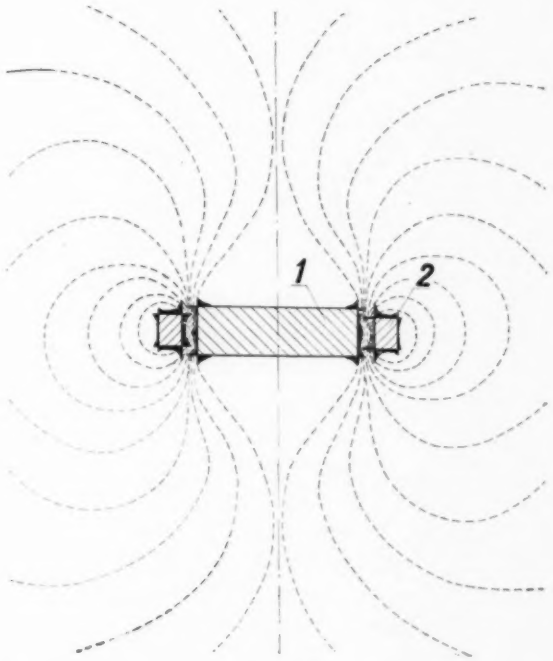

FIG. 1. Distribution of magnetic field and of peripheral density of eddy currents in the field of a single-turn heater coil.

For the power supply of induction heating sets, electron tube oscillators are used. Power oscillator tubes operate with anode voltages of about 10 kv, and, correspondingly, the voltage on the load in the anode circuit of the oscillator tube will be of the same order. To satisfy the operating conditions; i.e., to have the voltage across the heater coil no more than several hundred volts, it has been until these present experiments general practice to make use of intermediate circuits, but these complicate the tuning, increase the cost of the oscillator, and decrease the efficiency.

The authors have succeeded in developing a

[1] Pieces which have an axis of symmetry always have two equipotential surfaces in the form of planes. Pieces of a complicated shape may have curvilinear equipotential surfaces. The "model" method is therefore more easily adapted for symmetrical bodies.

[2] By peripheral density of eddy currents we mean the total current in a 1-cm width.

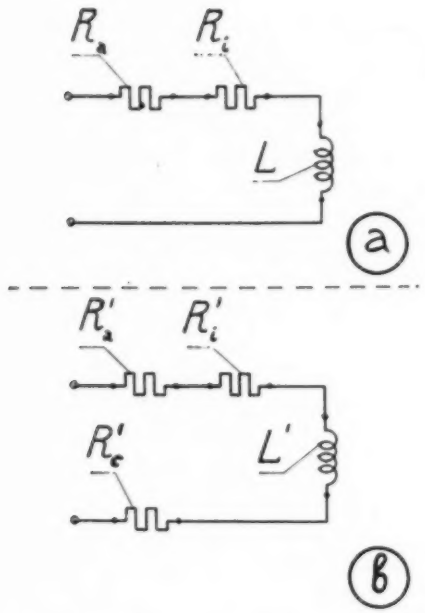

FIG. 2. Equivalent circuits of inductive heating: (a) without concentrator; (b) with concentrator.

"concentrator of eddy currents," which makes it possible for the magnetic field of a multi-turn coil to be transformed and directed so that the magnetic flux is concentrated on the "heatable" local areas of the treated piece. This device also protects the coil (to which the full 10-kv anode voltage may be applied) from the glowing surface of the piece.

The principle of action of a concentrator is based on the above-mentioned property of eddy currents; i.e., their ability completely to screen the inside of metal from a magnetic field. A metal brought into a high frequency magnetic field appears to press out the force lines from the volume it occupies. But, since the line integral $\oint Hdl$ is always equal to $4\pi AW$ (AW represents the ampere-turns of the coil), the "pressing out" of the field from one part of the space surrounding the coil involves the increase of magnetic field intensity in other parts of the same space.

If the metal body which causes the field redistribution were made from a superconductor, then the redistribution would not involve any additional losses. But in practice a concentrator is made from a material characterized by a certain resistivity; the best metal that can be used is silvered copper. Therefore in the concentrator itself there will always be some power dissipated.

Figure 2 shows equivalent circuits of inductive heating for the case where the piece is placed directly in the field of the multi-turn coil and for the case where a concentrator is inserted between the piece and the coil. In this figure R_a is the equivalent resistance of the piece heated, R_i the resistance of the coil, and R_c the loss resistance of the concentrator.

Figure 3 shows diagrams of circuit arrangements with concentrators. 1 is a choke coil; 2, an oscillator tube; 3, blocking condenser; 4, condenser of oscillatory circuit; 5, multi-turn heater coil; 6, concentrator; 7, the piece heated; 8, the grid condenser; and 9, the grid-leak. The oscillatory circuit (4–5) of Fig. 3a will offer high resistance only to the fundamental of the current. Therefore, independently of the wave form of the plate current, the heater coil voltage will be sinusoidal. It is easy to have the circuit (14–15) a multi-wave circuit so that it offers high resistance also to the third harmonic of plate current. Then the third harmonic will also produce useful heat in the piece treated. This utilization of the third harmonic increases the efficiency of the oscillator and makes it possible to obtain much greater power from a given type of tube. If P_a are permissible tube losses, then

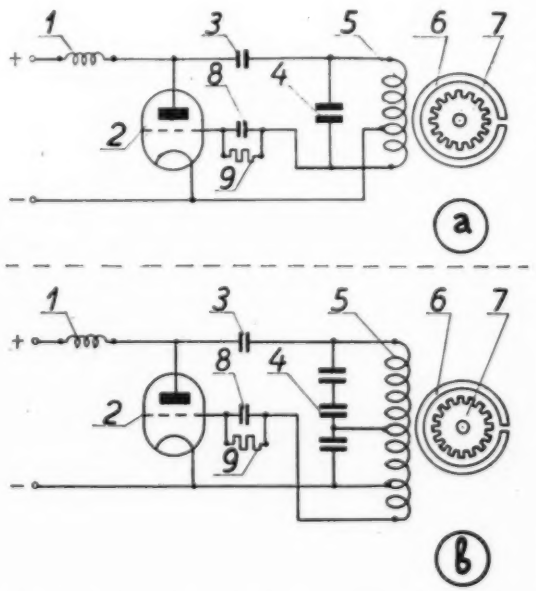

FIG. 3. Circuit arrangements with concentrators: (a) Only the fundamental of anode current is utilized. (b) Both the fundamental and third harmonic of anode current are utilized.

the power output in the oscillatory circuit will be $P_0=P_a/(1-\eta)$.

Figures 4 and 5 illustrate schematically some forms of concentrator designs. A concentrator consists of a massive copper bushing with a slot. Eddy currents flow on the surface facing the multi-turn coil on the slot sides and close themselves on the crest which faces the piece treated. Since this crest is considerably less in height than the surface facing the heater coil, the density of eddy currents will be greatest on the crest. The magnetic field of greatest intensity will therefore be in the interstice between the crest of the concentrator and the piece. Figure 4 shows a concentrator for heating working surfaces of pinions. Figure 5 is a concentrator for heating working surfaces of crown gears. The various parts are designated as follows: 1, multi-turn heater coil; 2, the body of concentrator; 3, the crest of concentrator; 4, the part heated; 5, water-cooling channel of the crest; 6, water-pipes; 7, clamp for fastening the piece heated; 8, protective casing; 9 and 10 (in Fig. 5 only), the beginning and the end of the multi-turn heater coil.

If L is the inductivity of the system as measured across the terminals of the multi-turn heater coil; C, the capacity of a condenser battery in parallel with the heater coil; and E, the voltage on the heater coil, the frequency of the current in the heater coil will, of course, correspond to the resonance frequency of the circuit; i.e., $\omega=1/(LC)^{\frac{1}{2}}$. Then the power given up to the piece heated will be

$$P_a=KE^2(C^{3/4}/L^{5/4})(\rho\mu)^{\frac{1}{4}}, \qquad (1)$$

where ρ and μ are the resistivity and the permeability of the material of the heated piece, respectively, and K is a factor depending only on the relative positions of the heater coil and piece.

The presence of a concentrator results in a considerable decrease in the inductivity of the system, because the concentrator reduces the cross section of the magnetic flux.[3] Therefore, heating in a concentrator requires fewer kilovoltamperes from the condenser battery than does heating in a simple multi-turn coil. Furthermore, the concentrator tends to increase the factor K in Eq. (1) by a large amount.

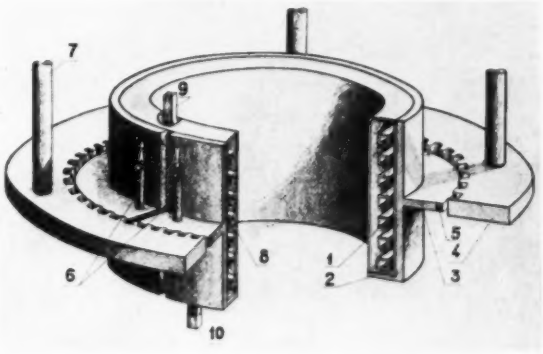

FIG. 5. Schematic view of a concentrator for heating crown gears.

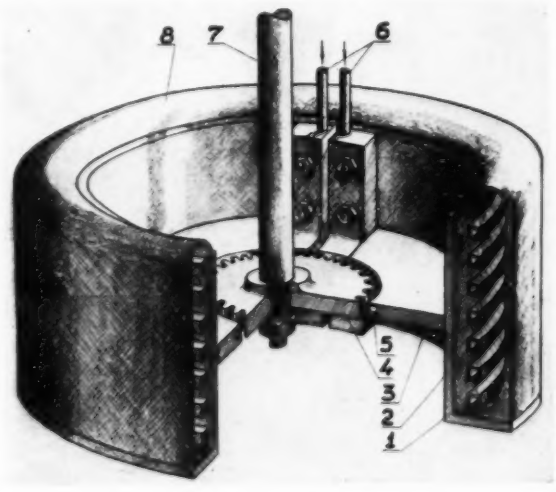

FIG. 4. Schematic view of a concentrator for heating pinions.

Referring to the equivalent circuit of Fig. 2, the expression for the efficiency when heating without the concentrator may be written:

$$\eta_1=R_a/(R_a+R_i).$$

The corresponding expression when the concentrator is used is

$$\eta_2=R_a'/(R_a'+R_i'+R_c).$$

The increase of the factor K of Eq. (1) contributes to the increase of R_a in the efficiency equation. Therefore, although the denominator of the expression for η_2 contains a new term R_c, nevertheless $\eta_2>\eta_1$, because R_a' in this expression is much greater than R_a in the equation for η_1.

[3] Inductivity is determined by the ratio of the magnetic flux section to the medial length of magnetic force lines.

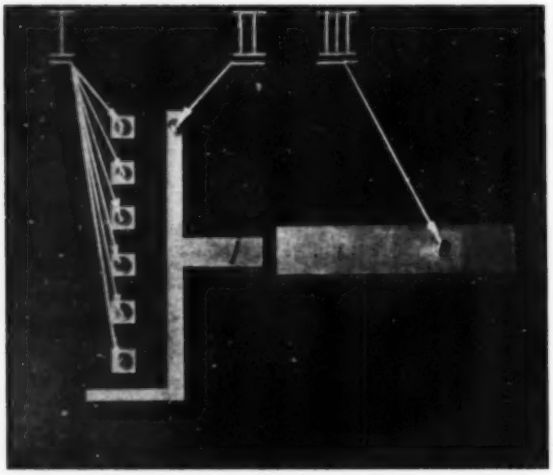

FIG. 6. Model for studying the distribution of eddy currents in concentrator: I. multi-turn coil, II. concentrator bushing, III. the piece heated.

We see, therefore, that the use of the concentrator increases the efficiency of inductive heating.

Figure 6 shows a photograph of a concentrator model by means of which the distribution of magnetic field and of peripheral eddy current density was studied in an electrolytical tank. Figures 7 and 8 illustrate the results obtained. The results of field investigations carried out by means of models had previously shown that uniform heating of the lateral surface of cylindrical bodies is obtained when the height of the heater coil is equal to $(h-2a)$, where h is the height of the cylinder heated, and a is the width of spacing between cylinder and heater coil. To prevent the overheating of teeth rims, the crest of the concentrator was made less in height than the gear.

Figure 9 shows a 200-kw concentrator. The primary consists of 8 turns of square copper tubing (10×10 mm). The concentrator bushing is made from copper sheets welded together. A 12-kv, 0.06-μf battery of condensers is connected in parallel to the primary. It was found that the natural frequency of the heating system varied from 160 to 230 kilocycles (wave-length 1900 to 1300 m) depending on the kind of piece treated. The voltage across the heater coil terminals varied from 5 to 9 kv (effective). The highest value of heater coil current was 870A. The kilovoltamperes of the condenser battery were 8000

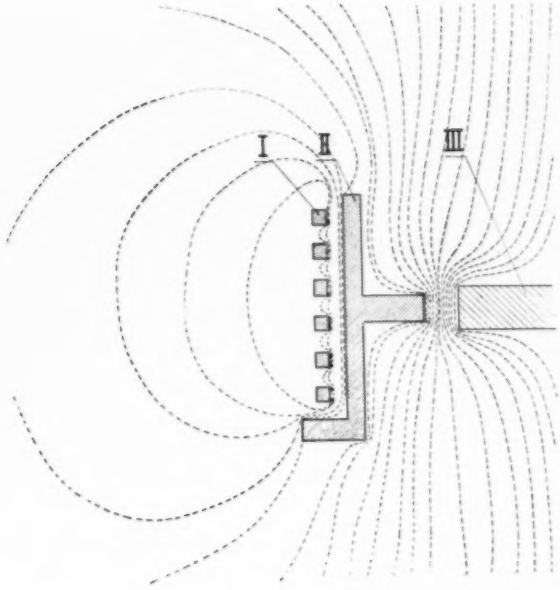

FIG. 7. Magnetic field distribution taken down with the model of Fig. 5.

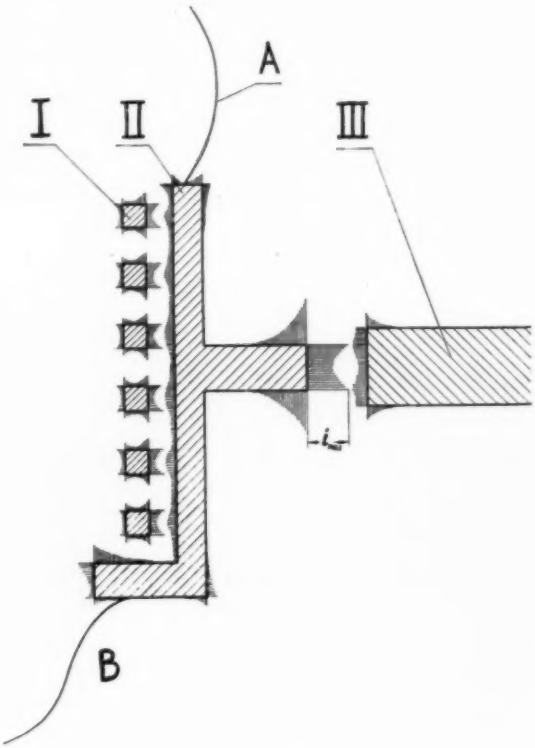

FIG. 8. Distribution of eddy current density in concentrator calculated from Fig. 7.

FIG. 9. 200-kw concentrator with protective casing taken off.

FIG. 10. Equipment with a 200-kw concentrator for hardening gears. (Dr. Babat is shown at the left of the photograph and Dr. Losinsky at the right.)

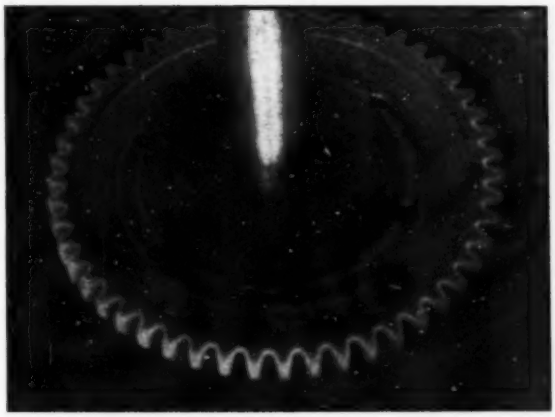

FIG. 11. A 260 mm $\times$30 mm gear being heated in the 200-kw concentrator. This picture was made four seconds after the current switched on.

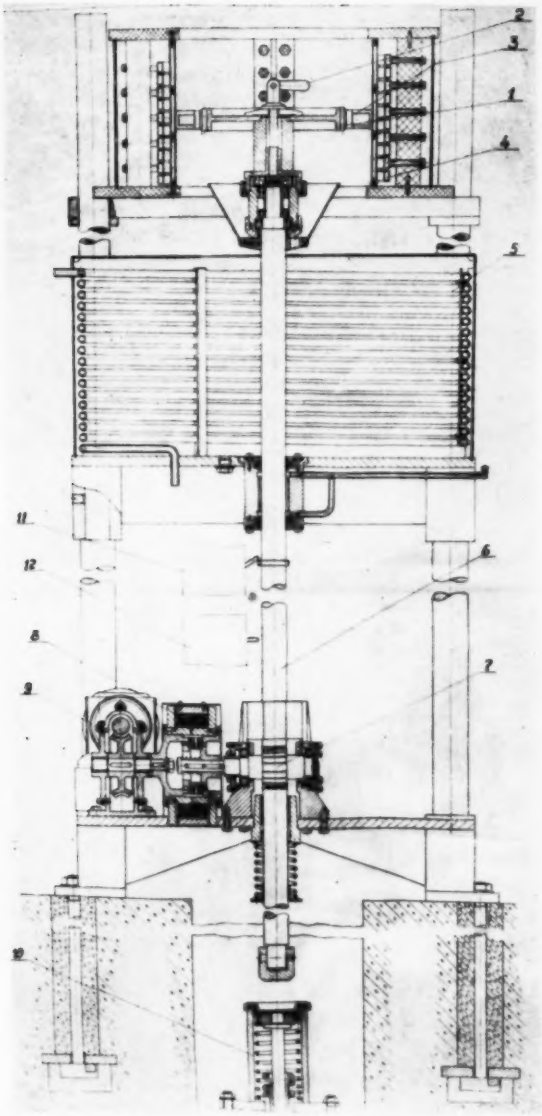

FIG. 12. A hardening machine for pieces in the form of disks and cylinders: 1, a gear being heated; 2, the fastening device; 3, the crest of the concentrator; 4, the primary of concentrator (made of 10$\times$20-mm copper tubing); 5, the tank with cooling liquid; 6, a bar moved by means of the gear; 7, 8, electromagnetic coupling; 9, motor; 10, choke adsorber; 11 and 12, end switches.

kva. Hence the power factor of the heating system, $\cos \varphi = 0.025$.

The current in the concentrator crest at maximum load was 7000A. Since, in copper, the depth of penetration of current at 150 kilocycles is 0.2 mm, the current density on the crest reached the large value of 3500 A/mm^2.

Figure 10 shows a general view of hardening equipment with a 200-kw concentrator. Figure

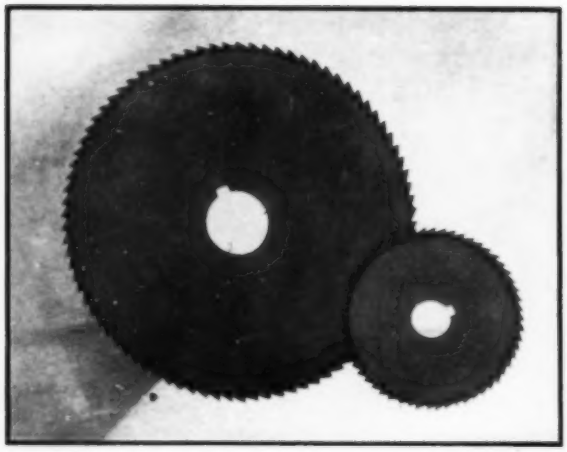

FIG. 13. Macrostructure of cutters $D=160$ mm and $D=70$ mm.

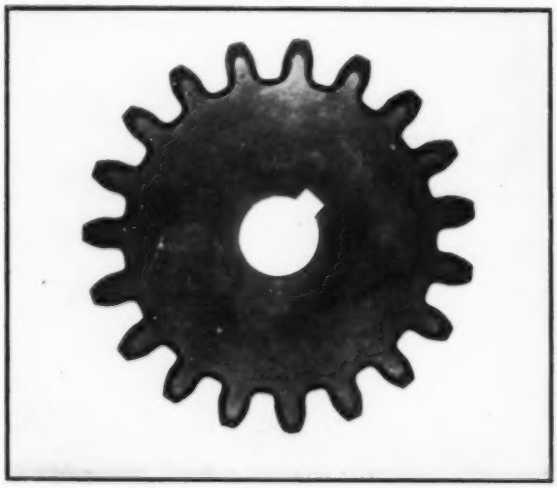

FIG. 14. Macrostructure of a gear.

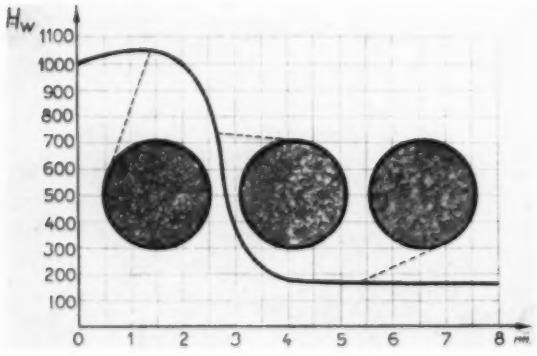

FIG. 15. Decrease of hardness from the surface of the hardened layer into the thickness of material.

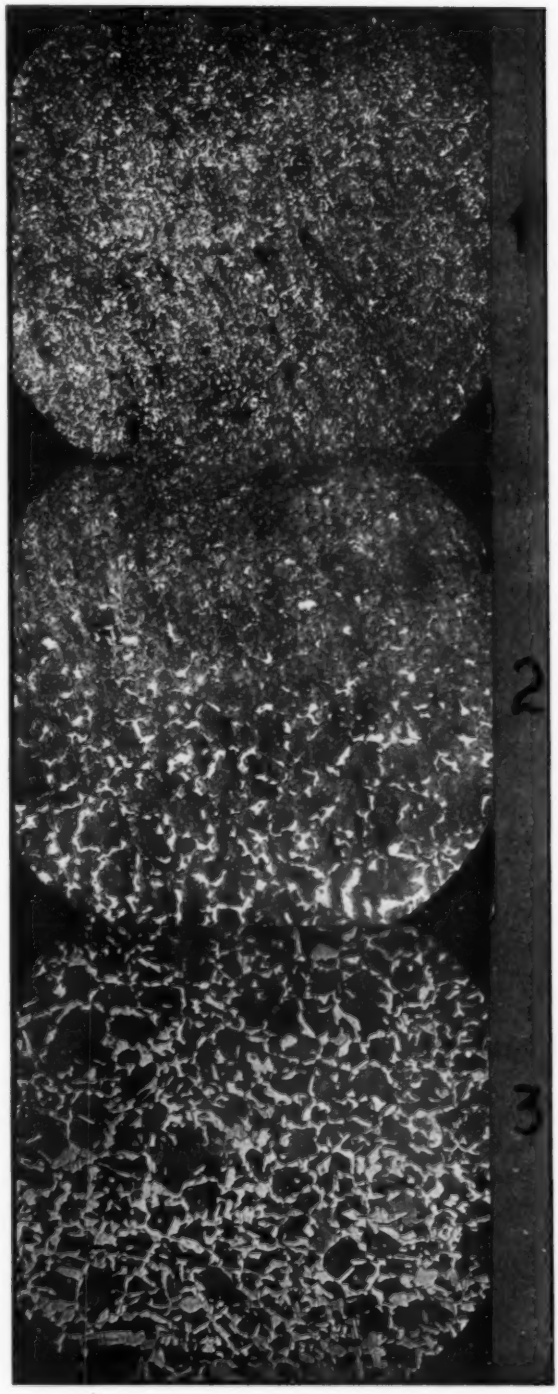

FIG. 16. Microphotograph of the structure of a surface hardened piece.

11 illustrates the heating of a gear in the concentrator.

The concentrator must not be considered as a device for solving all possible problems of zonal heating of steel pieces. For crank pins, for instance, the use of a simple transformer with a secondary which can be taken apart is more advantageous. For heating a big surface of a plate a simple multi-turn heater coil may be employed. For heating a great number of parts, however, the concentrator will be found to be the most handy device. A change from one type of parts heated to another type involves only a change in the inner bushing or, in some cases, in the crest alone. This may be accomplished in a few minutes. No tuning of oscillator when changing from one type of parts to another is required.

The voltage on the bushing (across the slot rims) is equal to the anode voltage divided by the number of heater coil turns and multiplied by the ratio of magnetic flux flowing between the crest and the piece to the overall magnetic flux of the heater coil.[4] With a heater coil consisting of 15 turns and 10 kv anode voltage, the effective value of voltage on the bushing will be 400 volts.

The power output of the concentrator may be controlled merely by varying the capacity of the condenser battery in parallel connection. With other conditions invariable, the power given up to the piece will vary with $C^{3/4}$.

The side of the concentrator which faces the piece heated is made of massive water-cooled copper. Therefore, occasional shocks, splashes of oil, or splashes of water cannot injure the concentrator.

After the piece has been heated in the concentrator, it must be quickly cooled. This may be accomplished by moving the piece in a bath filled with a cooling liquid (see Fig. 10). For supplying the cooling liquid, in some cases, the concentrator bushing itself may be utilized. The crest facing the piece heated should then be provided with a channel closed by a perforated lap; the cooling liquid may then be supplied under pressure through the perforations.

[4] With correct design of the bushing this ratio is 0.8–0.85.

Appendix

The hardening device shown in Fig. 10 was reconstructed from a drill press. If the work-piece is placed correctly with respect to the crest of the concentrator; i.e., if there is no eccentricity, then the heating is quite uniform and the presence of slots in the crest of the concentrator does not in the least affect the temperature distribution in the piece. The non-uniformity of heating becomes appreciable only with an eccentricity exceeding 1 mm. Rotating the work-piece completely eliminates all non-uniformity of heating.

Figure 12 shows a hardening machine with a concentrator for pieces in the form of disks. The work-piece (1) is fastened at the end of the bar (6) which is lifted by means of the motor (9). The accurate position of the work-piece with respect to the concentrator crest is secured by an end-switch (11). As soon as the treatment of the gear is completed, the electromagnetic coupling (8) is released, the bar glides down and the heated gear plunges in cooling liquid. A definite time length thereafter, the motor (9) and the coupling (8) are again on, and the piece is lifted up. The heating time required depends upon the thickness of the layer to be hardened. The thicker the layer, the more slowly must the heating proceed. A layer 1 to 2 mm thick may be heated in the course of 2 to 4 seconds. With a 5-mm layer, heating may last 10 seconds.

Figures 13 and 14 show samples hardened after treatment in the concentrator illustrated in Figs. 9 and 10. The pieces have been etched by Heine reagent, which causes the hardened layer to look darker than the core.

Figure 15 illustrates the hardness across a section of a gear, surface hardened. In Fig. 16 are shown microphotographs of the hardened layer (1), the intermediate zone (2), and the core material (3). It may be seen that the hardened layer consists of very fine martensite going smoothly over into the core structure.

Author Index to Volume 11

References with (L) are to Letters to the Editor

Albright, John G. Physics of the earth and atmosphere—568 (book reviews)
Allen, A. J. The cyclotron—569 (book review)
Atlee, Z. J., J. T. Wilson and J. C. Filmer. Lubrication in vacuum by vaporized thin metallic films—611

Babat, G. and M. Losinsky. Concentrator of eddy currents for zonal heating of steel parts—816
Bachman, C. H. Ring focusing of negative ions in a cathode-ray beam—83; Correction—240(L)
Baker, J. G. Mechanics applied to vibrations and balancing—626 (book review)
Ballard, Stanley S. Qualitative spectrochemical analysis in agriculture and geochemistry—750
—— **and L. A. Dean.** Use of radioactive phosphorus in soil studies—366
Bardeen, John. Electrical conductivity of metals—88
Barrett, Charles S. and Alfred H. Geisler. Atomic distribution in aluminum-silver alloys during aging—733
Bell, M. E. (see Berberich, L. J.)—681
Berberich, L. J. and M. E. Bell. Dielectric properties of the rutile form of TiO_2—681
Berkey, W. E. (see Slepian, Joseph)—765
Bingham, Eugene C. and Paul W. Kinney. Relation of fluidity to volume in organic liquids—192
Biot, Maurice A. Equations of finite differences applied to torsional oscillations of crankshafts—530
—— Influence of initial stress on elastic waves—522
Blackwood, O. H. Modern science—571 (book review)
Block, Raymond B. On the resistance to the uniform motion of a solid through a viscous liquid—635
Bradbury, N. E. Preferential and initial ionic recombination in gases—267
Breazeale, Francis. Remarks on the study of structural viscosity in liquids, and the derivation of equations for the flux of such liquids through tubes—187
Brennecke, Cornelius G. Conductivity measurements on potassium halides—202
Brickwedde, F. G. Temperature scale, a proposed change in definition—371
Brown, William Fuller, Jr. Ferromagnetic domains and the magnetization curve—160
Bundy, Francis P. Stresses in freely falling chimneys and columns—112

Carapella, Louis A. Graphical method for selecting suitable radiations for the precision determination of noncubic lattice constants and for indexing back-reflection lines in powder x-ray photograms—800
—— Graphical method for selecting suitable targets for precision determination of cubic lattice constants and for solving cubic powder patterns—510
Carley, Glenn R. Pendulum analysis in the scale industry—314
Chu, L. J. Calculation of the radiation properties of hollow pipes and horns—603
Cinnamon, C. A. and Albert B. Martin. Growth conditions for single and optically mosaic crystals of zinc—487
Collins, S. C. (see Jacobs, R. B.)—491
Condon, E. U. Electronic generation of electromagnetic oscillations—502
Cruzan, C. G. and H. A. Miley. Cuprous-cupric oxide films on copper—631

David, W. T. Concerning "Physics of flames and explosions of gases"—157(L)
Dean, L. A. (see Ballard, Stanley S.)—366
Dillon, J. H. Polonium alloy for spark plug electrodes—291; Answer to communication by R. D. Evans—562(L)
Dix, F. Johnson and G. W. Scott Blair. On the flow of suspensions through narrow tubes—574
Dow, R. B. and C. E. Fink. Computation of some physical properties of lubricating oils at high pressures. I. Density—353
Drucker, Daniel C. and Raymond D. Mindlin. Stress analysis by three-dimensional photoelastic methods—724
DuMond, Jesse and J. Paul Youtz. X-ray method of determining rates of diffusion in the solid state—357

Eckart, Carl. Static and dynamic electricity—568 (book review)
Ehrke, Louis F. and Charles M. Slack. Investigation into the gettering powers of various metals for the gases hydrogen, oxygen, nitrogen, carbon dioxide and air—129
Elmore, W. C. Electrolytic polishing. II—797
Evans, Robley D. Polonium alloy for spark plug electrodes—561(L)
Evinger, H. H. (see Muskat, M.)—739
Eyring, Henry (see Frisch, David)—75

Farwell, H. W. Tension and birefringence in a vinylite plastic—274
Filmer, J. C. (see Atlee, Z. J.)—611
Fink, C. E. (see Dow, R. B.)—353
Forsythe, W. E. Optical pyrometry—408
Fowler, J. L. and K. L. Hertel. Flow of a gas through porous media—496
Fox, G. W. and D. O. McCoy. Breakdown potentials of gases under alternating voltages—592
Fried, B. (see Weller, R.)—283
Frisch, David, Henry Eyring and John F. Kincaid. Pressure and temperature effects on the viscosity of liquids—75

Geisler, Alfred H. (see Barrett, Charles S.)—733
Gemant, Andrew. Measurement of solid friction of plastics—647
Goudsmit, S. and Ming-chen Wang. Introduction to the problem of the isochronous hairspring—806

Hartman, Paul L. (see Smith, Lloyd P.)—220
Hertel, K. L. (see Fowler, J. L.)—496
—— (see Sullivan, R. R.)—761
Hickman, Kenneth C. D. Trends in design of fractionating pumps—303
Hodge, A. H. (see Kent, R. H.)—240(L)
Hultgren, Ralph and M. H. Pakkala. Preparation of high melting alloys with the aid of electron bombardment—643
Hutchisson, Elmer. "A way of total peace"—749
—— Analytical physicist—301
—— Atom smashing *versus* humanity smashing—159
—— Columbus meeting—87
—— Congratulations to the A.S.M.—231
—— Modern masterpieces—1
—— National defense and the physicist—451; II—509; III—567
—— "The irresponsibles"—625
—— What is a physicist?—697

Jacobs, R. B. and S. C. Collins. Experimental study of heat interchangers—491

Kang, Bun Po (see Whitehead, J. B.)—596
Kent, R. H. and A. H. Hodge. Piezoelectric *vs.* spring pressure gauge—240(L)
Kincaid, John F. (see Frisch, David)—75
King, Ronold. Parasitic electronic oscillations and coupling frequencies in a power tube—615
Kingslake, R. Design of wide-aperture photographic objectives—56
Kinney, Paul W. (see Bingham, Eugene C.)—192
Kirkpatrick, Arnold. Some relations between molecular structure and plasticizing effect—255
Kistler, S. S. Thermoplastic behavior of linear and three-dimensional polymers—769
Kuiper, G. P. Stellar temperatures—241

Larsen, B. M. and W. E. Shenk. Temperature measurement with blocking-layer photo-cells—555
Lessells, John M. Symposium on tensile test of metals—420
Levy, Saul. Correlation method for the elimination of errors due to unstable excitation conditions in quantitative spectrum analysis—480
Lewis, Bernard and Guenther von Elbe. Answer to communication by W. T. David—158(L)
—— **and Guenther von Elbe.** Flame temperature—698
Loeb, Leonard B. and John M. Meek. Mechanism of spark discharge in air at atmospheric pressure. I—438; II—459
Losinsky, M. (see Babat, G.)—816
Lyons, W. James. Initial stage of plastic deformation in lead under compression—514

MacAdam, David L. Physics in color photography—46
Manning, Millard F. Electrodynamics—572 (book review)
—— Statistical thermodynamics—572 (book review)
Martin, Albert B. (see Cinnamon, C. A.)—487
Matteson, Robert and C. J. Vogt. Velocity of compressional waves in petroleum fractions at atmospheric and elevated pressures—658
McCoy, D. O. (see Fox, G. W.)—592
McFarlan, Ronald L. and J. Wallace Reddie. X-ray study of acetylsalicylic acid when incorporated in certain sugars—80
Meek, John M. (see Loeb, Leonard B.)—438, 459
Merchant, M. E. Mechanism of static friction—230(L)
***Meres, M. W.** (see Muskat, M.)—208
Miley, H. A. (see Cruzan, C. G.)—631
Miller, F. H. Note on Heaviside's expansion theorem—343
Mindlin, R. D. Proceedings of the fifth international congress for applied mechanics—571 (book review)
—— (see Drucker, Daniel C.)—724
Mooney, M. Theory of large elastic deformation—582
Morgan, F. (see Muskat, M.)—208
——, **M. Muskat and D. W. Reed.** Studies in lubrication. VI. Electrolytic models of full journal bearings—141; VIII. Lubrication of plane sliders—541
Morse, Philip M. Acoustic air-jet generator—568 (book review)
Morton, G. A. (see Piore, E. R.)—153
Murphy, George M. Raman effect and its chemical applications—569 (book review)
Muskat, Morris. Theory of lubrication—570 (book review)
—— (see Morgan, F.)—141, 541
—— **and H. H. Evinger.** Studies in lubrication. IX. Effect of the pressure variation of viscosity on the lubrication of plane sliders—739
——, **F. Morgan and M. W. Meres.*** Studies in lubrication. VII. Lubrication of plane sliders of finite width—208

Noel, Edward B. Development of water-cooled quartz mercury lamps—325
Norton, Francis J. Diffusion of hydrogen from water through steel—262

Offner, Franklin. Recorder for electrical potentials. Damping of piezoelectric systems—347
Ôkubo, H. Similarity of the stress distributions in a circular disk and a square plate—720
Osgood, Thomas H. Physics in 1939—2

Pakkala, M. H. (see Hultgren, Ralph)—643
Phillips, C. J. Glass as an electrical insulator—173
Pierce, J. R. Rectilinear electron flow in beams—548
Piore, E. R. and G. A. Morton. Behavior of willemite under electron bombardment—153
Pipes, Louis A. Analysis of symmetrical vibrating systems—279

Reddie, J. Wallace. (see McFarlan, Ronald L.)—80
Reed, D. W. (see Morgan, F.)—141, 541
Richardson, E. G. Optical properties of colloidal suspensions in relation to the measurement of particle-size frequency—653
Roeser, Wm. F. Thermoelectric thermometry—388
Rose, Albert. Mechanical model for the motion of electrons in a magnetic field—711
Rüdenberg, Reinhold. Electric oscillations and surges in subdivided windings—665

* Deceased.

Sabaroff, Samuel. Theory of frequency controlled oscillators—538
Sanders, Edward W. Wave propagation in shearing quartz oscillators of high frequency—299
Sawyer, R. A. and H. B. Vincent. Spectrochemical analysis of sheet steel at the Great Lakes Steel Company—452
Schnurmann, R. Mechanism of static friction—624(L)
Scott Blair, G. W. (see Dix, F. Johnson)—574
Shenk, W. E. (see Larsen, B. M.)—555
Shortley, G. H. Mathematical methods in engineering—626 (book review)
—— Mathematics applied to electrical engineering—626 (book review)
—— (see Weller, R.)—283
Slack, Charles M. (see Ehrke, Louis F.)—129
Slepian, Joseph and W. E. Berkey. Spark gaps with short time lag—765
Smith, Lloyd P. and Paul L. Hartman. Formation and maintenance of electron and ion beams—220
Squire, Charles F. Changes in the absorption spectrum of Pb and Ni films at low temperatures—779
—— Magnetic cooling; the production and measurement of temperatures below 1°K—232
Sullivan, R. R. and K. L. Hertel. Flow of air through porous media—761

Tyrrell, W. A. Moderne kurzwellen-empfangstechnik—570 (book review)

Valasek, Joseph. Fundamentals of photography—627 (book review)
—— Elementary photography—627 (book review)
—— Microscope—627 (book review)
—— Perception of light—626 (book review)
Vincent, H. B. (see Sawyer, R. A.)—452
Vogt, C. J. (see Matteson, Robert)—658
von Elbe, Guenther (see Lewis, Bernard)—158(L), 698

Walker, Eric A. Notes on the power factor testing of long lengths of cables—717
Wang, Ming-chen. (see Goudsmit, S.)—806
Warga, Mary E. Proceedings of the seventh summer conference on spectroscopy and its applications—570 (book review)
—— Wavelength tables—571 (book review)
Webb, J. H. Theory of the photographic latent-image formation—18
Weller, R., G. H. Shortley and B. Fried. Solution of torsion problems by numerical integration of Poisson's equation—283
Wells, A. J. Infra-red transmission of thin films of various organic materials—137
Wensel, H. T. Temperature and temperature scales—373
White, John E. Backfiring in mercury arc rectifiers—507(L)
Whitehead, J. B. and Bun Po Kang. Conductivity of insulating oils under alternating stress—596
Wilkins, T. R. Response of photographic materials to atomic particles—35
Wilson, J. T. (see Atlee, Z. J.)—611
Wilson, Robert R. Theory of the cyclotron—781
Worrell, Francis T. Photography, its principles and practice—71 (book review)
—— Photographic process—71 (book review)
Worthing, A. G. Temperature radiation emissivities and emittances—421

Youtz, J. Paul (see DuMond, Jesse)—357

Subject Index to Volume 11

(L) refers to Letters to the Editor.

"A way of total peace," Elmer Hutchisson—749
Absorption spectrum of Pb and Ni films at low temperatures, Changes in, Charles F. Squire—779
Acetylsalicylic acid, An x-ray study of, Ronald L. McFarlan and J. Wallace Reddie—80
Acoustic air-jet generator, Jul. Hartmann—568 (review)
Agriculture and geochemistry, Qualitative spectrochemical analysis in, Stanley S. Ballard—750
Air at atmospheric pressure, Spark discharge in, Leonard B. Loeb and John M. Meek, I—438; II—459
Air through porous media, Flow of, R. R. Sullivan and K. L. Hertel—761
Alloys, Aluminum-silver, Charles S. Barrett and Alfred H. Geisler—733
Alloys, High melting, Ralph Hultgren and M. H. Pakkala—643
Alternating stress, Conductivity of insulating oils under, J. B. Whitehead and Bun Po Kang—596
Alternating voltages, Breakdown potentials of gases under, G. W. Fox and D. O. McCoy—592
Aluminum hydrate films of importance in silicosis prevention, Identification of—182 (resumé)
Aluminum-silver alloys, Atomic distribution in, Charles S. Barrett and Alfred H. Geisler—733
Amplifier, Logarithmic, for direct currents—125 (resumé)
Analysis of sheet steel at the Great Lakes Steel Company, Spectrochemical, R. A. Sawyer and H. B. Vincent—452
Analysis of symmetrical vibrating systems, Louis A. Pipes—279
Analysis, Quantitative spectrum, Saul Levy—480
Analytical physicist, Elmer Hutchisson—301
Answer to communication by W. T. David, Bernard Lewis and Guenther von Elbe—158(L)
Atom smashing *versus* humanity smashing, Elmer Hutchisson—159
Atomic distribution in aluminum-silver alloys during aging, Charles S. Barrett and Alfred H. Geisler—733
Atomic particles, Response of photographic materials to, T. R. Wilkins—35

Backfiring in mercury arc rectifiers, John E. White—507(L)
Back-reflection lines in powder x-ray photograms, Louis A. Carapella—800
Behavior of willemite under electron bombardment, E. R. Piore and G. A. Morton—153
Beta-brass crystals, Young's modulus of—707 (resumé)
Birefringence in a vinylite plastic, H. W. Farwell—274
Blocking-layer photo-cells, Temperature measurement with, B. M. Larsen and W. E. Shenk—555
Breakdown potentials of gases under alternating voltages, G. W. Fox and D. O. McCoy—592
Bromine isotopes, Separation of, by centrifugation—125 (resumé)
Cables, Power factor testing of long lengths of, Eric A. Walker—717
Calculation of the radiation properties of hollow pipes and horns, L. J. Chu—603
Cathode-ray beam, Ring focusing of negative ions in, C. H. Bachman—83; Correction—240(L)
Centrifugation, Separation of bromine isotopes by—125 (resumé)
Changes in the absorption spectrum of Pb and Ni films at low temperatures, Charles F. Squire—779
Chimneys and columns, Stresses in freely falling, Francis P. Bundy—112
Colloidal suspensions, Optical properties of, E. G. Richardson—653
Color photography, Physics in, David L. MacAdam—46
Columbus meeting, Elmer Hutchisson—87
Compressional waves in petroleum fractions, Velocity of, Robert Matteson and C. J. Vogt—658
Computation of some physical properties of lubricating oils at high pressures. I. Density, R. B. Dow and C. E. Fink—353
Concentrator of eddy currents for zonal heating of steel parts, G. Babat and M. Losinsky—816
Concerning "Physics of flames and explosions of gases," W. T. David—157(L); Answer to communication by W. T. David, Bernard Lewis and Guenther von Elbe—158(L)
Conductivity measurements on potassium halides, Cornelius G. Brennecke—202
Conductivity of insulating oils under alternating stress, J. B. Whitehead and Bun Po Kang—596
Conductivity of metals, Electrical, John Bardeen—88
Conductivity of metals, Thermal—707 (resumé)
Congratulations to the A.S.M., Elmer Hutchisson—231
Cooling, Magnetic, Charles F. Squire—232
Copper, Cuprous-cupric oxide films on, C. G. Cruzan and H. A. Miley—631
Correction, C. H. Bachman—240(L)
Correlation method for the elimination of errors due to unstable excitation conditions in quantitative spectrum analysis, Saul Levy—480
Coupling frequencies in a power tube, Ronold King—615
Crankshafts, Torsional oscillations of, Maurice A. Biot—530
Crystal directions of the same metal, Recent experiments on the thermionic properties of—337 (resumé)
Crystals of zinc, Growth conditions for single and optically mosaic, C. A. Cinnamon and Albert B. Martin—487
Crystals, Young's modulus of beta-brass—707 (resumé)
Cubic lattice constants, Louis A. Carapella—510
Cubic powder patterns, Louis A. Carapella—510
Cuprous-cupric oxide films on copper, C. G. Cruzan and H. A. Miley—631
Cyclotron, The, W. B. Mann—569 (review)

Cyclotron, Theory of the, Robert R. Wilson—781

Damping of piezoelectric systems, Franklin Offner—347
Defense and the physicist, Elmer Hutchisson—451, II—509, III—567
Deformation, Elastic, M. Mooney—582
Density of lubricating oils at high pressures, R. B. Dow and C. E. Fink—353
Design of wide-aperture photographic objectives, R. Kingslake—56
Development of water-cooled quartz mercury lamps, Edward B. Noel—325
Dielectric properties of the rutile form of TiO_2, L. J. Berberich and M. E. Bell—681
Diffusion in the solid state, X-ray method of determining rates of, Jesse DuMond and J. Paul Youtz—357
Diffusion of hydrogen from water through steel, Francis J. Norton—262
Direct currents, Logarithmic amplifier for—125 (resumé)

Earth's magnetism—621 (resumé)
Eddy currents, Concentration of, for zonal heating of steel parts, G. Babat and M. Losinsky—816
Elastic deformation, Theory of large, M. Mooney—582
Elastic moduli of Cu_3Au through the order-disorder transformation—476 (resumé)
Elastic waves, Influence of initial stress on, Maurice A. Biot—522
Electric oscillations and surges in subdivided windings, Reinhold Rüdenberg—665
Electrical conductivity of metals, John Bardeen—88
Electrical insulator, Glass as an, C. J. Phillips—173
Electrodes, Spark plug, J. H. Dillon—291, 562(L); Robley D. Evans—561(L)
Electrodynamics, L. Page and N. I. Adams, Jr.—572 (review)
Electrolytic polishing. II, W C. Elmore—797
Electromagnetic oscillations, Electronic generation of, E. U. Condon—502
Electron and ion beams, Formation and maintenance of, Lloyd P. Smith and Paul L. Hartman—220
Electron bombardment, Behavior of willemite under, E. R. Piore and G. A. Morton—153
Electron bombardment, Preparation of high melting alloys with the aid of, Ralph Hultgren and M. H. Pakkala—643
Electron flow in beams, Rectilinear, J. R. Pierce—548
Electron microscope—629 (resumé)
Electronic generation of electromagnetic oscillations, E. U. Condon—502
Electronic work functions by contact potential measurement—338 (resumé)
Electrons in a magnetic field, Mechanical model for the motion of, Albert Rose—711
Elementary photography, Gilford G. Quarles—627 (review)
Emissivities and emittances, Temperature radiation, A. G. Worthing—421
Equations of finite differences applied to torsional oscillations of crankshafts, Maurice A. Biot—530
Experimental study of heat interchangers, R. B. Jacobs and S. C. Collins—491

Ferromagnetic domains and the magnetization curve, William Fuller Brown, Jr.—160
Films, Lubrication in vacuum by vaporized thin metallic, Z. J. Atlee, J. T. Wilson and J. C. Filmer—611
Films on copper, Cuprous-cupric oxide, C. G. Cruzan and H. A. Miley—631
Films, Pb and Ni, Charles F. Squire—779
Fission, Mechanism of nuclear—70 (resumé)
Flame temperature, Bernard Lewis and Guenther von Elbe—698
Flames and explosions of gases, W. T. David—157(L); Answer to communication by W. T. David, Bernard Lewis and Guenther von Elbe—158(L)
Flow of a gas through porous media, J. L. Fowler and K. L. Hertel—496
Flow of air through porous media, R. R. Sullivan and K. L. Hertel—761
Flow of suspensions through narrow tubes, F. Johnson Dix and G. W. Scott Blair—574
Fluidity, Relation of, to volume in organic liquids, Eugene C. Bingham and Paul W. Kinney—192
Flux of liquids through tubes, Derivation of equations for, Francis Breazeale—187
Formation and maintenance of electron and ion beams, Lloyd P. Smith and Paul L. Hartman—220
Fractionating columns, Packed—628 (resumé)
Fractionating pumps, Trends in design of, Kenneth C. D. Hickman—303
Frequency controlled oscillators, Theory of, Samuel Sabaroff—538
Friction, Mechanism of static, M. E. Merchant—230(L); R. Schnurmann—624(L)
Friction of plastics, Solid, Andrew Gemant—647
Fundamentals of photography, Paul E. Boucher—627 (review)

Gas analyses, Mass spectrometer for—628 (resumé)
Gas through porous media, Flow of a, J. L. Fowler and K. L. Hertel—496
Gases hydrogen, oxygen, nitrogen, carbon dioxide and air, Investigation into the gettering powers of various metals for, Louis F. Ehrke and Charles M. Slack—129
Gases, Preferential and initial ionic recombination in, N. E. Bradbury—267
Gases under alternating voltages, Breakdown potentials of, G. W. Fox and D. O. McCoy—592
Gauge, Piezoelectric *vs.* spring pressure, R. H. Kent and A. H. Hodge—240(L)
Geochemistry, Qualitative spectrochemical analysis in, Stanley S. Ballard—750
Gettering powers of various metals for the gases hydrogen, oxygen, nitrogen, carbon dioxide and air, Louis F. Ehrke and Charles M. Slack—129
Glass as an electrical insulator, C. J. Phillips—173
Graphical method for selecting suitable radiations for the precision determination of non-cubic lattice constants and for indexing back-reflection lines in powder x-ray photograms, Louis A. Carapella—800

Graphical method for selecting suitable targets for precision determination of cubic lattice constants and for solving cubic powder patterns, Louis A. Carapella—510
Great Lakes Steel Company, Spectrochemical analysis of sheet steel at, R. A. Sawyer and H. B. Vincent—452
Growth conditions for single and optically mosaic crystals of zinc, C. A. Cinnamon and Albert B. Martin—487

Hairspring, Isochronous, S. Goudsmit and Ming-chen Wang—806
Heat interchangers, Experimental study of, R. B. Jacobs and S. C. Collins—491
Heaviside's expansion theorem, F. H. Miller—343
Hydrogen arc for absorption spectroscopy—182 (resumé)
Hydrogen, Diffusion of, from water through steel, Francis J. Norton—262

Identification of aluminum hydrate films of importance in silicosis prevention—182 (resumé)
Influence of initial stress on elastic waves, Maurice A. Biot—522
Infra-red transmission of thin films of various organic materials, A. J. Wells—137
Initial stage of plastic deformation in lead under compression, W. James Lyons—514
Insulating oils under alternating stress, Conductivity of, J. B. Whitehead and Bun Po Kang—596
Insulator, Glass as an electrical, C. J. Phillips—173
Introduction to the problem of the isochronous hairspring, S. Goudsmit and Ming-chen Wang—806
Investigation into the gettering powers of various metals for the gases hydrogen, oxygen, nitrogen, carbon dioxide and air, Louis F. Ehrke and Charles M. Slack—129
Ion beams, Formation and maintenance of, Lloyd P. Smith and Paul L. Hartman—220
Ionic recombination in gases, Preferential and initial, N. E. Bradbury—267
Ions, Ring focusing of, in a cathode-ray beam, C. H. Bachman—83; Correction—240(L)
Isochronous hairspring, Introduction to the problem of the, S. Goudsmit and Ming-chen Wang—806
Isotope analyses, Mass spectrometer for—628 (resumé)
Isotopes, Bromine, Separation of, by centrifugation—125 (resumé)
Isotopes, Concentration of—628 (resumé)

Journal bearings, Electrolytic models of full, F. Morgan, M. Muskat and D. W. Reed—141

Latent-image formation, Theory of the photographic, J. H. Webb—18
Lattice constants, Cubic, Louis A. Carapella—510
Lattice constants, Non-cubic, Louis A. Carapella—800
Lead under compression, Initial stage of plastic deformation in, W. James Lyons—514
Linear polymers, Thermoplastic behavior of, S. S. Kistler—769
Liquids, Pressure and temperature effects on the viscosity of, David Frisch, Henry Eyring and John F. Kincaid—75
Liquids, Relation of fluidity to volume in organic, Eugene C. Bingham and Paul W. Kinney—192
Liquids, Remarks on the study of structural viscosity in, and the derivation of equations for the flux through tubes, Francis Breazeale—187
Logarithmic amplifier for direct currents—125 (resumé)
Lubricating oils at high pressures, Computation of some physical properties of, R. B. Dow and C. E. Fink—353
Lubrication in vacuum by vaporized thin metallic films, Z. J. Atlee, J. T. Wilson and J. C. Filmer—611
Lubrication, Studies in. VI. Electrolytic models of full journal bearings, F. Morgan, M. Muskat and D. W. Reed—141; VII. Lubrication of plane sliders of finite width, M. Muskat, F. Morgan and M. W. Meres*—208; VIII. Lubrication of plane sliders, F. Morgan, M. Muskat and D. W. Reed—541; IX. Effect of the pressure variation of viscosity on the lubrication of plane sliders, M. Muskat and H. H. Evinger—739

Magnetic cooling; the production and measurement of temperatures below 1°K, Charles F. Squire—232
Magnetic field, Mechanical model for the motion of electrons in, Albert Rose—711
Magnetism, Earth's—621 (resumé)
Magnetization curve, Ferromagnetic domains and, William Fuller Brown, Jr.—160
Mass spectrometer for routine isotope and gas analyses—628 (resumé)
Mathematical methods in engineering, T. v. Kármán and M. A. Biot—626 (review)
Mathematics applied to electrical engineering, A. G. Warren—626 (review)
Measurement of solid friction of plastics, Andrew Gemant—647
Mechanical model for the motion of electrons in a magnetic field, Albert Rose—711
Mechanics applied to vibrations and balancing, D. Laugharne Thornton—626 (review)
Mechanism of nuclear fission—70 (resumé)
Mechanism of spark discharge in air at atmospheric pressure, Leonard B. Loeb and John M. Meek, I—438, II—459
Mechanism of static friction, M. E. Merchant—230(L); R. Schnurmann—624(L)
Mercury arc rectifiers, Backfiring in, John E. White—507(L)
Mercury lamps, Development of water-cooled quartz, Edward B. Noel—325
Metal, Thermionic properties of different crystal directions of—337 (resumé)
Metals, Electrical conductivity of, J. Bardeen—88
Metals, Gettering powers of, for the gases hydrogen, oxygen, nitrogen, carbon dioxide and air, Louis F. Ehrke and Charles M. Slack—129
Metals, Symposium on tensile test of, John M. Lessels—420
Metals, Thermal conductivity of—707 (resumé)
Meteorological glossary—568 (review)
Microscope, New electron—629 (resumé)
Microscope, R. M. Allen—627 (review)

* Deceased.

Modern masterpieces, Elmer Hutchisson—1
Modern science, Hyman Levy—571 (review)
Moderne kurzwellen-empfangstechnik, M. J. O. Strutt—570 (review)
Molecular structure and plasticizing effect, Arnold Kirkpatrick—255

National defense and the physicist, Elmer Hutchisson—451, II—509, III—567
New electron microscope—629 (resumé)
New radiation pyrometer—475 (resumé)
Non-cubic lattice constants, Louis A. Carapella—800
Note on Heaviside's expansion theorem, F. H. Miller—343
Notes on the power factor testing of long lengths of cables, Eric A. Walker—717

Objectives, Design of wide-aperture, R. Kingslake—56
Oils at high pressures, Computation of some physical properties of lubricating, R. B. Dow and C. E. Fink—353
Oils, Insulating, J. B. Whitehead and Bun Po Kang—596
On the flow of suspensions through narrow tubes, F. Johnson Dix and G. W. Scott Blair—574
On the resistance to the uniform motion of a solid through a viscous liquid, Raymond B. Block—635
Optical properties of colloidal suspensions in relation to the measurement of particle-size frequency, E. G. Richardson—653
Optical pyrometry, W. E. Forsythe—408
Order-disorder transformation, Elastic moduli of Cu_3Au through the,—476 (resumé)
Order-disorder transformations—124 (resumé)
Organic materials, Infra-red transmission of thin films of, A. J. Wells—137
Oscillations, Electronic generation of electromagnetic, E. U. Condon—502
Oscillations of crankshafts, Torsional, Maurice A. Biot—530
Oscillators, Shearing quartz, Edward W. Sanders—299
Oscillators, Theory of frequency controlled, Samuel Sabaroff—538
Oxide films on copper, Cuprous-cupric, C. G. Cruzan and H. A. Miley—631

Packed fractionating columns and the concentration of isotopes—628 (resumé)
Parasitic electronic oscillations and coupling frequencies in a power tube, Ronold King—615
Particle-size frequency, Optical properties of colloidal suspensions in relation to the measurement of, E. G. Richardson—653
Pendulum analysis in the scale industry, Glenn R. Carley—314
Perception of light, W. D. Wright—626 (review)
Petroleum fractions at atmospheric and elevated pressures, Velocity of compressional waves in, Robert Matteson and C. J. Vogt—658
Phosphorus in soil studies, Use of radioactive, Stanley S. Ballard and L. A. Dean—366
Photo-cells, Temperature measurement with blocking-layer, B. M. Larsen and W. E. Shenk—555
Photoelastic methods, Stress analysis by three-dimensional, Daniel C. Drucker and Raymond D. Mindlin—724
Photographic latent-image formation, Theory of, J. H. Webb—18
Photographic materials, Response of, to atomic particles, T. R. Wilkins—35
Photographic objectives, Design of wide-aperture, R. Kingslake—56
Photographic process, Julian Ellis Mack and Miles J. Martin—71 (review)
Photography, Color, David L. MacAdam—46
Photography, its principles and practice, C. B. Neblette—71 (review)
Physicist, National defense and the, Elmer Hutchisson—451, II—509, III—567
Physics in color photography, David L. MacAdam—46
Physics in 1939, Thomas H. Osgood—2
Physics of stressed solids—475 (resumé)
Piezoelectric systems, Damping of, Franklin Offner—347
Piezoelectric *vs.* spring pressure gauge, R. H. Kent and A. H. Hodge—240(L)
Pipes and horns, Calculation of the radiation properties of, L. J. Chu—603
Plane sliders, Effect of the pressure variation of viscosity on the lubrication of, M. Muskat and H. H. Evinger—739
Plane sliders, Lubrication of, F. Morgan, M. Muskat and D. W. Reed—541
Plane sliders of finite width, Lubrication of, M. Muskat, F. Morgan and M. W. Meres*—208
Plastic deformation in lead under compression, Initial stage of, W. James Lyons—514
Plastic, Tension and birefringence in vinylite, H. W. Farwell—274
Plasticizing effect, Some relations between molecular structure and, Arnold Kirkpatrick—255
Plastics, Solid friction of, Andrew Gemant—647
Poisson's equation, Solution of torsion problems by numerical integration of, R. Weller, G. H. Shortley and B. Fried—283
Polishing, Electrolytic, W. C. Elmore—797
Polonium alloy for spark plug electrodes, J. H. Dillon—291; Robley D. Evans—561(L); Answer to communication by R. D. Evans, J. H. Dillon—562(L)
Polymers, Thermoplastic behavior of linear and three-dimensional, S. S. Kistler—769
Porous media, Flow of a gas through, J. L. Fowler and K. L. Hertel—496
Porous media, Flow of air through, R. R. Sullivan and K. L. Hertel—761
Potassium halides, Conductivity measurements on, Cornelius G. Brennecke—202
Potentials, Recorder for electrical, Franklin Offner—347
Powder patterns, Cubic, Louis A. Carapella—510
Powder x-ray photograms, Louis A. Carapella—800
Power factor testing of long lengths of cables, Eric A. Walker—717
Power tube, Parasitic electronic oscillations and coupling frequencies in a, Ronold King—615

* Deceased.

Preferential and initial ionic recombination in gases, N. E. Bradbury—267
Preparation of high melting alloys with the aid of electron bombardment, Ralph Hultgren and M. H. Pakkala—643
Pressure and temperature effects on the viscosity of liquids, David Frisch, Henry Eyring, and John F. Kincaid—75
Proceedings of the fifth international congress for applied mechanics, J. P. Den Hartog and H. Peters, Editors—571 (review)
Proceedings of the seventh summer conference on spectroscopy and its applications—570 (review)
Pumps, Trends in design of fractionating, Kenneth C. D. Hickman—303
Pyrometer, New radiation—475 (resumé)
Pyrometry, Optical, W. E. Forsythe—408

Qualitative spectrochemical analysis in agriculture and geochemistry, Stanley S. Ballard—750
Quantitative spectrum analysis, Elimination of errors due to unstable excitation conditions in, Saul Levy—480
Quartz oscillators of high frequency, Wave propagation in shearing, Edward W. Sanders—299

Radiation emissivities and emittances, Temperature, A. G. Worthing—421
Radiation properties of hollow pipes and horns, L. J. Chu—603
Radiation pyrometer—475 (resumé)
Radioactive phosphorus in soil studies, Stanley S. Ballard and L. A. Dean—366
Raman effect and its chemical applications, James H. Hibben—569 (review)
Recent experiments on the thermionic properties of different crystal directions of the same metal—337 (resumé)
Recorder for electrical potentials. Damping of piezoelectric systems, Franklin Offner—347
Rectifiers, Backfiring in mercury arc, John E. White—507(L)
Rectilinear electron flow in beams, J. R. Pierce—548
Relation of fluidity to volume in organic liquids, Eugene C. Bingham and Paul W. Kinney—192
Remarks on the study of structural viscosity in liquids, and the derivation of equations for the flux of such liquids through tubes, Francis Breazeale—187
Resistance to the uniform motion of a solid through a viscous liquid, Raymond B. Block—635
Response of photographic materials to atomic particles, T. R. Wilkins—35
Ring focusing of negative ions in a cathode-ray beam, C. H. Bachman—83; Correction—240(L)
Rutile form of TiO_2, Dielectric properties of the, L. J. Berberich and M. E. Bell—681

Scale industry, Pendulum analysis in, Glenn R. Carley—314
Separation of bromine isotopes by centrifugation—125 (resumé)
Silicosis prevention, Identification of aluminum hydrate films of importance in—182 (resumé)
Similarity of the stress distributions in a circular disk and a square plate, H. Ôkubo—720
Sliders, Lubrication of plane, F. Morgan, M. Muskat, and D. W. Reed—541; M. Muskat and H. H. Evinger—739; M. Muskat, F. Morgan and M. W. Meres*—208
Soil studies, Use of radioactive phosphorus in, Stanley S. Ballard and L. A. Dean—366
Solid state, X-ray method of determining rates of diffusion in the, Jesse DuMond and J. Paul Youtz—357
Solid through a viscous liquid, Resistance to the uniform motion of a, Raymond B. Block—635
Solids, Physics of stressed—475 (resumé)
Solution of torsion problems by numerical integration of Poisson's equation, R. Weller, G. H. Shortley and B. Fried—283
Some relations between molecular structure and plasticizing effect, Arnold Kirkpatrick—255
Spark discharge in air at atmospheric pressure, Mechanism of, Leonard B. Loeb and John M. Meek, I—438, II—459
Spark gaps with short time lag, Joseph Slepian and W. E. Berkey—765
Spark plug electrodes, Polonium alloy for, J. H. Dillon—291, 562(L); Robley D. Evans—561(L)
Spectrochemical analysis in agriculture and geochemistry, Qualitative, Stanley S. Ballard—750
Spectrochemical analysis of sheet steel at the Great Lakes Steel Company, R. A. Sawyer and H. B. Vincent—452
Spectrometer, Mass—628 (resumé)
Spectroscopy, Hydrogen arc for absorption—182 (resumé)
Spectrum analysis, Elimination of errors due to unstable excitation conditions in quantitative, Saul Levy—480
Spectrum of Pb and Ni films at low temperatures, Changes in the absorption, Charles F. Squire—779
Speech, Synthesizing—124 (resumé)
Static and dynamic electricity, William R. Smythe—568 (review)
Static friction, Mechanism of, M. E. Merchant—230(L); R. Schnurmann—624(L)
Statistical thermodynamics, R. H. Fowler and E. A. Guggenheim—572 (review)
Steel parts, Concentrator of eddy currents for zonal heating of, G. Babat and M. Losinsky—816
Steel, Spectrochemical analysis of sheet, R. A. Sawyer and H. B. Vincent—452
Stellar temperatures, G. P. Kuiper—241
Stress analysis by three-dimensional photoelastic methods, Daniel C. Drucker and Raymond D. Mindlin—724
Stress distributions in a circular disk and a square plate, Similarity of the, H. Ôkubo—720
Stressed solids, Physics of—475 (resumé)
Stresses in freely falling chimneys and columns, Francis P. Bundy—112
Studies in lubrication. VI. Electrolytic models of full journal bearings, F. Morgan, M. Muskat and D. W. Reed—141; VII. Lubrication of plane sliders of finite width, M. Muskat, F. Morgan, and M. W. Meres*—208; VIII. Lubrication of plane sliders, F. Morgan, M. Muskat and D. W. Reed—541; IX. Effect of the pressure variation of viscosity on the lubrication of plane sliders, M. Muskat and H. H. Evinger—739

* Deceased.

Subdivided windings, Electric oscillations and surges in, Reinhold Rüdenberg—665
Suspensions, Colloidal, E. G. Richardson—653
Suspensions through narrow tubes, Flow of, F. Johnson Dix and G. W. Scott Blair—574
Symposium on tensile test of metals, John M. Lessells—420
Synthesizing speech—124 (resumé)

Targets for precision determination of cubic lattice constants and for solving cubic powder patterns, Louis A. Carapella—510
Temperature and temperature scales, H. T. Wensel—373
Temperature effects on the viscosity of liquids, David Frisch, Henry Eyring and John F. Kincaid—75
Temperature, Flame, Bernard Lewis and Guenther von Elbe—698
Temperature measurement with blocking-layer photocells, B. M. Larsen and W. E. Shenk—555
Temperature radiation emissivities and emittances, A. G. Worthing—421
Temperature scale, a proposed change in definition, F. G. Brickwedde—371
Temperatures below 1°K, Production and measurement of, Charles F. Squire—232
Temperatures, Stellar, G. P. Kuiper—241
Tensile test of metals, Symposium on, John M. Lessells—420
Tension and birefringence in a vinylite plastic, H. W. Farwell—274
Terrestrial magnetism and electricity, J. A. Fleming, Editor—568 (review)
"The irresponsibles," Elmer Hutchisson—625
Theory of frequency-controlled oscillators, Samuel Sabaroff—538
Theory of large elastic deformation, M. Mooney—582
Theory of lubrication, M. D. Hersey—570 (review)
Theory of the cyclotron, Robert R. Wilson—781
Theory of the photographic latent-image formation, J. H. Webb—18
Thermal conductivity of metals—707 (resumé)
Thermionic properties of different crystal directions of the same metal, Recent experiments on—337 (resumé)
Thermoelectric thermometry, Wm. F. Roeser—388
Thermometry, Thermoelectric, Wm. F. Roeser—388
Thermoplastic behavior of linear and three-dimensional polymers, S. S. Kistler—769
Thin films of various organic materials, Infra-red transmission of, A. J. Wells—137
Three-dimensional photoelastic methods, Stress analysis by, Daniel C. Drucker and Raymond D. Mindlin—724
Three-dimensional polymers, Thermoplastic behavior of, S. S. Kistler—769
TiO_2, Dielectric properties of the rutile form of, L. J. Berberich and M. E. Bell—681
Torsion problems, Solution of, by numerical integration of Poisson's equation, R. Weller, G. H. Shortley and B. Fried—283
Torsional oscillations of crankshafts, Equations of finite differences applied to, Maurice A. Biot—530
Trends in design of fractionating pumps, Kenneth C. D. Hickman—303

Unstable excitation conditions in quantitative spectrum analysis, Saul Levy—480
Use of radioactive phosphorus in soil studies, Stanley S. Ballard and L. A. Dean—366

Velocity of compressional waves in petroleum fractions at atmospheric and elevated pressures, Robert Matteson and C. J. Vogt—658
Vibrating systems, Analysis of symmetrical, Louis A. Pipes—279
Vinylite plastic, Tension and birefringence in a, H. W. Farwell—274
Viscosity of liquids, Pressure and temperature effects on the, David Frisch, Henry Eyring and John F. Kincaid—75
Viscosity in liquids, Remarks on the study of structural, Francis Breazeale—187
Viscous liquid, Motion of a solid through, Raymond B. Block—635

Wave propagation in shearing quartz oscillators of high frequency, Edward W. Sanders—299
Wavelength tables, George R. Harrison—571 (review)
Waves, Elastic, Maurice A. Biot—522
What is a physicist? Elmer Hutchisson—697
Willemite under electron bombardment, Behavior of, E. R. Piore and G. A. Morton—153
Work functions, Electronic—338 (resumé)

X-ray method of determining rates of diffusion in the solid state, Jesse DuMond and J. Paul Youtz—357
X-ray photograms, Powder, Louis A. Carapella—800
X-ray study of acetylsalicylic acid when incorporated in certain sugars, Ronald L. McFarlan and J. Wallace Reddie—80

Young's modulus of beta-brass crystals—707 (resumé)

Zinc, Growth conditions for single and optically mosaic crystals of, C. A. Cinnamon and Albert B. Martin—487

UNUSUAL APPLICATIONS OF L&N EQUIPMENT

Applications of scientific instruments to special research problems are often unusual enough to be interesting, yet too limited to warrant detailed explanation.

For example, in an investigation of "Leaf Temperatures of Cotton . . .", the Department of Agriculture used a thermocouple connected to an L&N Galvanometer. The leaf was folded over one junction of the couple and the galvanometer deflection showed the temperature difference between the leaf and the surrounding air.

Some years ago, the Dept. of Agriculture had another interesting problem. They found it necessary to measure the temperature of a growing raspberry. A very small thermocouple connected to a manual indicator solved this one.

At the Harvard Forest, Petersham, Mass., a Leeds & Northrup Recorder integrates the amount of sunlight reaching the plants and trees. An Eppley Pyroheliometer which consists of a thermopile on a flat disc is exposed to the sunlight. Under the central junctions of the thermopile the disc is painted black to absorb radiation. Under the outer junctions, the disc is painted white and reflects radiation so that there is a temperature difference between outer and inner junctions, depending on the amount of sunlight reaching the disc. The emf generated is recorded by an L&N Recorder and is a measure of total radiation.

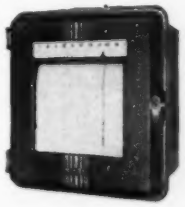

One investigation into the sleeping habits of humans used an L&N Conductivity Recorder.

Other applications include the measurement of temperature in a beehive, of various body temperatures in humans and animals, and hundreds of other researches which serve to illustrate the versatility and adaptability of Leeds & Northrup instruments. If you are using L&N equipment in an unusual way, we'll be interested to hear about it.

pH Indicator Is Accurate Even When Humidity Is 95%

Tube-Compartment Shield Helps Instrument Hold Accuracy Under Almost Any Ambient Condition; Prevents Delay and Inconvenience

As accurate in atmospheres of 95% relative humidity as it is under perfectly dry conditions, L&N's Universal pH Indicator practically eliminates interruptions caused by high humidity. Avoiding delays arising from inaccurate measurements and a lack of confidence in results, the user can go ahead in his work with the sure knowledge that his measurements are correct.

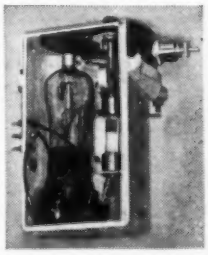

One side cut off of the tube compartment shows its construction

Advanced electrical design makes such performance possible. The vacuum tube is inclosed in an air-tight metal case which is equipped with a desiccator to prevent moisture and keep leakage currents from flowing over the tube surface. With this compartment, electrostatic conditions and humidity below 95% have no effect upon accuracy.

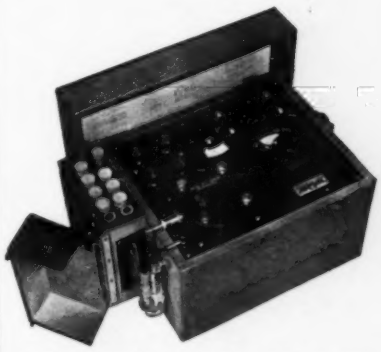

A full description of the Universal pH Indicator and other L&N pH instruments is contained in Catalog EN-96. A copy will be sent on request.

LEEDS & NORTHRUP COMPANY, 4978 STENTON AVE., PHILA., PA.

LEEDS & NORTHRUP

Measuring Instruments · Telemeters · Automatic Controls · Heat Treating Furnace

Jrl Ad E(9)

THE IGNITRON RECTIFIER

FOR HIGH-EFFICIENCY POWER CONVERSION

•

A Westinghouse development that is finding growing use at voltages of 750 volts and less

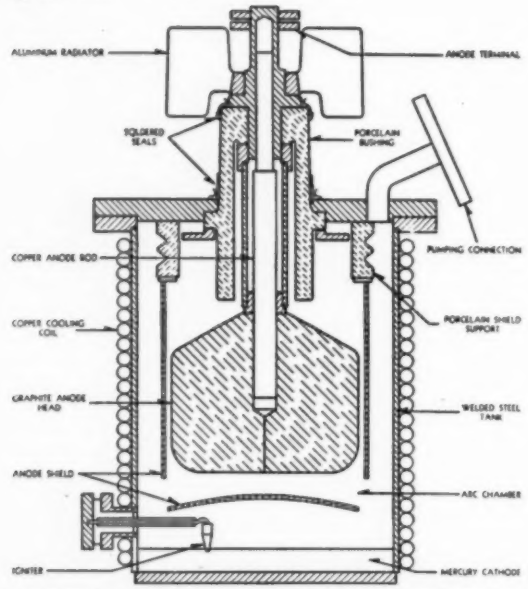

Basically, the Ignitron is a single-anode mercury-arc rectifier. The tube is fired by the igniter which, at the exact moment when power should be carried between anode and cathode, creates the cathode spot. Since there is no arc in the tank when the anode is negative with respect to the cathode, the need for shields and grids is minimized, and the electrodes can be placed closer together.

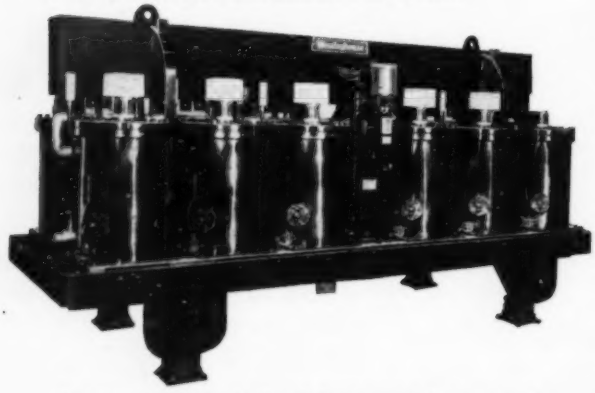

As a power rectifier, banks of six or more tubes are used. Ignitron rectifiers require no expensive foundations—they can be adapted to almost any space restrictions.

A chemical plant is installing a 50,000-ampere unit. Another has recently ordered a 240,000-ampere unit. A Class I railroad uses a 3000-kw unit at its busiest terminal. Such are a few items from recent news about Ignitron Rectifiers.

The Ignitron Rectifier is a comparatively recent development whereby groups of individual tanks or tubes replace the single-tank, multiple-anode design of the conventional mercury-arc rectifier. Each tube contains a single anode and cathode, plus an igniter or "starter." An arc is established only when the anode is positive with respect to the cathode.

With this method of excitation, the anode can be placed closer to the cathode, and less shielding is required. With a lower arc drop, efficiency is higher than that of the conventional multi-anode design (about 1½% higher at 600 V; 2½% higher at 250 V). Cooling is simplified, and corrosion minimized.

Simplified voltage control with practically no change in over-all efficiency is another advantage of the Ignitron Rectifier. By varying the d-c voltage, it is possible to shift load, to start at low voltages or to limit current.

Westinghouse ENGINEERING RESEARCH FOR INDUSTRY

KODACHROME DUPLICATES
of original Kodachrome Transparencies

THE Eastman duplicating service greatly enhances the utility of your Kodachrome pictures. Original transparencies may be preserved under ideal storage conditions and the duplicates used for routine purposes. The service is comprehensive, embracing the following:

1. *24 x 36 mm. Kodachrome Duplicates U*—from 24 x 36 mm. and Bantam Kodak Kodachrome Film transparencies, and Kodachrome Professional Film transparencies (except sizes 45 x 107 mm., 6 x 13 cm., and 11″ x 14″).
2. *24 x 36 mm. Kodachrome Duplicates M*—from the same film sizes as the 24 x 36 mm. Duplicates U. The process involves an additional step, however, and this results in more faithful reproduction of both color and scale of gradation.
3. *Kodachrome Professional Film Sizes* (except sizes 45 x 107 mm. and 6 x 13 cm.)—from 24 x 36 mm. and Bantam Kodak Kodachrome Film transparencies, and most sizes of Kodachrome Professional Film transparencies.
4. *16 mm. Kodachrome Motion Pictures*—from 16 mm. Kodachrome motion pictures, with or without incorporation of sound. Monochrome duplicates can also be made from any 16 mm. Kodachrome motion picture, with or without sound.

For further information about any phase of the Kodachrome Duplicating Service, and prices, consult your regular photographic dealer or write direct.

EASTMAN KODAK COMPANY, Rochester, N. Y.

PROVED PERFORMANCE
IN HIGH VOLTAGE AND HIGH FREQUENCY APPLICATIONS

OPENING NEW ENGINEERING HORIZONS

After three years of extensive field use, these unique IRC Resistor types have established themselves as essential tools wherever high voltage or high frequency problems are involved. Far beyond the experimental stage, they have paved the way to many important developments ranging from high voltage dividers and meter multipliers to high frequency and surge generator applications.

IRC Type MV Resistors are available in 5 standard sizes from 1 to 150 watts and from 150 to 10,000 megohms—also many special types.

IRC Type MP Resistors are designed for ultra-high frequency service where power dissipation is required. Five standard sizes, from 5 to 150 watts and from 5 to 25 ohms min. with 1000 megohms maximum.

Both of these types utilize the famous "Metallized" resistance principle and have the same voltage coefficient, frequency and stability characteristics as IRC Types BT and F Resistors.

Bulletin II gladly sent upon request.

IRC
INTERNATIONAL RESISTANCE CO., 419 N. Broad St., Philadelphia, Pa.

REPORTS ON
PROGRESS IN PHYSICS
VOLUME VI (1939)

A COMPREHENSIVE REVIEW by qualified physicists under the general editorship of
J. H. AWBERY, B.A., B.Sc.

434 pages *Illustrated* *$5.25 post free* *Bound in cloth*

The steady demand for the first five volumes has strengthened the Physical Society's belief that these annual *Reports* satisfy a long-felt want. Despite the abnormal times, the sixth volume is now ready and is as comprehensive in scope as any of the preceding volumes. This volume includes articles on:

Production and Measurement of Short-Wave Radiations
Induced Radioactivity
Separation of Isotopes
Stellar Interiors and Evolution
Theory of Molecular Structure
Luminescence of Solids
Theory of Elasticity of Rubber
Ultra-Short Waves on Wires
Impedance Networks
Measurement of Capacitance
Dielectric Breakdown in Solids
Teaching of Physics in Technical Institutions
The Cyclotron
The Meson
Spectroscopy
X-Rays and Crystals
Reactions in Solids
Fluid Motion
Sound
Heat
Superconductivity
Liquid Helium

Volumes I, II and IV (1934, 1935 and 1937) are now out of print. Volumes III and V (1936 and 1938) are still available, $5.00 each post free.

Orders, with remittance, should be sent to

THE PHYSICAL SOCIETY, 1 Lowther Gardens, Exhibition Road, London, S.W.7

JAGABI "LUBRI-TACT"
LABORATORY RHEOSTATS

Lubricated sliding contact. Four sizes, seventy-six different ratings carried in stock.

Also Compression Carbon Rheostats.

Bulletin 1620-R.

JAMES G. BIDDLE CO.
ELECTRICAL AND SCIENTIFIC INSTRUMENTS
1211-13 ARCH STREET PHILADELPHIA, PA.

CHRISTMAS SEALS

Help to Protect Your Home from Tuberculosis

An Important New Book

ELECTROMAGNETIC THEORY

By J. A. STRATTON

Associate Professor of Physics
Massachusetts Institute of Technology

International Series in Physics

615 pages, 6 x 9. $6.00

IN this advanced text and reference book the author places primary emphasis on dynamic rather than static field theory, postulating Maxwell's equations from the outset. A mathematical formulation of the general theory is followed by a comprehensive investigation of energy and stress relations. The properties of static fields are then discussed and the rest of the book is devoted to the propagation of plane, cylindrical, and spherical waves, the theory of radiation, and boundary-value problems.

Send for a copy on approval

McGRAW-HILL BOOK COMPANY, Inc.

330 West 42nd Street **New York, N. Y.**

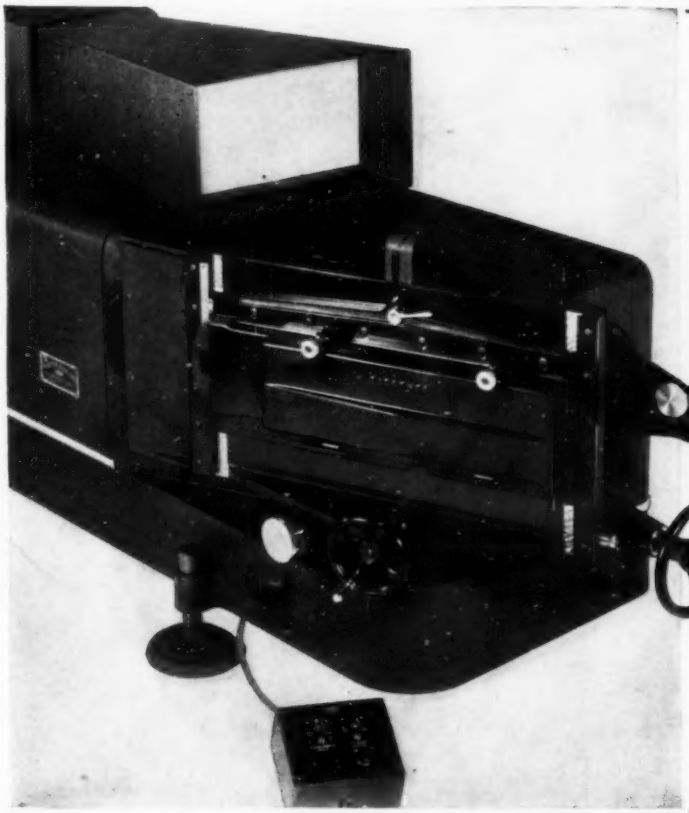

New! **TWO LENS QUARTZ**

SPECTROGRAPH

Range **1850Å to 12000Å**

One Plate **covers the region 2100Å–3300Å most used in analytical work.**

One Control **sets wave range, focuses, and tilts plate holder, *automatically*.**

Any Spectrum Line **can be brought to center of plate.**

Projection **of wavelength setting, and of range covered, on large translucent screen. Numbers 1 inch high, always visible.**

Littrow Weaknesses Avoided. **No stray light. No tilting of lenses necessary. No right angle reflecting prisms. Illuminating bench aligned with slit.**

The GAERTNER SCIENTIFIC CORPORATION

1212 Wrightwood Ave. ▲ Chicago ▲ U. S. A.

Linde

RARE GASES AND MIXTURES

NEON
ARGON
HELIUM
KRYPTON
XENON
MIXTURES

. . . Spectroscopically Pure
. . . Easily removed from bulb without contamination

Scientific uses for Linde rare gases include—

1. The study of electrical discharges.
2. Work with rectifying and stroboscopic devices.
3. Metallurgical research.
4. Work with inert atmospheres, where heat conduction must be increased or decreased.

Many standard mixtures are available. Special mixtures for experimental purposes can be supplied upon request.

The word "Linde" is a trade-mark of

The Linde Air Products Company
Unit of Union Carbide and Carbon Corporation
30 East 42nd Street UCC Offices in
New York, N. Y. Principal Cities

PORTABLE POTENTIOMETERS

Rubicon portable potentiometers are available in a variety of single and double range models suitable for thermocouple, pH and instrument calibration work. Guaranteed accuracy to .1%.

These sturdy, self-contained instruments are built to give years of satisfactory service under all conditions encountered in the laboratory, shop or field. They are outstanding values in their class.

Ask for Bulletin 270.

RUBICON COMPANY
Electrical Instrument Makers
29 North Sixth Street Philadelphia, Pa.

ANNOUNCING

Polaroid* Quarterwave Glass

Polaroid Quarterwave Glass is now offered in the form of inexpensive 1¾″ discs for use with Polaroid Light Polarizers in demonstrations in advanced optics — photoelastic stress analysis, microscopy and other applications involving circularly polarized light.

Polaroid Laboratory Quarterwave Plates, edge-ground, set of 2, 1¾″ diameter. No. 390: $7.50. Non-standard sizes up to 12″ x 12″ are also available. Prices on request.

For new complete catalog, write your laboratory supply house or Division 4

POLAROID CORPORATION
729 Main Street, Cambridge, Mass.

* T. M. REG. U. S. PAT. OFF.

THERMOCOUPLES for special uses

We manufacture many thermocouples with much higher electromotive force than is obtainable with the standard platinum-rhodium vs platinum couple.

A few typical couples are:

COUPLE	E. M. F., microvolts per °C in range 0-100°C.
Pt-Ir vs Au-Pd	47
Chromel P vs Au-Pd	63
Silver vs Bismuth	76
Bismuth-Tin vs Bismuth	126

These are for use at moderate temperatures only and the e.m.f's, cannot be guaranteed. They are supplied in all wire sizes.

Complete information will be furnished on request.

BAKER & CO., INC.
PLATINUM
113 Astor Street Newark, N. J.

LOW REFLECTION SURFACES

We are now prepared to produce low reflecting surfaces on a commercial basis by the high-vacuum distillation of metallic fluorides.*

By reducing the usual 4% reflection loss at each glass-air surface, a substantial improvement can be made in the light transmission and image forming characteristics of any optical system.

NATIONAL RESEARCH CORPORATION
100 BROOKLINE AVENUE
BOSTON, MASS.

*U. S. Pat. 2,207,656

SHALLCROSS
Standard Resistors

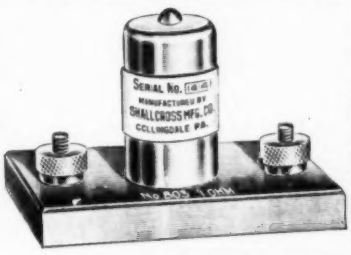

Nos. 803 to 810—Standard Resistors:

Secondary Standard Resistors mounted on a substantial base, fitted with dust covers, fill the need for high quality standards of moderate accuracy and price.

Specifications

SECONDARY STANDARD RESISTORS

NO.	RESISTANCE	TYPE WINDING	ACCURACY PERCENT	MAXIMUM LOAD	PRICE
*803P	1	Bifiliar	0.1	1 watt	$ 7.50
803	1	Bifiliar	0.1	1 watt	5.00
804	10	Bifiliar	0.1	1 watt	5.00
805	100	Bifiliar	0.1	1 watt	5.00
806	1,000	Bifiliar	0.1	1 watt	5.00
807	10,000	Balanced Rev. Pie	0.1	1 watt	7.50
808	100,000	Balanced Rev. Pie	0.1	1 watt	10.00
809	1,000,000	Balanced Rev. Pie	0.1	1 watt	30.00
810	10,000,000	Nickel Chrome	0.1	1 watt	60.00

*803P is fitted with both current and potential binding posts.

WRITE FOR BULLETIN NO. 810-BC

SHALLCROSS MFG. COMPANY
INSTRUMENTS ● RESISTORS ● SWITCHES
COLLINGDALE, PA.

RECERTIFICATION
of
STANDARD CELLS

Industry is continually demanding more and more accuracy from science. With proper treatment your Eppley precision type standard cells will meet this demand, but we wish to point out that according to authoritative sources the emf of cadmium cells should be redetermined at intervals of not more than two years.

In this connection we are pleased to offer the services of a finely equipped laboratory and a competent personnel. Our saturated standards, maintained in closely controlled oil baths, are regularly compared with the national standards at the National Bureau of Standards in Washington.

We will be pleased to examine and report on the condition of your cells without charge. For recertification a charge of Three Dollars ($3.00), plus postage and insurance is made. Approximately two weeks should be allowed for recertification.

EPLAB

THE EPPLEY LABORATORY, INC.
SCIENTIFIC INSTRUMENTS
NEWPORT, R.I.
U.S.A.

CLIFFORD MANUFACTURING CO.
564 E. FIRST STREET, BOSTON
BOSTON CHICAGO DETROIT LOS ANGELES
PRODUCERS OF BELLOWS EXCLUSIVELY
SERVING AUTOMATIC CONTROL MANUFACTURERS

POSITION WANTED

Physicist-Chemist—B.S. Chemistry, M.S. Physics. Eight years industrial research in heavy chemicals and powder metallurgy including pilot plant design and operation, employed, desires connection with a small growing concern. Address Box J3-16. Rm. 1502, 175 Fifth Ave., New York, N. Y.

THE NATIONAL RESEARCH COUNCIL OF CANADA invites applications from British subjects for positions in the Radio Laboratory, Division of Physics and Electrical Engineering, for

I. Engineers

Qualifications: — graduation in honors Physics, Engineering Physics or Electrical Engineering from a recognized university. Post-Graduate training and experience in Radio desirable. Experience in the design and operation of radiofrequency equipment. Experience in transmitter design and construction. Mathematical ability in the theoretical type of calculations arising from Radio work.

II. Radio Technicians

Qualifications: — Technical School training or equivalent, in Radio Communications, practical machine shop training an asset. Ability to construct transmitters and/or receivers and carry out preliminary tests.

Application forms may be obtained from the Secretary-Treasurer, National Research Council, Ottawa, Ontario, Canada.

INDEX TO ADVERTISERS

Name *Page*

BAKER & COMPANY, INC. vi
Platinum, palladium, gold, and silver, and their alloys, in wire and sheet form. Laboratory ware and special apparatus.

JAMES G. BIDDLE COMPANY iv
"Jagabi" Rheostats; Adam Hilger and Kipp & Zonen Optical Instruments; "Pointolite" Lamps; Electrical Testing and Speed-measuring Instruments.

CENTRAL SCIENTIFIC COMPANY .....Cover 4
Manufacturers of Cenco Physical Apparatus and Instruments to meet all requirements of University, College and High School Physics Laboratories. Specializing in high vacuum pumps and development of instruments and apparatus for various sciences.

CLIFFORD MFG. COMPANY viii
Hydron metallic bellows for temperature and pressure control devices. Data for engineers.

EASTMAN KODAK COMPANY iii
Purified Organic Chemicals for research purposes; Plates for Photography, Photomicrography, Spectroscopy, Photometry, Astronomy; Wratten Light Filters; Cameras and Films.

THE EPPLEY LABORATORY, INC. vii
Standards of e.m.f. (standard cells). Precision electrical instruments; potentiometers, bridges, temperature bridges, volt boxes. Thermopiles and pyrheliometers.

GAERTNER SCIENTIFIC CORPORATION v
Spectroscopes, Spectrometers, Spectrographs, Spectrophotometers, Heliostats, Measuring Microscopes, Comparators, Cathetometers, Reading Telescopes, Interferometers, Chronographs, Dividing Machines, etc.

GENERAL RADIO COMPANY .....Cover 3
Manufacturers of electronic measuring instruments; vacuum-tube voltmeters, amplifiers and oscillators; wave analyzers, noise meters and analyzers, stroboscopes; laboratory standards of capacitance, inductance and frequency; impedance bridges, decade resistors and condensers; air condensers and variable inductors; rheostats, Variacs, transformers; other laboratory accessories.

INTERNATIONAL RESISTANCE COMPANY iii
Manufacturers of metallized and wirewound fixed and variable Resistors including high voltage and high frequency types.

LEEDS & NORTHRUP COMPANY i
Manufacturers of Galvanometers, Resistors, Bridges, Condensers, Inductances, Potentiometers, Testing Sets; Temperature Measuring, Recording and Controlling Apparatus; Instruments for Measuring and Controlling Conductivity of Electrolytes and Hydrogen Ion Concentrations.

THE LINDE AIR PRODUCTS CO. vi
Oxygen, Argon, Helium, Krypton, Neon, Xenon, Rare Gas Mixtures, Nitrogen, Hydrogen, Calcium Carbide, Acetylene, equipment for Oxy-Acetylene welding and cutting.

MCGRAW-HILL BOOK COMPANY, INC. v

NATIONAL RESEARCH CORPORATION vii
Specialists in industrial applications of high vacuum in the fields of physics and chemistry; research, design, consulting; low reflecting glass surfaces, special products produced under low pressure.

POLAROID CORPORATION vi
Polaroid experimental kit for demonstrating Polarized light. Hand book.

RUBICON COMPANY vi
Galvanometers, electrometers, potentiometers, Wheatstone and Kelvin bridges, resistance boxes, hydrogen ion and conductivity apparatus.

SHALLCROSS MFG. COMPANY vii
Taylor High Voltage Resistors, Kilovoltmeters, Megohm Decade Resistance Boxes, Bridges, Resistance Standards, Test Sets, Attenuators, and other laboratory apparatus. Solid silver contact rotary selector switches, Super Akraohm, non-reactive wirewound resistors. Special apparatus built to specifications.

WESTINGHOUSE ELECTRIC & MANUFACTURING COMPANY ii

Simplified Sound Measurements

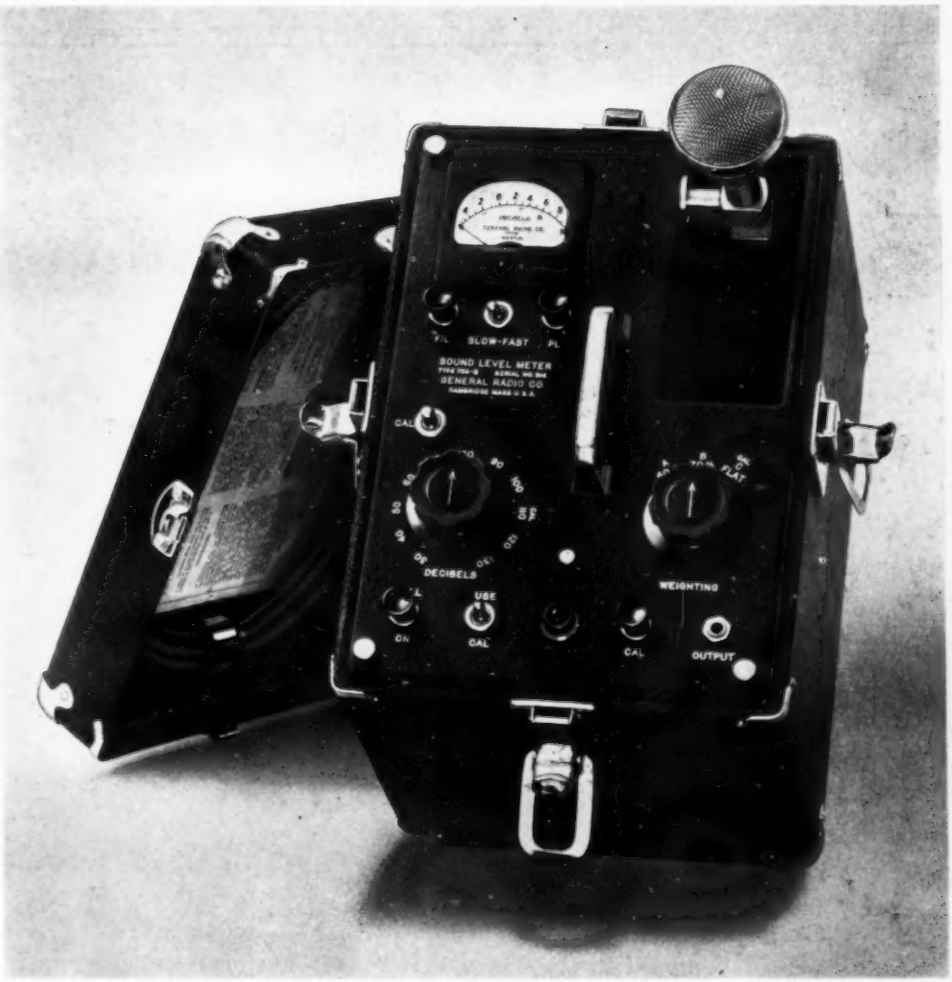

With this Accurate, Highly Stable Meter

WITH THE IMPROVED General Radio Sound-Level Meter the intensity of sound can now be measured conveniently, quickly and accurately by anyone. This instrument is widely used throughout industry for all types of noise measurements and studies. It is completely self-contained and portable and will measure the intensity of sound from a whisper to a steam whistle.

FEATURES:

1 **EXCEPTIONALLY WIDE RANGE**—24 to 140 db

2 **SIMPLIFIED CONTROLS**—complete db range covered by a single control knob

3 **IMPROVED MICROPHONE**—special type of great sensitivity, highly rugged, unaffected by ordinary changes in temperature and humidity

4 **PLUG-IN MICROPHONE**—normally used directly on folding socket on instrument but can be detached and used with cable and tripod if desired

5 **SLOW-FAST METER**—two speeds—control switch selects either; "fast" position, meter movement corresponds to A. S. A. standards; "slow" position, meter heavily damped to measure average level fluctuations.

6 **INTERNAL CALIBRATION SYSTEM**—calibration can be checked quickly from built-in calibrator

7 **THREE WEIGHTING NETWORKS**—low level, high level and substantially flat over-all response

8 **NO COILS**—instrument contains no coils or inductances and accordingly reads accurately in the presence of any ordinary magnetic field

TYPE 759-B SOUND-LEVEL METER **$195.00**

● Write for Bulletin 658 for Information

GENERAL RADIO COMPANY, Cambridge, Massachusetts

Only A Few Remain—

71546

RCA PORTABLE CATHODE RAY OSCILLOGRAPH

The oscillograph is enclosed in an attractive case with gray wrinkle finish and snap handle. Operation is through five radiotron tubes: a full wave rectifier; two amplifiers; timing axis oscillator; and a cathode ray tube with 1-inch screen.

71546 Oscillograph, 115 volts, 50–60 cycles.... } special } $21.50
71546A Oscillograph, 115 volts, 25–60 cycles.... } prices } $23.50

80806

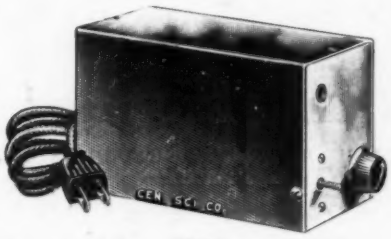

80807

For showing the wave forms of sound, No. 80806 Carbon Type Microphone at $1.25 is a desirable accessory. When this is connected through No. 80807 Modulated Oscillator Coupling Unit and a radio receiver for amplifying and reproducing the sound impulses, and the oscillograph is connected into the circuit, the wave forms may be observed. The price of No. 80807 Modulated Oscillator Coupling Unit, which oscillates between 900 and 1200 kilocycles and requires either A. C. or D. C. from 105 to 125 volts, is $6.50.

CENTRAL SCIENTIFIC COMPANY

SCIENTIFIC INSTRUMENTS — TRADE MARK CENCO REG. U.S. PAT. OFF. — LABORATORY APPARATUS

New York • Boston • CHICAGO • Toronto • San Francisco

LANCASTER PRESS, INC., LANCASTER, PA.